EE-MSFC-1900

EE-MSFC-1900

(NASA-CR-120685) CALCULATIONS FOR INTERPRETATION OF SOLAR VECTOR MAGNETOGRAPH DATA Final Report, Oct. 1970 - May 1975 (Teledyne Brown Engineering) 164 p HC $6.25 CSCL 03B
N75-29986
Unclas
G3/93 33026

Final Report

CALCULATIONS FOR INTERPRETATION OF SOLAR VECTOR MAGNETOGRAPH DATA

May 1975

TELEDYNE
BROWN ENGINEERING

Cummings Research Park • Huntsville, Alabama 35807

FINAL REPORT
EE-MSFC-1900

CALCULATIONS FOR INTERPRETATION OF SOLAR VECTOR MAGNETOGRAPH DATA

By

A. R. Dunn, Ph.D.

May 1975

Prepared For

ELECTROMAGNETIC AND SOLID STATE DIVISION
SPACE SCIENCES LABORATORY
GEORGE C. MARSHALL SPACE FLIGHT CENTER
HUNTSVILLE, ALABAMA

Contract No. NAS8-26376

Prepared By

RESEARCH DEPARTMENT
ELECTRONICS AND ENGINEERING
TELEDYNE BROWN ENGINEERING
HUNTSVILLE, ALABAMA

ABSTRACT

This report describes the work which has been done on Contract No. NAS8-26376 between October 1970 and May 1975. The report is divided into three self-contained sections, each dealing with a separate portion of the performance period. In Section 1, the work done between October 1970 and October 1971 is discussed. Section 2 covers the period from October 1971 to June 1973. Section 3 covers the period from June 1973 to May 1975.

APPROVED:

N E Chatterton

N. E. Chatterton, Ph.D.
Manager
Research Department

SECTION 1

ANALYSIS OF SUNSPOT SPECTRAL DATA

TABLE OF CONTENTS

LIST OF ILLUSTRATIONS

LIST OF TABLES

INTRODUCTION

Observations of the profile of the neutral iron line at 0.5250216 micrometer (5,250.216 Å) are described in this section. The reduction of the observations to obtain residual intensities, line widths, and the locations of the Zeeman components is discussed. The components of magnetic field strength along the line of sight are determined and plotted in the form of a sunspot map. Finally, the steps to be followed in a more complete analysis of the data are outlined.

SUNSPOT SPECTRUM OBSERVATIONS

This section describes the analysis of sunspot spectral observations made during July 1969 by Dr. M. J. Hagyard with the spectrograph of the McMath solar telescope at the Kitt Peak National Observatory. (The spectrograph and telescope are described in Reference 1). Although both photographic and photoelectric observations were made, the photographic data are of primary interest here.

Because the spectra were intended for Zeeman effect studies, the polarization form of the observed intensity had to be known. A partial linear polarization is introduced within the telescope in the reflection at the primary mirror; this was compensated in the observations by placing a glass flat in the light path. The only remaining instrumental effect is then a possible phase shift introduced at the primary. Such a phase shift would not be detectable in the results before a more advanced stage in the analysis is reached. In order to check for residual instrumental polarization, photoelectric and photographic observations were made of the photosphere, which should be intrinsically unpolarized. Photospheric intensities were measured in right and left circularly polarized light and in light linearly polarized at 0, 45, and 90 degrees to the entrance slit. No dependence of intensity upon polarization form was observed for any of the photospheric observations; residual instrumental polarization is, therefore, negligible.

Control over the polarization form of the observed light was achieved by placing polarizers in front of the spectrograph slit. The slit was always parallel to the east-west direction on the Sun. Immediately preceding the slit was a calcite analyzer oriented to pass only those light components which were linearly polarized parallel to the slit. The calcite analyzer was preceded by a soleil compensator, which can be adjusted to form a quarter-wave or a half-wave plate. The form of polarization transmitted is defined by specifying the angle α between the compensator's axis and the transmission direction of the calcite analyzer. The polarization forms transmitted by the compensator-analyzer combination are summarized in Table 1; the sequence numbers 1 through 5 were used to identify the combinations throughout the observations.

A predisperser was used to eliminate overlapping orders. The slit width was 0.1 millimeter for all observations; the effective slit length was determined by the soleil compensator setting. The exposure times were either 6 or 12 seconds, and stepwedge calibrations were made for both these exposure times. All the spectra discussed in this report were photographed on 14 July 1969 between 2:40 and 3:15 p.m. M.S.T. The sunspot observed was then located near the center of the disk ($\cos \theta = 0.939$). The spot penumbra was approximately circular, but the umbra was divided by a light bridge. The position of the umbral center was marked on the spectra by a wire placed perpendicular to the slit. A second wire was placed parallel to the slit near the red end of the observed spectral range for a permanent position marker.

The spectrograph slit was first placed just south of the sunspot, with the length of the slit directed east-west on the Sun. A sequence of five exposures was made in the order given in Table 1. The slit was then moved 1 millimeter toward the north pole of the solar image, and the exposure sequence was repeated. The procedure was repeated, the slit being moved north by 1 millimeter each time, until the entire spot had been traversed. The solar image formed by the McMath telescope is approximately 800 millimeters in diameter, so a displacement of 1 millimeter in the image corresponds to approximately 1,740 kilometers on the Sun. Twelve positions on the Sun were observed with an exposure time of 6 seconds. The three positions containing the sunspot umbra were also photographed with a 12-second exposure time.

TABLE 1. OBSERVED POLARIZATION FORMS

SEQUENCE NUMBER	SOLEIL COMPENSATOR SETTING	α (deg)	FORM OF TRANSMITTED LIGHT
1	$\lambda/4$ plate	+45	Left circularly polarized
2	$\lambda/4$ plate	-45	Right circularly polarized
3	$\lambda/2$ plate	0	Linearly polarized parallel to slit
4	$\lambda/2$ plate	+22.5	Linearly polarized at 45 deg to slit*
5	$\lambda/2$ plate	+45	Linearly polarized at 90 deg to slit*

*Recall that a half-wave plate alters the plane of vibration by 2α.

The photographic spectra were converted to digital form by measuring the photographic density as a function of position on the film with a digitizing microdensitometer. The films cover approximately 5×10^{-4} micrometers (5 Å) of the solar spectrum centered at 0.525 micrometer (5,250 Å); a shorter region of approximately 1.5×10^{-4} to 2×10^{-4} micrometers (1.5 to 2.0 Å) containing the neutral iron line at 0.5250216 micrometer (5,250.216 Å) was measured. The position scale was converted to dispersion in Å/mm by referring to the locations of the spectral lines and the wire position marker. The microdensitometer sample spacing could then be expressed in terms of angstroms on the film; the sampling points were found to be spaced at 5.88×10^{-7} micrometer (5.88 mÅ) intervals.

The films were sampled in a uniform pattern, which simplifies the correlation of the scans with their proper positions in the sunspot. The pattern is shown in Figure 1.

The spectral dispersion was along the north-south direction, so each microdensitometer scan was made parallel to the dispersion and had a height equal to the microdensitometer slit height of 1 millimeter. The width of spectrum sampled at each scan step was determined by the microdensitometer slit width of 30 micrometers. At the dispersion of the film, this represents a sample width of 4.20×10^{-7} micrometers (4.20 mÅ).

The center of the umbra is marked on the film by the image of the wire placed perpendicular to the slit. Microdensitometer scans were made beginning at the wire and working eastward, the final scan being entirely in the photosphere. These scans were labelled a through f. Scans were then made westward from the wire into the penumbra; these were labelled g through i. For those exposures which did not contain the entire sunspot, the same pattern was followed, but the reference line was the centerline of the film instead of the center of the umbra.

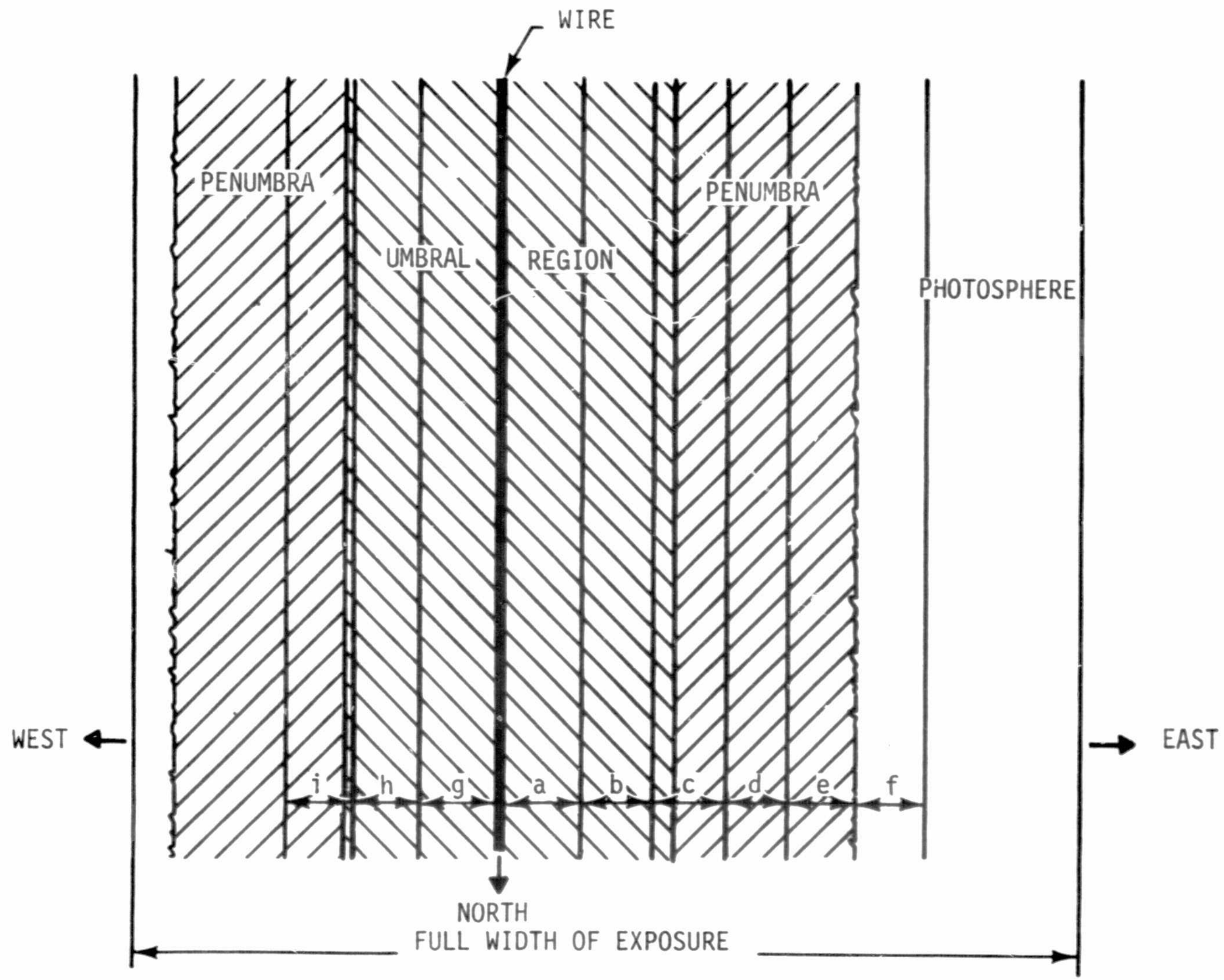

FIGURE 1. MICRODENSITOMETRY PATTERN FOR SUNSPOT OBSERVATIONS

The digital intensity data are labelled with three symbols which describe the position of the observed region and the polarization form of the recorded intensity. For example, in the label X-2-c, the Roman numeral X designates the north-south location of the region observed, in terms of millimeters on the primary solar image; 2 is the polarization form, in this case right-hand circular polarization; c is the east-west location of the measured strip, in terms of millimeters on the film. There are 564 strips in the 15 exposures made on 14 July 1969, but not all of these contain sunspot spectra.

The microdensitometer output represented measured film density in the sample areas of the film. The digital output data were recorded on magnetic tape and were converted to intensities by use of the characteristic curves derived from the stepwedge calibration exposures. The magnetic tapes thus contain intensities uniformly spaced 5.88×10^{-7} micrometers (5.88 mÅ) apart, defining a region approximately 1.5×10^{-4} to 2×10^{-4} micrometers (1.5 to 2. Å) long. The intensity values are in arbitrary units, in the sense that the continuum level shown on the tape records is usually considerably less than 1.00. The intensity values are in correct proportion to one another but should be rescaled to bring the continuum up to 1.00. These digital data were the values used in the analysis to be described in the subsection entitled "Line Profile Data Reduction Program".

REDUCTION OF THORIUM CALIBRATION WAVELENGTHS TO STANDARD CONDITIONS

To obtain a laboratory determination of the wavelengths of the solar spectrum lines, a thorium emission spectrum and a solar disk spectrum were exposed in parallel rows on the same film. The observed solar wavelengths can then be determined by measuring their distances from thorium standard reference lines (reference standards are discussed in References 2 and 3; precise determinations of additional thorium wavelengths are given in References 4, 5, and 6). This procedure refers the solar lines to the wavelengths for the thorium lines at the time of observation; the observed wavelength actually depends slightly upon the conditions of observation.

Because the index of refraction of air depends upon its temperature and pressure, and upon the wavelength of radiation being studied, measured wavelengths are reduced to the values they would have in some chosen standard conditions. The usual standard conditions are dry air at temperature 15° C, pressure 760 millimeters of mercury; or vacuum. Air values are used more often as standards for wavelengths in the visible range.

In 1952, a meeting of the Joint Commission for Spectroscopy, sponsored by the International Astronomical Union, the International Union of Pure and Applied Physics, and the International Council of Scientific Unions, recommended adoption of Edlén's formula for converting wavelengths in standard air to wavelengths in vacuum (Ref. 7). In the same paper, Edlén also gives a simple formula for converting measured wavelengths to values for standard air. This simple formula can be used when the conditions of measurement are not very far from the standard conditions. An additional correction for the presence of water vapor should be made in high-precision work.

A short FORTRAN program (Figure 2) has been written to correct wavelengths to standard air using Edlén's formula. The partial pressure of water vapor was not measured with the wavelengths to be corrected, so a moisture correction could not be included. The program uses the following version of Edlén's formula:

$$\lambda_2^0 - \lambda_2 = \left(\Delta\lambda_2 - \Delta\lambda_1 \cdot \frac{\lambda_2}{\lambda_1}\right)\left(\frac{0.0013882\ p}{1 + 0.00367\ t} - 1\right)$$

where

λ_2^0 - unknown wavelength in standard air

λ_2 - measured value to be corrected

λ_1 - reference wavelength for standard air

$\Delta\lambda_1$, $\Delta\lambda_2$ - vacuum corrections to λ_1 and λ_2

p - air pressure, mm Hg

t - temperature, °C.

The vacuum corrections $\Delta\lambda_1$, $\Delta\lambda_2$ are tabulated in Table 3 of Reference 8.

The program has been tested on the two examples of wavelength corrections given by Babcock (Ref. 9). The results of the test are summarized in Table 2.

TABLE 2. RESULTS OF TESTING EDLÉN CORRECTION PROGRAM

p (mm)	t (°C)	λ_1 (μ)	λ_2 (μ)	BABCOCK (μ)	DUNN (μ)
620	20	0.4500	0.300	-6.4×10^{-7}	-6.6×10^{-7}
720	25	0.400	0.800	$+5.2 \times 10^{-7}$	$+5.2 \times 10^{-7}$

```
REDUCTION OF WAVELENGTHS TO STANDARD AIR     10/22/70

REFS. -- INTRO. TO  TABLE OF WAVENUMBERS 2000A TO 7000 A , N.B.S.
MONOGRAPH 3, VOL. 1 (GET VACUUM CORRECTIONS FROM
TABLE 3 OF THIS REF.), EDLEN, JOSA VOL. 43, PG. 339, 1953,
BABCOCK, AP. J., VOL. 111, PG. 60, 1950.
EDLEN FORMULA
MUST TREAT WAVELENGTHS IN 2 PARTS TO MINIMIZE LOSS OF
SIGNIFICANCE.  CHARACTERISTIC WILL BE READ AS INTEGER
VARIABLE, MANTISSA AS REAL VARIABLE.  LW1C, W1M ARE REFERENCE
WAVELENGTH, D1 IS ITS VACUUM CORRECTION.  LW2C, W2M, D2 ARE
SAME QUANTITIES FOR WAVELENGTH  TO BE CORRECTED.
D2 IS THE TABULATED VALUE FOR THE MEASURED WAVELENGTH.  D2, D1
AND REF. WAVELENGTH ARE VALUES FOR STANDARD AIR.
NEGLECT MOISTURE CORRECTION.
P IS PRESSURE IN MM HG, T IS TEMPERATURE IN DEGREES C.

   KPU=2
   KPR=3
   READ (KPU, 1) LW1C, W1M, D1
 1 FORMAT (I6, 2F10.0)
   WRITE (KPR, 3)
 3 FORMAT (1H ,37HWAVELENGTHS CORRECTED TO STANDARD AIR)
   WRITE (KPR, 7)
 7 FORMAT (1H ,37HADD CORRECTION TO MEASURED WAVELENGTH)
   WRITE (KPR, 5) LW1C, W1M
 5 FORMAT (1H ,21HREFERENCE WAVELENGTH=, I6, 1H+, F10.6)
   WRITE (KPR, 4)
 4 FORMAT (1H , 19HMEASURED WAVELENGTH, 6X,15HCORRECTION IN A)
   READ (KPU, 2) P, T
 2 FORMAT (2F10.0)
10 READ (KPU, 1) LW2C, W2M, D2
   LOOK FOR LAST CARD (BLANK)
   IF (LW2C-0) 6, 60, 6
 6 W2C= LW2C
   W1C= LW1C
   A= W2C/(W1C + W1M)
   B= W2M/(W1C + W1M)
   FAC= (1.3882E-3*P/(1.0 + T*3.67E-3))-1.0
   CORR= (D2-D1*(A + B))*FAC
   WRITE (KPR, 8) LW2C, W2M, CORR
 8 FORMAT (1H ,3X,I6,1H+,F10.6, 8X, F10.6)
   GO TO 10
60 CALL EXIT
   END
```

FIGURE 2. EDLÉN CORRECTION TO MEASURED WAVELENGTHS

In practice, the corrections derived from this program will not be required. Unless the measurement conditions deviate grossly from standard, the wavelength corrections will be very small for wavelengths which lie within approximately 5×10^{-3} micrometers (50 Å) of the line used for a wavelength reference. The observed thorium calibration spectrum is very short, covering the range 0.5248 to 0.5256 micrometer (5,248 to 5,256 Å), approximately. There is no problem here of measuring wavelengths from a reference standard hundreds or thousands of angstroms away. The variation in wavelength caused by laboratory air will be negligible over the short observed wavelength range.

LINE PROFILE DATA REDUCTION PROGRAM

The sunspot spectra are to be used to determine sunspot magnetic field strengths from the profiles of the magnetically sensitive neutral iron line at 0.5250216 micrometer (5,250.216 Å). The digital intensity data described in the first subsection require additional reduction to prepare the profiles for determination of magnetic field strengths. A FORTRAN program (Figure 3) has been written to perform the reduction.

The intensity data are used here without correction for the effect of stray light. Stray light strongly distorts measured umbral continuum intensities, but the distorting effect is much smaller in the case of residual intensity in a spectral line which is present in both the sunspot and the photosphere. The 0.5250216 micrometer (5,250.216 Å) line is, in fact, stronger in spot umbrae than in the photosphere. The observed sunspot profiles without stray light correction are generally stronger than the photospheric 0.5250216-micrometer (5,250.216 Å) line in the Utrecht Atlas; and it was thought that in this case the distortion of the profiles by penumbral and photospheric stray light was smaller than the distortion by such other causes as blending of Zeeman components, absorption by telluric water vapor, and blending with the neighboring faint molecular line.

The digital intensity values appear on the magnetic tape in order of decreasing wavelength; the values are spaced 5.88×10^{-7} micrometers (5.88 mÅ) apart. The spectral range runs from the marker wire near 0.5254 micrometer (5,254 Å), to approximately 0.5249 micrometer (5,249 Å). The portion of spectrum between 0.5252 and 0.5253 micrometer (5,252 and 5,253 Å) reaches the true continuum in the photosphere, according to the Utrecht Atlas. Examination of the sunspot spectral data shows that the measured intensities are generally largest in the 0.5252 to 0.5253-micrometer (5,252 to 5,253 Å) interval, so these intensities

```
C     PROFILE PARAMETERS        12/15/70     ARD
C     7094 VERSION        1/5/71
C     FIND MINIMUM VALUES, HALFWIDTH, AND EQUIVALENT WIDTH OF 5250.2
C     PROFILE.
C     Y'S ARE UNSCALED INTENSITIES, CONT IS CONTINUUM LEVEL FOR SCAN,
C     RLAM IS RESIDUAL INTENSITY, W IS EQUIVALENT WIDTH.  LAST Y
C     VALUE WILL BE FOLLOWED BY Y= 2.0 TO SIGNAL END OF DATA.  ID IS
C     IDENTIFICATION NUMBER FOR SCAN, IBC IS 'BROADENING CODE'
C     DESCRIBING EXPECTED FORM OF ZEEMAN BROADENING.  I21 IS LEFT OF
C     PROFILE CENTER.  IT IS THE RIGHT HAND POINT OF ITS INTERVAL.
C     I22 IS THE LEFT HAND POINT OF THE SAME INTERVAL.  I11 AND I12
C     ARE RESPECTIVELY THE LEFT AND RIGHT HAND POINTS OF AN INTERVAL TO
C     THE RIGHT OF THE PROFILE CENTER.
      DIMENSION Y(10), RLAM(150), RMIN(6)
      DIMENSION XMIN(6)
      DIMENSION NUN(5), FT(3), FNNT(3), FOT(2)
      DIMENSION FAT(2), MALL(2)
      DIMENSION ILOSE(9)
      DATA FOT/8H(I1,2A6)/
      DATA FNNT/18H(2A6,I3,I5,1X,9A6)/
      DATA FAT/5H(5A6)/
      DATA FT/15H(I1,F6.4,9F7.4)/
      KPU= 5
      KPR= 6
      WRITE (KPR, 15)
      WRITE (KPR, 16)
   15 FORMAT (49H POSITIONS ARE IN TERMS OF DATA SPACING INTERVALS)
   16 FORMAT (26H AN INTERVAL IS ABOUT 5 MA)
C     AN INTERVAL IS 5.88 MA FOR DATA OF 14 JULY 1969
  300 CALL REDTPD (8,FOT,IER,1, ICK, 2, MALL)
      IF (IER .EQ. 2) GO TO 67
      IF (ICK .NE. 1) GO TO 300
C     LOOK FOR DATE (FIRST RECORD IN SCAN)
   68 READ (KPU, 1) ID, IBC, IRR, CONT
    1 FORMAT (3I5, F10.0)
C     IBC IS NUMBER OF RESOLVED AND UNRESOLVED MINIMA OBTAINED FROM VISUAL
C     INSPECTION OF PROFILE PLOTS.  IT IS USED ONLY AS A MEANS OF
C     CHECKING THE PROGRAM, WHICH DETERMINES THE NUMBER, TYPES,
C     AND POSTIONS OF MINIMA IN A DIFFERENT WAY.  IBC= (NO. OF RESOLVED
C     MIN.)*10 + NO. OF UNRESOLVED MIN.
      IF (ID) 67, 67, 301
C     NOW READ 2ND RECORD AND CHECK TO MAKE SURE YOU HAVE THE RIGHT
C     SCAN
```

FIGURE 3. LISTING OF LINE PROFILE REDUCTION PROGRAM

```
301 CALL REDTPD (8, FNNT, IER, 2, NUN, 1, IROLL, 1, IPAP, 9, ILOSE)
    IF (IROLL .EQ. IRR) GO TO 30
 18 CALL REDTPD (8, FOT, IER, 1, ICK, 2, MALL)
    IF (IER .EQ. 2) GO TO 67
    IF (ICK .NE. 1) GO TO 18
    CALL REDTPD (8,FNNT,IER,2,NUN,1,IROLL,1,IPAP,9, ILOSE)
    IF (IROLL .NE. IRR) GO TO 18
C   IF IRR NOT EQUAL TO IROLL, SAVE IRR AND CONT AND SKIP TO NEXT
C   SCAN
 30 CALL REDTPD (8, FAT, IER, 5, NUN)
 66 J=1
C   J IS USED TO COUNT  STORE  VALUES
    WRITE (KPR, 12) ID, IROLL
 12 FORMAT (1H , 8HID. NO.=, I5, 7H IROLL=, I5)
    YT = CONT * .475
  5 CALL REDTPD (8, FT, IER, 1, ICK, 10, Y(1))
  2 FORMAT (10F7.4)
    DO 7 I= 1, 10
    IF (Y(I)-YT) 4, 7, 7
  4 IF (Y(I)) 300, 300, 9
  9 STORE = Y(I)
    WRITE (KPR, 74) STORE
 74 FORMAT (1H , F10.5)
 73 IF (I-10) 71, 70, 70
 70 CALL REDTPD (8, FT, IER, 1, ICK, 10, Y(1))
    I= 1
    GO TO 72
 71 I= I + 1
 72 IF (Y(I)-YT) 73, 73, 104
104 IF (J-3) 17, 8, 6
 17 J= J + 1
  7 CONTINUE
    GO TO 5
  8 K=1
    DO 119 KK= 1, 15
C    WRITE THE 150 POINTS AFTER THE THIRD 'STORE' INTO RLAM ARRAY
C   BUT START WITH 1ST DATA POINT OF NEXT GROUP OF 10, NOT NEXT
C   DATA POINT
    CALL REDTPD (8, FT, IER, 1, ICK, 10, Y(1))
    DO 6 I= 1, 10
    RLAM(K)= Y(I)/CONT
    K= K + 1
  6 CONTINUE
119 CONTINUE
 11 CALL REDTPD (8, FOT, IER, 1, ICK, 2, MALL)
    IF (IER .EQ. 2) GO TO 67
    IF (ICK .NE. 1) GO TO 11
```

FIGURE 3 - Continued

```
C     FIND MINIMA WITHIN 5250.2
   13 ICHK= 0
C     ICHK IS VARIABLE USED TO COUNT MINIMA
      I10 = 10
      I1= 1
      DO 250 KK= 1, 15
      WRITE (KPR, 251) (RLAM(I), I= I1, I10)
  251 FORMAT (1H , 10F7.4)
      I1= I1 + 10
      I10 = I10 + 10
  250 CONTINUE
      I = 40
      NR= 0
      NUR= 0
   81 DELM= RLAM(I)-RLAM(I-1)
      DEL= RLAM(I+1) - RLAM(I)
      DELP= RLAM(I+2) - RLAM(I+1)
      IF (DELM) 83, 82, 83
   82 I= I + 1
      GO TO 81
   83 IF (DELP) 84, 88, 84
   88 IF (DEL) 89, 90, 89
   90 IF (RLAM(I+3)-RLAM(I+2)) 89, 89, 91
   91 ICHK= ICHK + 1
      RMIN(ICHK)= RLAM(I+1)
      XMIN(ICHK) = I + 1
      I = I + 1
      NUR= NUR + 1
      WRITE (KPR, 155) ICHK, XMIN(ICHK), RMIN(ICHK), NR, NUR
C     IN THIS CASE, WANT TO ARRIVE FINALLY AT STATEMENT NO. 82
C     WITH I= ORIGINAL I + 2, SO INCREASE I TWICE
  155 FORMAT (10H MIN. NO. ,I5,5X,2HI=,F6.2,5X,5HRLAM=,F8.4,2I7)
      GO TO 89
   84 IF (DEL) 85, 92, 85
   85 IF (ABS(DELM + DEL) - (ABS (DELM) + ABS (DEL))) 86, 87, 87
   92 IF (DELM) 93, 89, 89
   93 IF (DELP) 89, 89, 94
   94 ICHK= ICHK + 1
      RMIN(ICHK) = RLAM(I)
      XS= I
      XMIN(ICHK) = XS + 0.500
      NR= NR + 1
      WRITE (KPR, 155) ICHK, XMIN(ICHK), RMIN(ICHK), NR, NUR
      GO TO 89
   86 IF (DELM) 96, 89, 89
   96 IF (DEL) 89, 89, 97
   97 ICHK= ICHK + 1
      ISV = I
```

FIGURE 3 - Continued

```
      NR= NR + 1
      RMIN(ICHK)= RLAM(I)
      XMIN(ICHK) = I
      WRITE (KPR, 155) ICHK, XMIN(ICHK), RMIN(ICHK), NR, NUR
      GO TO 89
   87 IF (ABS(DEL) - ABS (DELP)) 98, 89, 89
   98 IF (ABS(DEL) - ABS(DELM)) 99, 89, 89
   99 ICHK = ICHK + 1
      RMIN(ICHK) = RLAM(I)
      XMIN(ICHK) = I
      NUR= NUR + 1
      WRITE (KPR, 155) ICHK, XMIN(ICHK), RMIN(ICHK), NR, NUR
   89 IF (I-65)  82, 100, 100
  100 IF (RLAM(I) - .800) 82, 82, 101
  101 ITRY= 10*NR + NUR
      IF (IBC-ITRY) 103, 102, 103
  103 WRITE (KPR, 105) NR, NUR, ITRY, IBC
  105 FORMAT (4H NR=,I5,3X,4HNUR=,I5,3X,5HITRY=,I5,3X,
     116HBROADENING CODE=, I5)
      WRITE (KPR, 107)
  107 FORMAT (25H CHECK DATA FOR THIS SCAN)
  102 IF (ICHK-3) 19, 20, 20
   19 ICHK = ICHK + 1
      RMIN(ICHK) = 1.00
      GO TO 102
   20 IF (RMIN(1) - RMIN(2)) 21, 21, 22
   21 ABSMN= RMIN(1)
      GO TO 23
   22 ABSMN= RMIN(2)
   23 DO 924 I= 3, 6
      IF (RMIN(I)-ABSMN) 57, 57, 924
   57 ABSMN= RMIN(I)
  924 CONTINUE
      WRITE (KPR, 128) ABSMN
  128 FORMAT (1H , F10.4)
C     START HALFWIDTH CALCULATION
   24 HMIN= 0.50*(1.0 + ABSMN)
      I1= ISV
C     ISV IS LOCATION OF FIRST RESOLVED MIN.  THERE MUST ALWAYS BE
C     AT LEAST ONE OF THEM.
C     WORK TO RIGHT OF PROFILE CENTER FIRST
   25 TEST= HMIN - RLAM(I1)
      IF (TEST) 59, 58, 58
   58 I1= I1 + 1
      GO TO 25
   59 I12= I1
      I11= I1 - 1
C     NOW WORK TO LEFT OF PROFILE CENTER
      I2= ISV
```

FIGURE 3 - Continued

```
   26 TEST= HMIN - RLAM(I2)
      IF (TEST) 48, 49, 49
   49 I2= I2 - 1
      GO TO 26
   48 I22= I2
      I21= I2 + 1
      FRAC= (HMIN-RLAM(I21))/(RLAM(I22)-RLAM(I21))
C     LINEAR INTERPOLATION TO GET POSITIONS OF HALFWIDTH POINTS
C     THIS SHOULD BE OK BECAUSE PROFILE SHOULD BE NEARLY LINEAR IN
C     THIS RANGE
      XI21= I21
      POS2= XI21 - FRAC
      FRAC= (HMIN-RLAM(I11))/(RLAM(I12)-RLAM(I11))
      XI11= I11
      POS1= XI11 + FRAC
      FWHM= POS1 - POS2
      WRITE (KPR, 60) POS2, POS1, FWHM
   60 FORMAT (1H ,19HHALFWIDTH POINTS AT, F7.3,5H  AND,F7.3,
     17H  FWHM=, F7.3)
C     START EQUIVALENT WIDTH CALCULATION
      I= I22
C     LOOK FOR ENDS OF PROFILE
   27 X= RLAM(I)-RLAM(I-1)
      IF (X) 46, 47, 47
   46 I= I - 1
      GO TO 27
   47 ISTRT= I
      WRITE (KPR, 147) ISTRT
  147 FORMAT (1H , 6HISTRT=,  I5)
      I= I12
   28 X= RLAM(I+1) - RLAM(I)
      IF (X) 45, 45, 44
   44 I= I + 1
      GO TO 28
   45 ISTP= I
      WRITE (KPR, 148) ISTP
  148 FORMAT (1H , 5HISTP=, I5)
      NI= (ISTP-ISTRT + 1)/2
      XI= ISTP - ISTRT + 1
      XI2= XI/2.
      XI= NI
      IF (XI-XI2) 29, 43, 29
   43 ISTP= ISTP - 1
   29 SUM= 0.
      DO 41 I= 1, 150, 2
C     WILL NEVER GET TO I = 150
      IS = ISTRT + I
```

ORIGINAL PAGE IS
OF POOR QUALITY

FIGURE 3 - Continued

```
      SUM= RLAM(IS)*4. + RLAM(IS + 1)*2. + SUM
      IF (IS -(ISTP - 3)) 41, 62, 41
   41 CONTINUE
   62 S= RLAM(ISTRT) + RLAM(ISTP) + 4.*RLAM(ISTP - 1)
      SUM= (S + SUM)/3.
      DLAM= ISTP - ISTRT
      W= DLAM - SUM
      WRITE (KPR, 65) W
   65 FORMAT (3H W=,5X,F10.5,5X,22H IN DATA SPACING UNITS)
      GO TO 68
   67 WRITE (KPR, 10)
   10 FORMAT (9H END FILE)
      STOP
      END
```

FIGURE 3 - Concluded

ORIGINAL PAGE IS
OF POOR QUALITY

were adopted as the continuum values for the sunspot scans, and the remaining intensities were scaled to them. The continuum intensity was determined for each scan by inspection of the magnetic tape print-out, and that value was read as the variable "CONT" for the line profile reduction program.

Starting at the red end of the region, and including the image of the wire, the measured intensity falls below 50 percent of the continuum intensity three times before the 0.5250216-micrometer (5,250.216 Å) line is reached. This fact was used to isolate the 0.5250216-micrometer (5,250.216 Å) profile from the rest of the spectrum. The minima deeper than some fraction of CONT were counted, and the third minimum was known to be λ5250.6, the strong line immediately adjacent to λ5250.2. (The fractional value used was usually 0.475. However, because the relative intensities of the spectral lines are different on different scans, this value was sometimes adjusted to avoid counting unwanted lines or overlooking one of the desired minima. It was always possible to find a fraction which would select the three desired minima.)

When the third minimum has been found, the program tests the succeeding intensity values until it finds the next local intensity maximum, which represents the dividing line between the λ5250.6 profile and the λ5250.2 profile. (The intensity usually does not quite return to the continuum level between the two profiles.) The next spectral line, then, will be λ5250.216. An array of 150 values is set aside for that profile. One hundred fifty intensities following the local maximum are read into this array, called RLAM, and the rest of the unscaled digital values are not used. The intensities are scaled by dividing them by CONT before they are stored; they are stored as residual intensities.

The program next locates the intensity minima within the 0.5250216-micrometer (5,250.216 Å) profile.* These minimum value locations will be used later as the positions of the Zeeman components. The program begins searching at the fortieth point in the profile. In a few cases, unresolved minima appeared before the fortieth point, so the starting index should probably be changed. The presence of such neglected minima can always be detected because the program prints the 150 RLAM values for each profile.

The program searches for two kinds of minima, called "resolved" and "unresolved". A "resolved" local minimum is defined as an intensity value which lies between two greater intensities. The intensity value immediately adjacent on one side may be equal to the minimum value. For example, in the sequence 0.5210, 0.5009, 0.4841, 0.4995, 0.5196, the value 0.4841 would be selected as a resolved minimum. Its position would be given by its index: in this case, 3. In the sequence 0.5210, 0.5009, 0.4841, 0.4841, 0.4995, the resolved minimum would again be the lowest intensity value, 0.4841, but the position would be taken as halfway between the two intensity points with that value, or 3.5. An "unresolved" local minimum is defined as the left-hand point of an interval which is bounded by two intervals having slopes of the same sign but greater magnitude. Because the digital data are smooth, the use of minima found over a region only four or five points long is successful; noise fluctuations are rarely detectable on this scale.

As a check, the number of resolved and unresolved minima is also estimated visually from plots of the profile scans, and a code

*All positions found by this program are the array indices of the corresponding intensity values. They may be converted to wavelength values by using the fact that adjacent intensity values are separated by 5.88 $\times 10^{-7}$ micrometers (5.88 mÅ).

number (IBC) equal to ten times the number of resolved minima plus the number of unresolved minima is read for each scan. This code number is checked against the number of minima found by the program, and a warning message is printed if they do not agree. Lack of agreement is not necessarily a sign of error, since the program's selection criteria are not exactly the same as those of the eye. However, the warning message provides a screening mechanism which selects the scans that are most likely to contain errors. The data can then be checked to ensure that the correct scan is being read and that the 0.5250216-micrometer (5,250.216 Å) line has been correctly isolated.

The program next determines the full width of the 0.5250216-micrometer (5,250.216 Å) profile at half the minimum intensity, where the minimum intensity, I_{min}, is taken to be the intensity of the deepest minimum in the profile. The intensities I_{half} at half minimum are then equal to $(1.00 + I_{min})/2$. The program searches outward on both sides of the profile from the deepest minimum until it finds the intervals containing the intensities I_{half} and interpolates, if necessary, to find the positions of the I_{half} values.

Finally, the program defines the ends of the profile as the positions near the continuum at which intensity reaches local maximum values. The indices corresponding to these local maxima are printed. The equivalent width W_λ is then obtained by direct integration of the profile between the end points, using the defining equation

$$W_\lambda = \int_{\lambda_1}^{\lambda_2} [1 - I(\lambda)]\, d\lambda$$

where

λ - wavelength

λ_1 and λ_2 - ends of the profile

$I(\lambda)$ - residual intensity as a function of wavelength.

The card input and program output are summarized in Tables 3 and 4.

TABLE 3. LINE PROFILE REDUCTION PROGRAM INPUT

VARIABLE NAME	DESCRIPTION
ID	Identification number for program output. Each scan has a unique number; they range from 1 to 564.
IBC	Code number for visual estimate of number of minima within profile.
IRR	Identification number of the scan on the magnetic tape. Two scans on different tapes may have the same IRR.
CONT	Continuum level obtained from the magnetic tape printout.

One card for each scan: ID, IBC, IRR, CONT Format (3I5, F10.0)

TABLE 4. LINE PROFILE REDUCTION PROGRAM OUTPUT

1) ID, IRR for identification of scan

2) Intensities of the three minima preceding $\lambda 5,250.216$

3) 150-value array containing the profile of $\lambda 5,250.216$

4) For each minimum found, a line is printed containing its position and intensity, and a two-digit code defined like IBC, giving a running total of the number of resolved and unresolved minima found in the profile.

5) Total number of resolved and unresolved minima, the two-digit minimum-count code (ITRY) for the entire profile, and the IBC value read, for comparison.

6) Warning message if ITRY is not equal to IBC.

7) Intensity of the deepest minimum in the profile.

8) Locations of the I_{half} points and the full width at half minimum in the data spacing units.

9) and 10) Ends of the profile.

11) Equivalent width, in data spacing units.

MAGNETIC FIELD STRENGTH DETERMINATIONS FROM THE 5,250.216 Å LINE

METHODS OF DETERMINING FIELD STRENGTHS

Determination of sunspot magnetic field strengths from the Zeeman splitting of spectral lines is discussed in detail in several textbooks (see, for example, Refs. 10 and 11). Reference 10 also contains a discussion of Unno's theory of spectral line formation in a magnetic field. Unno's technique was one of the first to permit calculation of absorption Zeeman profiles in a stellar atmosphere. It has been used by a number of investigators and is still used occasionally. It assumes a Milne-Eddington atmosphere; profiles which are formed in pure absorption and LTE; a uniform magnetic field; and a ratio of line to continuous absorption which is constant with depth.

Two more recent approaches are those of Beckers (Refs. 12 and 14) and of Moe (Ref. 13). Reference 13 also contains a summary of other methods. [A discussion by Staude (Ref. 15) of notational differences in recent papers is helpful in interpreting the literature.] Moe's method is probably the most popular one now. It is simple to program and permits calculation of profiles for any desired atmospheric model. (Refs. 16 and 17 contain results obtained by Moe's method.)

Moe's method consists of a different procedure for solving Unno's transfer equations for the Stokes parameters. Again, the line profile is assumed to be formed in LTE, and the magnetic field is assumed homogeneous over the region of line formation. The requirement of depth-independence of the absorption coefficients, however, is relaxed. The ratio of line to continuous absorption is represented as a product of a depth-dependent, wavelength-independent factor and a depth-independent, wavelength-dependent factor. The emergent intensities of the Stokes parameters I, Q, and V can then be written analytically and can be evaluated by numerical integration for a given model atmosphere. Numerical calculations are practical only for lines formed in pure absorption, although Moe indicates the form of the solution for scattering lines.

THE IRON LINE AT 5,250.216 Å

The iron line at 0.5250216 micrometer (5,250.216 Å) is often used for magnetograph field determinations. It has a strong triplet splitting and, in general, appears to conform with von Klüber's criteria for suitable lines for magnetic field measurements (Ref. 18).

Upon closer acquaintance, however, the line has revealed some unfavorable characteristics. It is a strong line with a low excitation potential and a large scattering component (Ref. 19). Detailed analysis is further complicated by the fact that the upper level of the line is split. Because the line is strong, it tends to saturate easily; this property has been suggested as the reason the line sometimes appears to have an "anomalous" Zeeman π-component (Refs. 20 and 21). The line is extremely temperature-sensitive, becoming stronger in regions of lower temperature (Ref. 22). Moreover, Moe has recently discovered a weak molecular line in the red wing of the profile, so the 0.5250216-micrometer (5,250.216 Å) line usually observed is actually a blend.

Some of the properties of the line are given in Table 5.

TABLE 5. PROPERTIES OF FE I λ5,250.216

Transition	$a^5D_0 - z^7D_1$	Ref. 10, p. 179
Lower and Upper Excitation Potentials	0.121 eV, 2.471 eV	Ref. 10, p. 179
Zeeman Pattern	$\underline{(0)\ 3}$	Ref. 10, p. 179
Lande g Value	3	Ref. 23, p. 382
*Log *gf* (g is statistical weight of lower level; *f* is oscillator strength for transition)	-4.46	Refs. 24 and 25
*Photospheric Fe Abundance	$\log\left(\frac{N_{Fe}}{N_H}\right) = -5.2$	Ref. 26

*The proper choice of abundance and *f*-values of iron is not yet established; other published values are as justifiable as those given here. (See, for example, Refs. 27, 28, and 29.) Fortunately, the *gf*-abundance product, which is the quantity needed for line profile calculations, is better known than either of its constituent factors.

PRELIMINARY DETERMINATION OF SUNSPOT MAGNETIC FIELD

For simple triplet splitting, the magnetic field strength along the line of sight can be derived immediately from

$$\Delta\lambda_H = \frac{eH}{4\pi m_e c^2} \lambda_0^2$$

where

$\Delta\lambda_H$ - separation of the π and σ Zeeman components, cm

λ_0 - undisturbed wavelength, cm

H - field strength, gauss

e - electron charge, e.s.u.

m_e - electron mass, g

c - speed of light, cm sec^{-1}.

A simple FORTRAN program has been written to calculate field strengths from the triplet splittings obtained from the spectral data. The results are field strength components, in gauss, along the line of sight. This solution gives no information about the field orientation and is limited to determination of field strengths large enough to produce resolvable Zeeman components. The field strengths will be required for calculating line profiles in the spot; they can also be used to construct a crude sunspot map of the projected field vectors.

The program is given in Figure 4; the results, in the form of a sunspot map, are given in Figure 5. Figure 5 is not drawn to scale. The length of a cell in the East-West direction represents approximately 1, 750 kilometers on the Sun. The length in the North-South direction

```
C     CALCULATE MAGNETIC FIELD STRENGTHS FOR TRIPLET SPLITTING
C     READ POSITIONS OF MINIMA ND ASSUME THESE ARE CENTERS OF COMPONENTS
      KPU= 2
      KPR= 3
      RFAD (KPU, 1) W, G
    1 FORMAT (F10.0, F5.0)
C     WAVELENGTH OF UNSHIFTED LINE IN ANGSTROMS, LANDE G VALUE
C     CONVERT W TO CM
      W= W*1.0E-8
    2 READ (KPU, 3) ID, XL, XC, XR
    3 FORMAT (I5, 5X, 3F10.0)
C     READ POSITIONS OF COMPONENTS IN DATA SPACING UNITS
C     IF A COMPONENT DOES NOT APPFAR, LEAVE IT OUT
C     IF ALL 3 COMPONENTS ARE PRESENT, ASSUME ZEEMAN SPLITTING IS
C     AVERAGE OF THE 2 VALUES THUS DETERMINED.
C     THIS PROGRAM ASSUMES AT LEAST 2 MINIMUM VALUES ARE READ FOR
C     EVERY LINE
      NXL= XL
      IF (NXL-0) 2, 5, 6
    5 DLH= (XR-XC)*5.88E-11
C     DLAMBDAH IN CM
      GO TO 10
    6 NXC= XC
      IF (NXC-0) 2, 7, 8
    7 DLH= (XR-XL)*2.94E-11
      GO TO 10
    8 NXR=XR
      IF (NXR-0) 2, 9, 11
    9 DLH= (XC-XL)*5.88E-11
      GO TO 10
   11 DLH=((XC-XL)+(XR-XC))*2.94E-11
   10 H= DLH/(4.67E-5*G*W*W)
      WRITE (KPR, 12) ID, H
   12 FORMAT (4H ID=,I5,10X,2HH=,E12.5,7H  GAUSS)
      GO TO 2
   13 CALL EXIT
      END
```

FIGURE 4. FIELD STRENGTH PROGRAM

SOUTH

	i	h	g	a	b	c	d	e	f
I									
II									
III			914	1,065	761	609			
IV	457	837	1,040	1,421	1,408				
V, VI	608	990	1,614	1,599	1,738	1,325	761		
VII, VIII	1,319	1,598	1,928	1,796	1,631	1,370			
IX, X	1,760	1,985	1,991	2,132	1,959	1,724			
XI	1,637	1,979	2,025	2,008	1,781	1,903			
XII	1,085	1,551	1,979	1,941	1,614	1,218			
XIII	1,066	1,243	1,040	1,446	761				
XIV	685	913	799	952	685				
XV			761						

EAST

NORTH

FIGURE 5. LINE-OF-SIGHT FIELD STRENGTHS IN GAUSS, OBSERVATIONS OF 14 JULY 1969

is approximately 175 kilometers on the Sun, and the separation of observations in the North-South direction is approximately 1500 kilometers. The Roman numerals along the left side of the figure and the lower case letters along the top are the labels of the observations corresponding to the plotted locations.

DETAILED MAGNETIC FIELD DETERMINATION

The complete determination of magnetic field strength and inclination can be summarized in a diagram (Figure 6). The three operations in the left-hand column (observations, determination of Zeeman splitting, and calculations of field strength components along the line of sight) have been completed. The remainder of the diagram is discussed below.

The dependence of the observed profile shapes upon the magnetic field configuration and upon the properties of the atmosphere is so complicated that the only practical way of determining the fields is to calculate line profiles for a number of magnetic field strengths and inclinations and compare these to the observed profiles. The initial field strength derivation can be used to obtain starting values for the field strength, and profiles can be calculated for a given strength at a number of different orientations. Most theoretical procedures assume homogeneous fields. This assumption is a limitation in principle but not in practice, since the spatial resolution of the observations is small. The observed profiles represent averages over an area on the Sun of approximately 175 by 1, 750 kilometers; they are averages over the depth range where the line is formed. The fields, therefore, could not be determined to smaller scale, even if the theory permitted it.

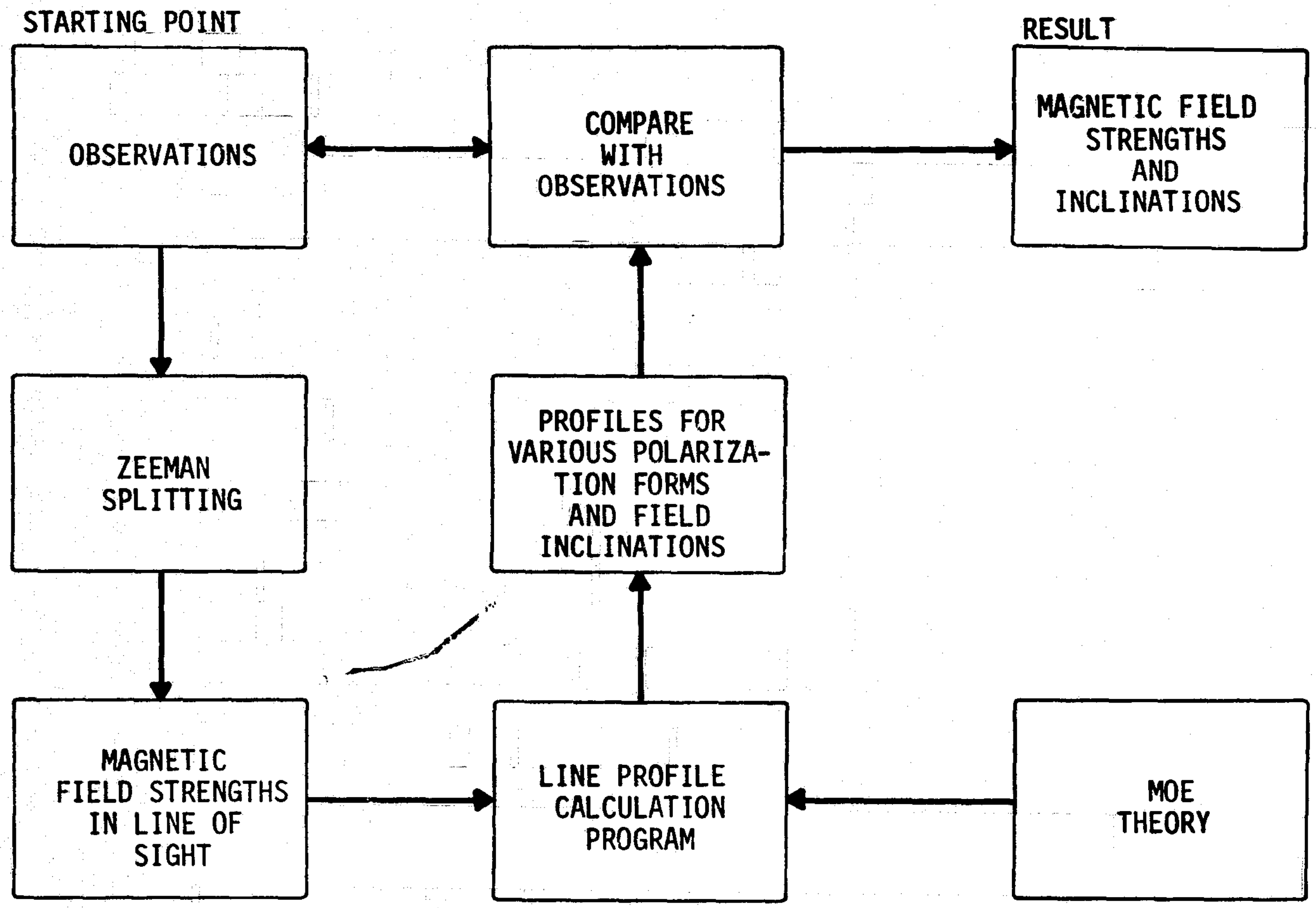

FIGURE 6. SUMMARY OF MAGNETIC FIELD CALCULATION

The solution consists of intensities of the Stokes parameters; these can be combined to yield calculated intensities corresponding to the five observed polarization forms. The calculated profiles can then be compared to the observations, and the field strengths and inclinations in the sunspot will be assumed to be those which yield the best matches to the observed profiles.

Because the theory is restricted to Zeeman triplets, this procedure cannot be used to derive field properties from lines with more complicated Zeeman patterns. Another line in the observed spectral region has a large triplet splitting: the neutral chromium line at 0.5247574 micrometer (5,247.574 Å), with Zeeman pattern $\frac{(0)\ 5}{2}$. The same analysis could be performed for this line. Because the chromium line has approximately the same strength as the iron line (and, therefore, forms at approximately the same depths), its analysis would serve as a check on the iron line calculations but would not provide information concerning the fields at different depths in the sunspot.

REFERENCES - SECTION 1

1. Brault, J. W., C. D. Slaughter, A. K. Pierce, and R. S. Aikens, Solar Physics, Vol. 18, p. 366, 1971

2. Transactions of the International Astronomical Union, Vol. 1, p. 35, 1922

3. Transactions of the International Astronomical Union, Vol. 11a, p. 97, 1961

4. Valero, F. P. J., Journal of the Optical Society of America, Vol. 58, p. 484, 1968

5. Valero, F. P. J., Journal of the Optical Society of America, Vol. 58, p. 1048, 1968

6. Giacchetti, A., R. W. Stanley, and R. Zalubas, Journal of the Optical Society of America, Vol. 60, p. 474, 1970

7. Edlén, B., Journal of the Optical Society of America, Vol. 43, p. 339, 1953

8. National Bureau of Standards Monograph No. 3, Table of Wavenumbers 2000Å to 7000Å, Vol. 1, 1960

9. Babcock, H. D., Astrophysical Journal, Vol. 111, p. 60, 1950

10. Bray, R. J. and R. E. Loughhead, Sunspots, Chapman and Hall Ltd., London, 1964 (Chapter 5)

11. von Klüber, H., "Spectroscopic Determinations of Solar Magnetic Fields", in Solar Physics, ed. J. Xanthakis, Interscience, 1967

12. Beckers, J. M., Solar Physics, Vol. 9, p. 372, 1969

13. Moe, O. K., Solar Physics, Vol. 4, p. 267, 1968

14. Beckers, J. M., Solar Physics, Vol. 10, p. 262, 1969

15. Staude, J., Solar Physics, Vol. 18, p. 24, 1971

16. Staude, J., Solar Physics, Vol. 12, p. 84, 1970

REFERENCES - SECTION 1 - Concluded

17. Staude, J., Solar Physics, Vol. 15, p. 102, 1970

18. von Klüber, H., Zeitschrif für Astrophysik, Vol. 24, p. 121, 1948

19. Obridko, V. N., Soviet Astronomy, AJ, Vol. 9, p. 398, 1965

20. Göhring, R., Solar Physics, Vol. 8, p. 271, 1969

21. Beckers, J. M. and E. H. Schröter, Solar Physics, Vol. 7, p. 22, 1969

22. Harvey, J. and W. Livingston, Solar Physics, Vol. 10, p. 283, 1969

23. Condon, E. U. and G. H. Shortley, The Theory of Atomic Spectra, Cambridge University Press, 1963

24. Corliss, C. H. and B. Warner, Astrophysical Journal Supplement Series, Vol. 8, p. 395, 1964

25. Bridges, J. M. and W. L. Wiese, Astrophysical Journal Letters, Vol. 161, p. L71, 1970

26. Withbroe, G. L., Solar Physics, Vol. 9, p. 19, 1969

27. Cowley, C., Astrophysical Letters, Vol. 5, p. 149, 1970

28. Wolnik, S. J., R. O. Berthel, and G. W. Wares, Astrophysical Journal, Vol. 162, p. 1037, 1970

29. Ross, J. E., Nature, Vol. 225, p. 610, 1970

SECTION 2

TOPICS RELATED TO MAGNETOGRAPH OPERATION

TABLE OF CONTENTS

LIST OF ILLUSTRATIONS

LIST OF TABLES

INTRODUCTION

The results of several studies of factors related to the practical use of solar magnetographs are collected in this section. Special emphasis is placed on uncertainties in the observed quantities and in their interpretation. The work reported was done between October 1971 and June 1973.

Several factors which influence magnetograph operation are discussed in this section, with special attention being given to uncertainties in the final results. A preliminary error estimate of ±20 percent is suggested as a reasonable value on the basis of experience with other systems.

The spectral line for which the Marshall Space Flight Center (MSFC) magnetograph was designed is shown to possess a number of disadvantages. Line profiles in sunspots cannot be calculated for this line, even approximately; the height of formation in the solar atmosphere is not known; and the strength of the line changes significantly for different regions on the solar disk. These disadvantages are largely a consequence of the fact that the line in question, λ5250.216 of neutral iron, has a very low excitation potential (e.p. = 0.121 electron volt for lower level). A number of Zeeman triplet lines have lower excitation potentials of 2.0 electron volts or higher, and these lines would show these disadvantages to a much smaller degree. It is therefore recommended that serious consideration be given to choosing a new line of higher excitation as an alternative magnetograph line. Such a line also would be more likely to be observable at higher temperatures than those prevailing in sunspots and might permit the magnetograph to be used for study of magnetic stars.

PROPERTIES OF THE NEUTRAL IRON LINE, λ5250.216

The MSFC Real Time Solar Magnetograph was designed to measure the degree of polarization in the neutral iron line at 525.0216 nanometers (5250.216 angstroms). This line has a lower-level excitation potential of 0.121 electron volt; the central intensity in the photosphere as shown in the Utrecht Atlas is 0.39 (Ref. 1); the equivalent width in Moore, Minnaert, and Houtgast's table of solar spectrum wavelengths is 62 milliangstroms (Ref. 2). The line is strengthened in sunspots. In a magnetic field, it shows a triplet Zeeman pattern with a strong splitting of about 4 milliangstroms per 100 gauss of field. The properties of the line are summarized in Table 1.

The very low excitation potential of the lower level suggests that the line has a strong scattering component. That suggestion is supported by observations which show that the strength of the profile does not vary greatly with position on the solar disk; such behavior is characteristic of scattering lines. Therefore, a valid theoretical treatment must consider both the absorption and scattering mechanisms.

Although a scattering matrix for the line has been derived (Ref. 3), the detailed calculation of a scattering line profile is very complicated. Obridko has done a calculation for a simple case (Ref. 4), but treatment of scattering alone using a realistic sunspot model is not yet practical. A calculation combining the effects of absorption and scattering for a realistic sunspot model is even more difficult.

For this reason, most calculations of λ5250 profiles assume pure absorption. Some recently published calculations of λ5250 profiles and of other profiles in sunspots are listed in Table 2.

TABLE 1. PROPERTIES OF Fe I λ5250.216

Transition	$a^5 D_0 - z^7 D_1$
Lower and Upper Excitation Potentials (eV)	0.121, 2.471
Zeeman Pattern	$\frac{(0)\ 3}{1}$
Landē g Value	3
Log gf (g is statistical weight of lower level; f is oscillator strength for transition)*	-4.46
Photospheric Iron Abundance*	$\log \left(\frac{N_{Fe}}{N_H}\right) = -5.2$

*The proper choice of abundance and f-values of iron is not yet established; other published values are as justifiable as those given here. The gf-abundance product is better known than either of its constituent factors.

TABLE 2. LINE PROFILE CALCULATIONS IN SUNSPOTS

AUTHOR	SPECTRAL LINE	SUNSPOT MODEL	PHOTOSPHERIC MODEL	REFERENCE
Moe and Maltby	λ5250.2		Holweger	5
Hénoux	Na D, Mg b (wings)	Hénoux		6
Hénoux	Weak to medium Fe I, Fe II, Cr I, Cr II, Ti I, Ti II	Hénoux		6
Yun	Na D (wings)	Yun		7
Beckers	λ5250.2		Bilderberg Continuum Atmosphere	8
Göhring	λ5250.2		Arbitrary η_0	9
Göhring	λ5250.2		Holweger	9
Moe	λ5250.2		Combination of Müller-Mutschlecner and Goldberg	10
Staude	λ5250.2	Hénoux		11

Although some of this work was elaborate, only one author, Staude, has published profiles of λ5250.2 calculated with a sunspot model. (Moe states that he has succeeded in making a similar calculation but has published no results.) As will be shown later, the profiles calculated in sunspots do not appear to be valid.

In sunspot spectra, a weak line of titanium oxide is blended with the red wing of λ5250, and this blend should be considered in a precise profile calculation. Each line modifies the radiation field seen by the other, and a rigorous approach requires that the source functions for both lines be modified correspondingly. Since in this case the strengths of the lines are so different, it is probably acceptable to assume that the titanium oxide line has negligible effect on the source function for the iron line and that the titanium oxide line is so weak that the effect of the modification of its source function by the iron line would be found to be of the order of the observational uncertainty or smaller. Then the separate profiles can simply be superimposed; the residual intensity for the combined line will be given by:

$$R(\lambda)_{Fe+TiO} = R(\lambda)_{Fe} - [1.00 - R(\lambda)_{TiO}]. \qquad (1)$$

No blend calculations, even on this level of approximation, have been published. Moe has calculated but not published sunspot profiles for λ5250 in which he treated the presence of blends by adjusting the continuum level. His reasoning is that the apparent continuum under the conditions prevailing in sunspots is likely to be crowded with weak, unresolved molecular lines. This approach yields profiles which agree well with observations, but the physical validity of the argument is questionable. Moreover, it will be shown that in this case the fact that calculated profiles agree with observations is not sufficient evidence that the calculation is correct.

The low excitation potential of the lower level of the line causes the absorption coefficient to be sensitive to the temperature and electron pressure in the model atmosphere. Figure 1 shows the fraction of iron atoms in the lower level as a function of depth in the sunspot model atmosphere (the model is that of Hénoux, Ref. 6). The top curve in the figure, marked by triangles, is the relation for λ5250. The lower curve, shown for reference, is the corresponding set of values for the neutral iron line at 617.3348 nanometers. This line has a lower excitation potential of 2.213 electron volts (Ref. 12); it is used for comparison because self-consistent profiles can be calculated for it in sunspots. The number of atoms capable of absorbing λ6173 decreases by about a factor of ten with increasing height in the atmosphere, but the number for λ5250 is nearly constant over most of the range and is close to its peak value at the top of the atmosphere. [The N_i values were calculated using the Boltzmann and Saha equations, assuming that iron could exist in neutral and singly-ionized forms; this calculation, of course, implicitly assumes the atmosphere is in local thermodynamic equilibrium (LTE).]

Figure 2 shows η_λ, the ratio of line-to-continuous absorption coefficients, as a function of depth in the Hénoux model atmosphere. Again, the triangles are used to signify λ5250 and circles to signify λ6173. The η_λ values for both lines rise sharply toward the top of the atmospheric model, primarily because the opacities fall rapidly over the same range. The effect of the increase in η_λ is much more serious for λ5250 because of the different line absorption coefficients for the two lines; the coefficient for λ6173 is much smaller at the top of the atmosphere, compared both to its own peak value and to the values for λ5250. The coefficient for λ5250 declines more slowly with height and has a much larger average value. Figure 2 also

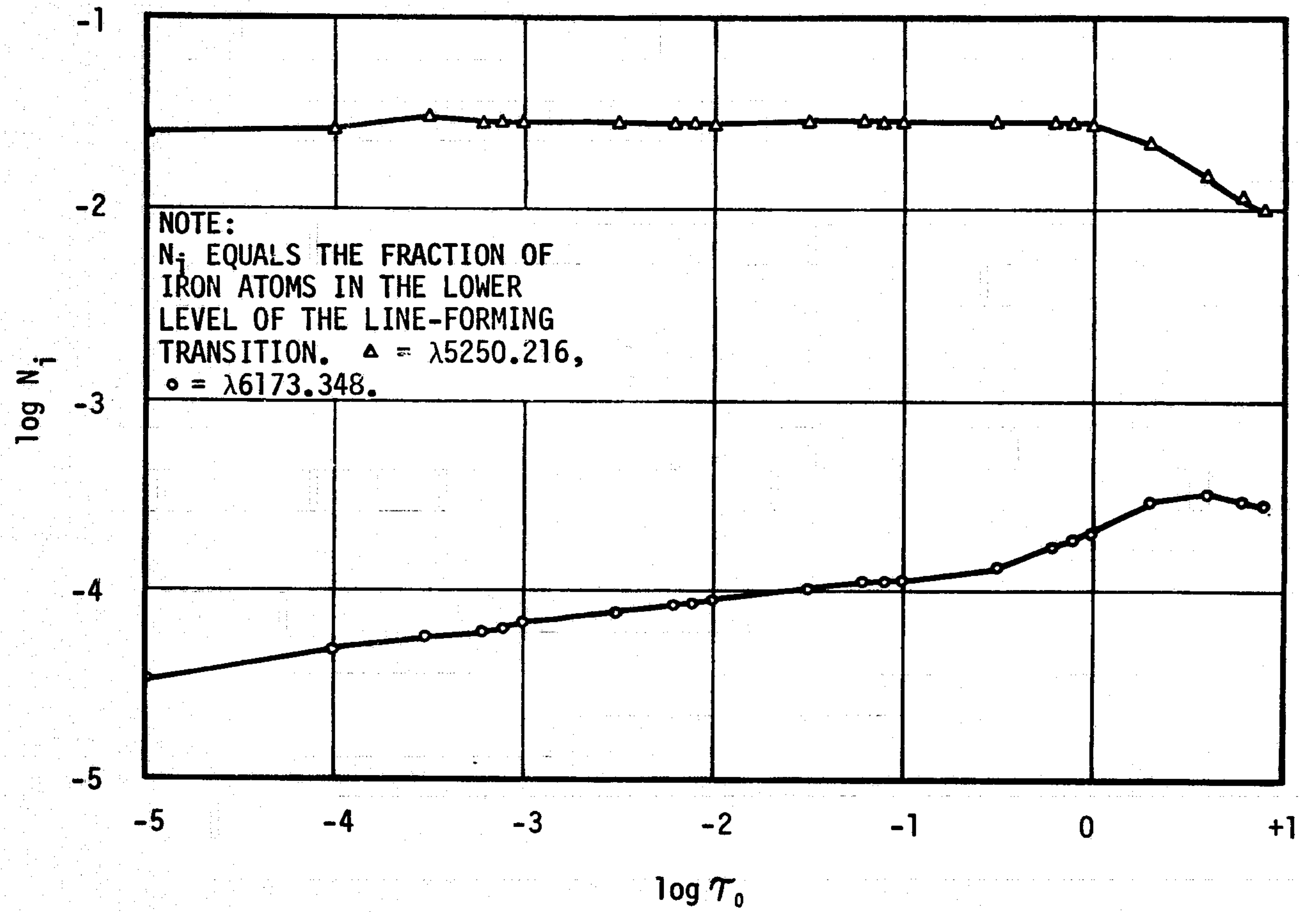

FIGURE 1. DEPTH DEPENDENCE OF LOG N_i

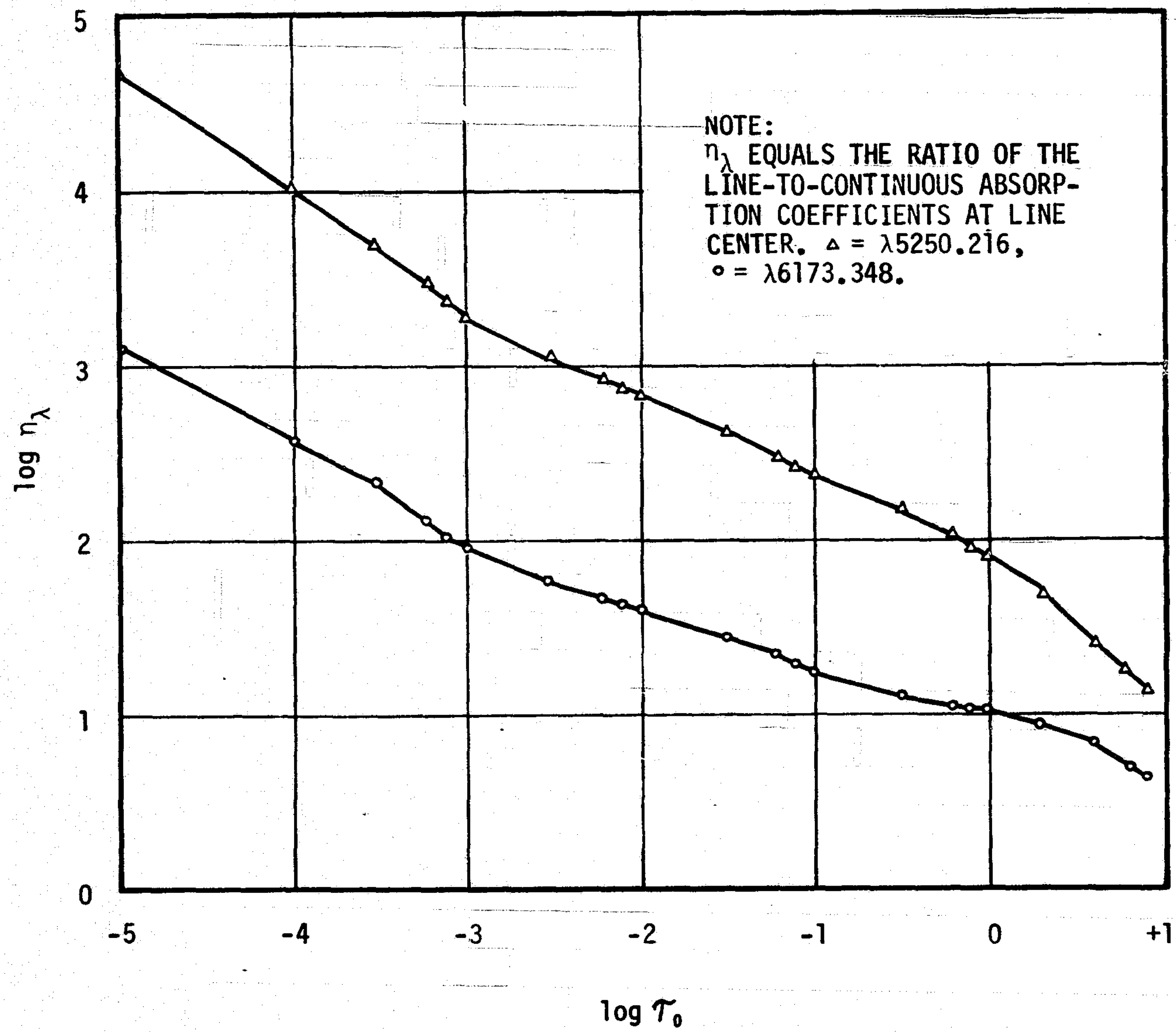

FIGURE 2. DEPTH DEPENDENCE OF LOG η_λ

provides the reason why Moe's addition of continuous absorption improved the appearance of his calculated profiles without correcting the fundamental difficulty: adding continuous absorption will reduce the ordinate values of the curves of Figure 2, but the values of the line absorption coefficients also are important to the result, and they are unchanged by the addition of continuous absorption.

When combined, these effects are sufficient to make impossible a self-consistent LTE profile calculation of λ5250 in sunspots. The residual intensities, R_λ, may be evaluated by direct integration of

$$R_\lambda = \frac{1}{I_\lambda^c} \int_0^\infty B_\lambda (t_\lambda) \exp^{-t_\lambda/\mu} \frac{dt_\lambda}{\mu} \tag{2}$$

where

$$t_\lambda = \int_0^{\tau_\lambda} (1 + \eta_\lambda)\, d\tau_\lambda$$

and

$B_\lambda\ (t_\lambda)$ - source function (here, the Planck function)

t_λ - optical depth in the line at wavelength λ

τ_λ - optical depth in the continuum at wavelength λ ($\tau_0 = \tau_\lambda \doteq 500$ nanometers)

I_λ^c - continuum intensity at wavelength λ and position on the solar disk given by $\mu = \cos\ \theta$

η_λ - ratio of line-to-continuous absorption at wavelength λ .

The calculations were done at the disk center ($\mu = 1.00$) for zero magnetic field. (The addition of a magnetic field will not affect the derived contribution relation, since the line-to-continuous absorption ratio for circularly polarized light in a longitudinal magnetic field is equal to the value in the zero field case.) The f-values were taken from Corliss and Warner (Ref. 13). The iron abundance ($\log_{10} N_{Fe}/N_H$) was set equal to -5.20 (Ref. 14). The microturbulent velocity in the sunspot was assumed to be constant with depth and equal to 1.0 kilometers per second.

The contributions of the various depths to the emergent intensity are displayed in Figure 3 by plotting the differences, $\Delta R_\lambda/\Delta(\log_{10} \tau_0)$, as a function of $\log_{10} \tau_0$; the ΔR_λ values were obtained from the integration of Equation (2). The $\Delta(\log_{10} \tau_0)$ intervals in each case are the depth intervals at which the Hénoux model is tabulated; the differences are plotted at the centers of their depth intervals.

As Figure 3 shows, the intensity contribution to λ5250 is at its maximum at the top of the model, with the peak value being undefined. Integration of these values over depth clearly will not yield a completely defined emergent intensity. On the other hand, the contributions to λ6173 are essentially all within the depth range of the model, so the residual intensity obtained by integrating those values over depth can be considered to be significant.

For photospheric conditions, the temperatures and electron pressures are high enough that the number of atoms in the lower level of the λ5250 transition is reduced, and self-consistent LTE profiles can be calculated. The λ5250 profiles calculated for photospheric models are therefore valid insofar as their underlying assumptions are valid. However, it does not seem reasonable to expect that profiles

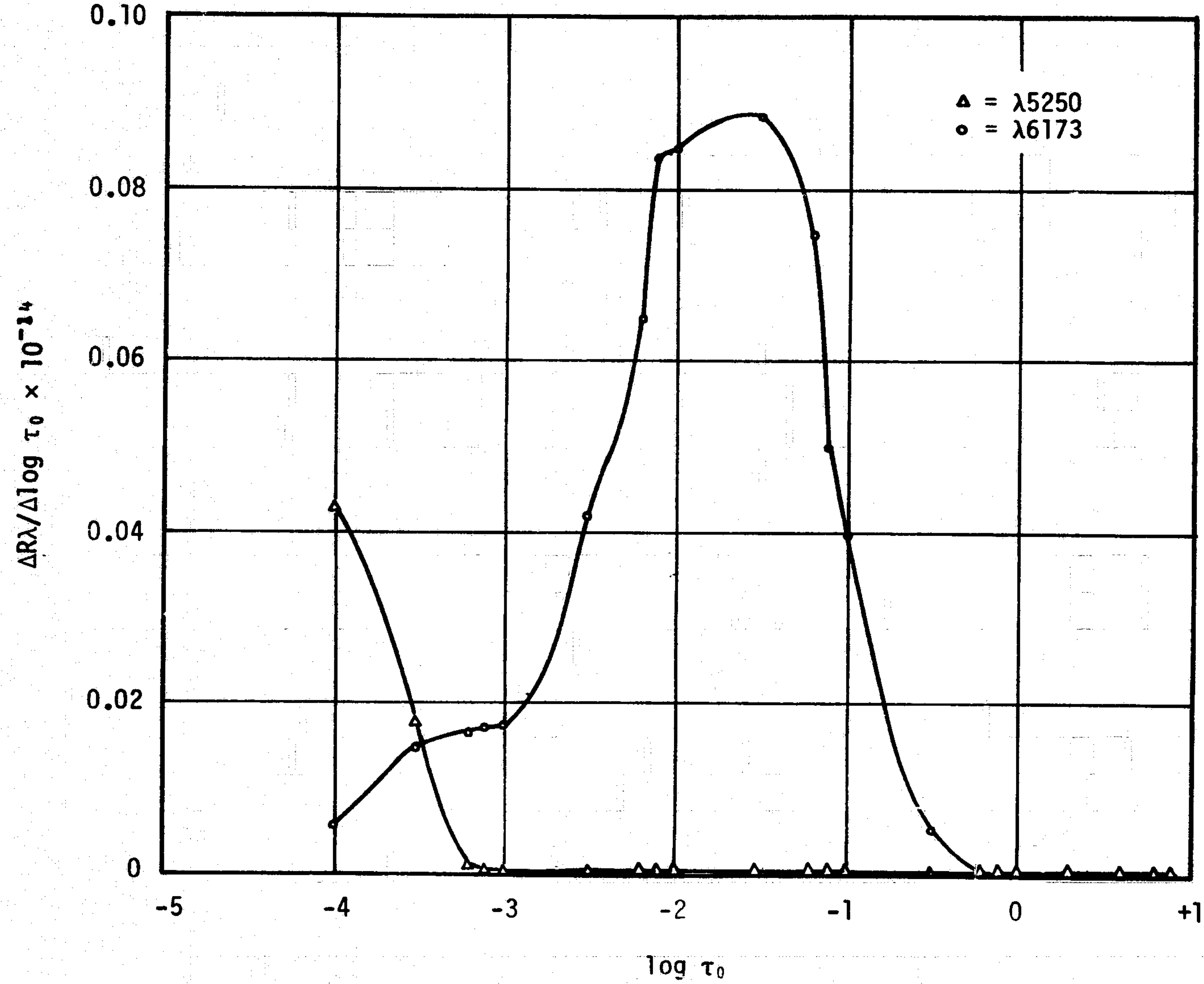

FIGURE 3. CONTRIBUTIONS OF DEPTHS IN THE HÉNOUX ATMOSPHERE TO EMERGENT INTENSITY IN λ5250 and λ6173

calculated for photospheric models will also be representative of sunspot conditions, and they therefore should not be used to interpret sunspot observations. (In practice, most magnetographs which use the $\lambda 5250$ line and depend on calibration from calculated profiles were calibrated using profiles calculated with photospheric models.)

Because $\lambda 5250$ is quite strong in sunspots, its profile is often saturated. When saturated profiles in different polarization states are superimposed, the intensity distribution of the combination may appear quite different from the distributions in the separate components. Often, in fact, the combination appears to have a spurious Π component, usually shifted somewhat from the normal position (Refs. 5, 9, 11, 15, and 16). This so-called "anomalous Π component" further complicates the analysis of $\lambda 5250$ observations.

Another source of complication of the theoretical treatment of $\lambda 5250$ is the effect of polarization of the atomic sublevels involved in the transition. If the splitting in a magnetic field is not complete, so that different sublevels overlap, then the sublevels are not independent, and phase relations exist between their wave functions. This interference between sublevels is called "level-crossing interference". The Hanle effect is an example of level-crossing interference.

The sublevel polarization is distinct from the polarization introduced by the Zeeman splitting. An unusually brief and clear description of the various sources of polarization has been given by Lamb (Ref. 17); it is quoted in the following paragraph.

> The polarization of light in solar absorption and emission lines may result from the action of one or more of three distinct processes. First, in the presence of a magnetic field the light in absorption or

emission lines may become partially polarized simply as the result of Zeeman splitting. Although the radiation absorbed or emitted at each frequency in the line by an assembly of atoms is then at least partially polarized, if atomic level polarization does not accompany the Zeeman splitting and if the assembly is optically thin in the line the total radiation absorbed or emitted, when integrated in frequency over the whole of the line, will be isotropic and unpolarized (one speaks of no "net" polarization of the line). Second, the light in Zeeman split absorption or emission lines formed in an assembly which is not optically thin may show a different partial polarization at each frequency from that of an optically thin assembly. Even in the absence of atomic level polarization, this phenomenon usually leads to net polarization of the light in the line. Finally, light in absorption or emission lines may become polarized as a result of the polarization of one or both of the atomic levels involved in the formation of the line, since in this case the assembly will preferentially absorb, emit, and scatter radiation of a particular polarization and angular distribution in radiative processes beginning at each of the polarized levels. Generally speaking, atomic level polarization leads to net polarization of the light in the line, whether or not the line also undergoes Zeeman splitting or the assembly is optically thin.

The study of these effects is still in its infancy; both Lamb and L. L. House have been working actively in this field (see Ref. 18, for example). A fairly complete analysis can be done only for certain simple resonance lines. The sublevel structure of λ5250 is far too complicated to permit an analysis of that transition with the techniques now in use. It should be observed, however, that Lamb (Ref. 17, p. 159) has estimated from collisional relaxation rates that "at photospheric densities the energy 'overlap' of states within the same atomic level will not be significant [for λ5250] when the magnetic field strength is greater than 10^2 G." Presumably, level-crossing interference also will be unimportant for lines formed in the lower depths of sunspots. For lines formed at greater heights, however, level-crossing interference may become important. The exact height of formation of $\lambda 5250$ is uncertain, but it probably is formed in the upper photosphere. Therefore, the possibility of the existence of level-crossing interference in this line cannot yet be eliminated.

ALTERNATIVE SPECTRAL LINES FOR MAGNETOGRAPH OPERATION

Because a theoretical calibration from calculated sunspot profiles for λ5250 cannot now be accomplished, it may be advantageous to consider adopting another spectral line for magnetograph operation. With this in mind, a number of Zeeman triplet lines within about 200 angstroms on either side of λ5250 were examined for suitability as magnetograph lines. The results of this preliminary study are summarized in Table 3. The lines were first checked for the presence of blends, using the photospheric tracings in the Utrecht Atlas (Ref. 1) and a photographic sunspot spectrum borrowed from the Kitt Peak National Observatory. The lines which did not appear to be badly blended in those two references were investigated further. In Table 3, "UA" signifies Utrecht Atlas; "KPNO", the Kitt Peak photographic spectra; and "MMH", the Moore, Minnaert, and Houtgast solar wavelength table (Ref. 2). The spectral line identifications in this last reference are useful for detecting and identifying blends.

It must be emphasized that probably no strong line can be found to be entirely free of blends in sunspots because of the large number of molecular lines which can form under these conditions. The presence of weak blended lines therefore cannot disqualify a spectral line for magnetograph use.

Spectral lines at greater distances from λ5250 also might be considered. Some interest now exists in the polarization of lines in the near infrared (Ref. 19), but these would not be suitable for use in a magnetograph located near sea level because of the strong telluric absorption by water vapor at long wavelengths. Harvey (Ref. 20) has published a list of lines with large Zeeman splittings, which could be

TABLE 3. PRELIMINARY SURVEY OF SPECTRAL LINES NEAR 5200 ANGSTROMS

WAVELENGTH (Å)	RESULT OF BLEND STUDY	CONCLUSION
5082.351 (NiI, multiplet number 130)	KPNO and UA spectra suggest blends are not serious; according to MMH, it may be blended in the wings with lines of C_2 and MgH • $g\lambda^2 = 39 \times 10^{-10}$ cm^2 (von Klüber) • Transition: z $^3P^o_1$ - e $^3P_1$ • Excitation potential of lower level = 3.642 electron volts • According to von Klüber, line is weakened in sunspots	Probably best avoided because of small splitting and weakness in sunspots
5145.104	Both KPNO and UA spectra show serious blends	Not usable
5202.351	KPNO spectrum shows serious blend, confirmed by MMH	Not usable
5215.190 (FeI, multiplet number 553)	UA spectrum shows blend in red wing; continuum is depressed in this region. • Transition: z $^5D^o_2$ - e $^5D_1$ • Excitation potential of lower level = 3.26 electron volts	Not usable
5217.398 (FeI, multiplet number 553)	Profile looks fairly clean in UA and KPNO spectra; MMH suggests possible blend • $g\lambda^2 = 41 \times 10^{-10}$ cm^2 • Transition: z $^5D^o_4$ - e $^5D_3$ • Excitation potential of lower level = 3.197 electron volts	Probably could be used but is not a good choice because of small splitting (see entry for λ5263)
5229.862 (FeI, multiplet numbers 553, 1090)	Profile looks clean in UA but KPNO spectrum shows possible blend in red wing • $g\lambda^2 = 41 \times 10^{-10}$ cm^2 • Transition: z $^5D^o_1$ - e $^5D_0$ • Excitation potential of lower level = 3.269 electron volts	Probably could be used but is not a good choice because of small splitting (see entry for λ5263)
5247.576 (CrI, multiplet number 18)	• $g\lambda^2 = 69 \times 10^{-10}$ cm^2 • Transition: a $^5D_0$ - z $^5P^o_1$ • Excitation potential of lower level = 0.957 electron volts This line, like λ5250, would be an excellent magnetograph line if it had a higher excitation potential. Attempts to calculate absorption profiles for sunspot models have shown that a profile cannot be defined for the same reasons that profiles are not defined for λ5250.	This line has no advantages over λ5250

TABLE 3 - Concluded

WAVELENGTH (A°)	RESULT OF BLEND STUDY	CONCLUSION
5253.470 (FeI, multiplet number 553)	Appearance of profile is good in UA and KPNO spectra; MMH shows blends with two faint lines • $g\lambda^2 = 41 \times 10^{-10}$ cm² • Transition: $z\ ^5D^o_1 - e\ ^5D_1$ • Excitation potential of lower level = 3.27 electron volts Zeeman splitting is not detectable in the KPNO spectrum. For a field of 2000 gauss, the value of $\Delta\lambda_H$ should be about 38 milliangstroms, compared to about 90 milliangstrom for λ6173 for about the same field strength. If a $\Delta\lambda_H$ as small as 2.5 milliangstroms could be resolved, the lower limit on measurable field strength would be about 130 gauss.	Splitting may be too small for line to be a good choice. It is probably usable.
5263.316	Appears badly blended in UA and KPNO spectra	Not usable
5273.172	Appears badly blended in UA and KPNO spectra	Not usable
5283.631	Appears badly blended in UA and KPNO spectra	Not usable
5302.309 (FeI, multiplet number 553)	Profile looks clean in UA but KPNO spectrum appears blended • $g\lambda^2 = 42 \times 10^{-10}$ cm² • Transition: $z\ ^5D^o_1 - e\ ^5D_2$ • Excitation potential of lower level = 3.269 electron volts	Not usable because of conspicuous blend in sunspots and small splitting
5324.193 (FeI, multiplet number 553)	Profile looks clean in UA but appears to be blended with a weak line, possibly Cr I, in KPNO • $g\lambda^2 = 42.5 \times 10^{-10}$ cm² • Transition: $z\ ^5D^o_4 - e\ ^5D_4$ • Excitation potential of lower level = 3.20 electron volts For a field of 2000 gauss, $\Delta\lambda_H$ = 39.6 milliangstroms	Probably usable. (This is the line used by the Aerospace Corporation magnetograph.)
5339.939	Profile looks blended in both UA and KPNO spectra	Not usable
5393.178 (FeI, multiplet number 553)	Profile looks blended in both UA and KPNO spectra, confirmed by MMH	Not usable

examined. Zwaan and Buurman have compiled a list of sunspot lines which are very weak in the photosphere and which therefore should not be distorted in shape by the effects of stray light. This list does not appear to have been published. One of the lines listed, according to Reference 21, is λ6064.626 of neutral titanium. Another relevant reference is Reference 22, in which Wittmann reports the results of examining a number of red lines for the presence of blends. This material would form a starting point for a more extensive search of the solar spectrum.

SOURCES OF ERROR FOR SOLAR MAGNETOGRAPH

EFFECTS WHICH DEPEND SOLELY ON POSITION ON THE SOLAR DISK

As is well known, the radiation observed at the center of the solar disk characterizes a greater range in depth than that observed at the limb. A crude numerical estimate of this effect can be made by using the Eddington-Barbier relation,

$$\tau_\theta \simeq \cos\theta = \mu \quad ,$$

where τ_θ represents the maximum optical depth in the solar atmosphere which can be observed at solar position angle θ.

Since the geometrical depth, d, in the atmosphere is approximately proportional to the log of the optical depth,

$$d_{ph} \simeq K_{ph} \log \tau_{ph}$$

$$d_{pe} \simeq K_{pe} \log \tau_{pe}$$

$$d_u \simeq K_u \log \tau_u \quad ,$$

where

ph - photosphere

pe - penumbra

u - umbra.

In general,

$$K_{ph} \neq K_{pe} \neq K_u$$

and

$$d_{ph} \neq d_{pe} \neq d_u \quad .$$

The approximate form of the relation between d and μ across the solar disk can be shown by letting K = 1. The zero point in the geometrical depth scale is arbitrary; here it has been chosen so that d = 1 at μ = 1, which is the deepest level observed.

μ	d	
1.00	1.00	↑
0.90	0.955	
0.80	0.903	
0.70	0.846	
0.60	0.779	Increasing depth
0.50	0.700	
0.40	0.603	
0.30	0.478	
0.20	0.301	
0.10	0.000	

Thus, for a given solar feature the depth observed at μ = 0.5 will be about 0.7 of that observed at μ = 1. This property can be very useful, since it allows a partial determination of the variation of observable quantities with depth in the Sun.

Foreshortening toward the limb will tend to decrease the spatial resolution of the observations. The magnetograph aperture has a projected size of about 5 minutes of arc square, at the distance of the Sun from the Earth. The aperture will accept a distance on the Sun at the center of the disk of 2.17×10^5 kilometers. If the aperture is placed so that its outer edge is just at the limb, the linear distance it subtends on the Sun becomes 5.84×10^5 kilometers, or more than two and one-half times as large as at the disk center.

Finally, any observation using line profiles will be affected to some extent by the tendency of profiles to broaden and flatten toward the solar limb. This tendency should not be reflected in the degree of polarization in the profile, so the effect for a polarization magnetograph will be mostly that of reducing the signal level somewhat, since both the brightness of the Sun and the depth of the line profile, which provides contrast, are reduced. The "limb darkening" is observed to be smaller in the umbrae of sunspots than in the photosphere; the photospheric and penumbral limb darkening are approximately the same.

EFFECTS CAUSED BY CHANGES IN STRENGTH AND SHAPE OF LINE PROFILE

One assumption which is implicit in the entire magnetograph design and operation is that the line absorption coefficient in each of the Stokes parameters is identical to the line absorption coefficient in the absence of a magnetic field, although it may be shifted in wavelength by an amount which corresponds to the Zeeman splitting. Knowledge of the form of the line absorption coefficient is, in principle, sufficient to determine the shape and strength of the line profile corresponding to a transition between known levels in a model atmosphere of known properties; therefore, the interpretation of the magnetograph results can be derived from the properties of the line profile thus determined. It follows that anything which alters the shape or strength of the line profile on the Sun will affect the interpretation of the magnetograph measurements.

The profile of $\lambda 5250.216$ is particularly susceptible to alteration by varying local conditions on the Sun. Since determining and using a separate magnetograph calibration for each of these local areas is difficult, an average calibration usually is used. The local variations will then result in errors when the average calibration is used to interpret results in the variant regions.

The local variations can be dependent on time and on position of the solar disk. They also vary in magnitude. A quantitative estimate of their effects is almost impossible to achieve, but qualitative descriptions can be given.

The effect on line profiles of motion of the solar gas is well known. If the scale of the motion is small compared to the range of depths over which the lines are formed (microturbulence), the line profile is broadened and its equivalent width is increased. If the scale of the motion is large compared to the range of line-formation depths (macroturbulence), the profile is broadened but its equivalent width is unchanged. Large-scale motions may also shift the entire profile in wavelength or cause it to become asymmetrical. The turbulence effects depend upon position on the solar disk: the profiles tend to broaden and flatten toward the limb.

The normal variation toward the limb can be determined and compensated for in the reduction and analysis. (If it is not compensated, errors of residual intensity of 0.10 or more -- 10 percent of the continuum value -- can result.) In a system which uses a filter to isolate the line, and does not have an entrance slit, shifts of the entire profile must be compensated in that way also. Most of the uncompensable error will come from undetected asymmetries and from unresolved random motions in umbrae, penumbrae, and active regions. The uncompensable errors in residual intensity in each Stokes parameter probably will be less than 0.05; the relative error in each measurement, of course, will depend upon the part of the profile in which the measurement is made. Since the average degree of circular polarization, P_V, is found by combining signals measured in two different polarization states, and since both signals may contain errors which are comparable in absolute value and partially interdependent, the resulting error in P_V cannot be estimated for a general case. Wiehr (Ref. 23) discusses errors caused by miscentering of the line profile in the original polarimeter designs used at the Crimea observatory and at the Locarno station of the Göttingen observatory; these errors can be very large.

Of the spectral lines used for magnetic field determinations, λ5250.2 shows some of the largest natural variations in strength. The line has moderate strength in the photosphere; it is stronger in sunspots and weaker in photospheric magnetic regions. Chapman and Sheeley (Ref. 24) give the photospheric equivalent width as 62 milliangstroms; the equivalent width they measured in photospheric magnetic regions is 27 percent smaller. The equivalent width in sunspots is difficult to determine because the spot spectra are usually contaminated by stray light, and no reliable estimate has been found.

The strength variations are thought to be caused partly by temperature effects and partly by magnetic saturation (Refs. 24, 25, and 26); the temperature effects appear to be confined to the line cores. Whatever the cause, the variations in profile strength have been responsible for discrepancies between magnetograph results obtained with λ5250 and with other lines. Usually, the calibration for λ5250 is based on an "average" profile for the solar disk and thus cannot account for the strength variations. Harvey and Livingston (Ref. 27) found that the fields they measured using λ5250 appeared to underestimate the true field strength by a factor of about 2 in the linear portion of the profile and about 5 near the line core; Chapman and Sheeley (Ref. 24) have estimated that a calibration using an average disk profile of λ5250 will yield magnetic field strengths which are too low by a factor of 1.5 to 2; and measurements made with molecular lines also differ consistently from the λ5250 values (Ref. 28).

Therefore, calibrations based only on disk-average profiles of λ5250 generally appear to yield estimates of magnetic field strength which are much too low. Some supplementary information is needed. Indeed, Harvey et al (Ref. 25) now use data from λ5233 to establish the average field strength in the areas they observe, and use the λ5250 observations to provide finer detail.

ERRORS WHICH ORIGINATE WITHIN THE TELESCOPE AND THE MAGNETOGRAPH

The magnitudes of errors arising within the magnetograph and the telescope will be determined by making measurements of auxiliary sources or solar regions whose characteristics are known. Although a complete description of the errors cannot be made until that has been done, a general review of some of the possible sources of error can be given here.

The magnetograph contains a flat glass plate to be used to compensate for residual polarization introduced by the telescope. Even after this compensation has been made, a careful check should be made for residual polarization in all modes to be measured, because residual polarization is very difficult to remove completely. Furthermore, if any residual polarization can be measured, it may be possible to remove its effect in the data analysis. Residual polarization studies should be made for a number of different source intensities and telescope orientations.

One of the chronic difficulties experienced with umbral and penumbral observations is contamination of the fainter solar intensities by stray light from brighter regions. The scattering processes which redistribute the light occur in the Earth's atmosphere and within the telescope. The net polarization produced by the atmospheric scattering should be negligible, but the redistribution of light at the telescope optical surfaces may introduce a net polarization. Thus, a small polarized component of stray light may exist which would tend to distort the relative intensities measured in different polarization states. This component, if present, would probably be essentially linear and therefore less serious for the circular polarization measurements. Nevertheless, it is a possibility that should be examined, since such polarized stray light might cause an appreciable distortion if the signal level is very low.

A more serious possibility is that of intercommunication or "crosstalk" between signals. If, for example, some fraction of unpolarized intensity is mixed with a circularly polarized component, a sizable error can result. Instruments which use electrically switched polarizing crystals are subject to this type of signal leakage, so the possibility of its existence should be examined (see, for example, Reference 25).

ERRORS CAUSED BY LIMITED RESOLUTION

The Cassegrain telescope to which the magnetograph is attached has a diameter of about 30.5 centimeters. The corresponding Rayleigh criterion value at $\lambda = 5250$ angstroms is 0.43 second of arc; this will be assumed to be the diffraction-limited spatial resolution of the telescope. The design goal for the magnetograph optics is a spatial resolution of 2.5 seconds of arc for the 5-by-5 minute of arc field size, and

1 second of arc for the 2-by-2 minute field size obtained with the magnification system (Ref. 29, p. 2-11). The resolution values 1 or 2.5 seconds thus represent the best possible performance of the system; the resolution may be further limited by atmospheric seeing.

The typical daylight seeing values at the telescope tower have not yet been completely determined; in most locations, however, 1 second of arc is considered excellent, and 2 seconds or more are more usual (Ref. 12, p. 19). Moreover, the seeing usually varies rapidly with time, even on the best days, so an observation of more than a few seconds in length probably will show distortion. A reasonable prediction would be that on average days, observations made with the 5-minute field size should not be severely seeing-limited; the full resolution of the 2-minute field will be attained only at times of exceptionally good seeing.

Good spatial resolution is required for precise mapping of magnetic fields on the Sun. (A really fine discrimination of position is not possible from the Earth, since here an angle of 1 second of arc corresponds to a linear distance of about 725 kilometers at the center of the solar disk.) Spatial resolution is also important because the Sun shows many surface inhomogeneities of sizes near the limit of resolution or smaller. At maximum resolution, the smearing of these inhomogeneities will be smallest, and the resulting distortions of the observations will be minimized. Several of these inhomogeneities are briefly described below:

- Umbral dots are small, bright transient regions which appear in sunspot umbrae. The mean diameter of the dots measured by Beckers and Schröter (Ref. 30) was 420 kilometers (about 0.6 second of arc); the mean lifetime was 1500 seconds. (The lifetime was defined as the time between the occurrence of half-maximum brightness in the increase and decrease of the dot's intensity.) Umbral dots may be associated with inhomogeneities in the umbral magnetic field.

- Penumbral filaments (Ref. 12, p. 75) are irregular, elongated bright regions in the penumbra. The lengths of the filaments vary a good deal; a representative value for large spots is about 10 seconds of arc. Their lifetimes are of the order of a few hours, so a prominent penumbral filament in an observed region probably would be noticed.

- Magnetic knots are small regions in the photosphere which are characterized by unusually strong magnetic fields (Ref. 31). The strengths of many spectral lines, including $\lambda 5250$, decrease in these regions. A typical field strength is 1000 gauss; diameters are about 1000 kilometers. Lifetimes of knots are greater than 30 minutes.

- Pores are small sunspots with no penumbrae (Ref. 31). Their diameters are 2 to 5 seconds of arc, so at times of very poor seeing they may not be resolved. They typically have brightnesses of about half that of the surrounding photosphere and field strengths greater than 1500 gauss.

- Nonmagnetic gaps (Ref. 31) are regions in the photosphere where the strength of certain spectral lines decreases and the continuum brightness increases, but there is no strong local magnetic field. The diameters of these regions are about 1100 kilometers, and lifetimes are about 40 minutes.

Any of these inhomogeneities is capable of producing some distortion of the magnetograph record, especially at times of poor seeing. The amounts of such distortion will be determined largely by the magnitudes of the effects of errors arising within the telescope and magnetograph.

It is apposite to quote here a statement made by Deubner and Liedler in their discussion of the magnetograph at the Fraunhofer Institut (Ref. 32): "In attempting to calibrate the vectormagnetograph, it has been shown here that due to our limited knowledge of the nature of these inhomogeneities (on the solar surface), which doubtless exists, the construction of a universal calibration curve is more or less impossible or even meaningless. Such a calibration would be valid only for the single spot from which it was derived during a particular state of development, and only for the prevailing spot field."

ERRORS ASSOCIATED WITH UNCERTAINTIES IN THEORY

Calibration curves relating magnetograph signal levels to magnetic field strengths on the Sun must be based, ultimately, on some theory of line formation in magnetic fields. As will be shown later, theory does not yet permit a precise prediction of signal levels for all conditions on the Sun.

Approximate calibration curves have already been calculated. While they are not exactly applicable, they should serve to show the general behavior of signal as a function of field strength. The relations thus obtained consist of a series of nested curves, one for each value of the field orientation angle. These curves are fairly closely spaced; since in some cases the spacing may be of the order of the uncertainty of the signal, the interpretation could be ambiguous even supposing that the calibration curves were precisely known. Moreover, the curves are not monotonic; the signal increases with increasing field strength until a field of the order of 1000 gauss is reached; as the field increases beyond that value, the signal drops abruptly. Therefore, an additional ambiguity exists in the region around the peak unless independent information is available to show on which branch of the curve the signal lies. To make matters worse, at present there is no way to determine an absolute calibration curve for λ5250, so given signal values cannot be attributed to specific field strengths. This comes about partly through the inherent difficulties of calculating the polarized intensities in a solar magnetic field, and partly through the properties of the transition producing λ5250.216.

Only one or two transitions can be treated in detail in solar magnetic fields, and the calculations for these cases are so cumbersome as to be impractical for the large number of repetitions needed to define a calibration curve. House and Cohen (Ref. 33) described the calculations necessary to define the scattering in a magnetic field (with simplifying approximations) for a resonance line which gives rise in a magnetic field to a normal Zeeman triplet. The field must be weak. The transition considered is $^1S_0 \rightarrow {}^1P_1$, which for the solar astrophysical case would be found only in the resonance lines of neutral calcium and magnesium, in the visible wavelengths.

The 5250.216 angstrom line comes from the transition $^5D_0 \rightarrow {}^7D_1$ (Ref. 34); the lower excitation potential is 0.12 electron volt, the upper 2.47 electron volt. The line is therefore one of low excitation but not a resonance line. One would expect it to have a strong scattering component, and this expectation is reinforced by its behavior on the Sun, where the variation in line strength from center to limb is less than would be expected for a line formed in pure absorption (Ref. 4). Nevertheless, the line also has a strong absorption component. It cannot be correctly treated by either a pure scattering or a pure absorption approximation, and these are the only computational methods which are practical for the large number of calculations required. The two most often used procedures for calculations in a magnetic field, described in References 10 and 35, require that pure absorption or pure scattering be assumed.

There is general agreement that, because of the intrinsic differences between the regions, calibration curves established for the photosphere should not be used in interpreting sunspot observations. The calculation of expected signal values in sunspots is even more difficult than in the photosphere. All the difficulties of the photospheric calculation remain, and in addition the existing sunspot models do not permit a self-consistent profile calculation under any set of assumptions (Ref. 36).

The interpretation of the observations is even more uncertain because of several magneto-optic effects which can alter the plane of polarization after it is produced in the spectral line transition on the Sun. The Hanle effect usually is mentioned in this connection; others may enter as well (see Ref. 37, for example). The effects are much more severe for linear than for circular polarization. Indeed, Beckers has stated, "There is no simple relationship between the amount and direction of linear polarization and the strength and direction of the magnetic field. Only with very large approximation can one say that the degree of polarization is related to the total field strength and the direction to the longitudinal magnetic field strength." (See Ref. 38, p. 13.)

Many magnetograph calibrations take advantage of the fact that, for small fields, the measured signal is (approximately) directly proportional to the field strength. This relation can be used if it is understood that it applies to small fields only and that the proportionality "constant" depends explicitly on position on the solar disk, so that the value used must be correct for the solar coordinates of the sunspot (see Ref. 12, p. 194, and Ref. 29, p. 1-17). Adjustment of the "constant" according to disk position will be discussed in a later section of this report.

PROBABLE ERRORS IN FIELD STRENGTHS DETERMINED FROM ZEEMAN SPLITTING

The results of a determination of magnetic fields in sunspots from the Zeeman splitting of λ 5250 illustrates the error which can enter a well-documented field strength determination. The observations and method of deriving field strengths are described in Section 1. The calculated field strengths were reviewed to estimate the error in the final values. Most of the field strengths are averages of several values obtained from separate spectra made of the same location in the sunspot, so the deviations of the separate values from the average form a part of the error estimate. When the calculated field strength values were reviewed, the identification of the separate Zeeman components was also reviewed. In some cases, the identifications were revised, causing changes in the average field value for the location. These changes generally were small. A value which departed greatly from the average of the other values was discarded in one location (square XI-g of the magnetic field map). The final map is shown in Figure 4; it does not differ appreciably from the one given in Reference 39. The deviations from the mean values shown in the map are tabulated for each location in the sunspot in Table 4.

The average deviation for all the values from their separate means is 180 gauss; the uncertainty caused by scatter in the individual magnetic field values for this sunspot, therefore, is ±180 gauss.

The final values are uncertain for other reasons also. Because the splittings are determined from the observed positions of the Zeeman components, uncertainties in wavelength will affect the results. The spectral intensities were recorded at wavelength intervals of 5.88 milliangstroms, so this interval size imposes a limit to the wavelength resolution. If the location of a Zeeman component is defined as the wavelength of its minimum measured intensity, the uncertainty in that location is at least ± 5.88/2 milliangstroms.

SOUTH

	i	h	g	a	b	c	d	e	f
I									
II									
III			906	908	805	605			
IV	151	830	1,070	1,250	1,230				
V, VI	944	1,330	1,430	1,680	1,670	1,4[illegible]0	604		
VII, VIII	926	1,400	1,900	1,780	1,670	1,360			
IX, X	1,680	2,010	1,990	2,060	1,770	1,640	1,360		
XI	1,510	2,020	2,060	1,940	1,680	1,300			
XII	1,120	1,670	1,840	1,750	1,450	1,440			
XIII	1,060	1,240	1,580	1,210	755				
XIV	680	754	792	966	680				
XV			755						

EAST

NORTH

FIGURE 4. REVISED LINE-OF-SIGHT FIELD STRENGTHS IN GAUSS FOR SUNSPOT OBSERVATIONS OF JULY 14, 1969

TABLE 4. DEVIATIONS OF SEPARATE FIELD STRENGTH VALUES FROM MEAN VALUE FOR LOCATION

LOCATION IN SUNSPOT	MEAN FIELD STRENGTH (gauss)	NUMBER OF VALUES AVERAGED	AVERAGE DEVIATION FROM MEAN (gauss)
IIIa	908	2	152
IIIb	805	3	67
IIIc	605	1	0
IIIg	906	1	0
IVa	1,250	4	609
IVb	1,230	3	686
IVg	1,070	5	315
IVh	830	2	75
IVi	151	1	0
V, VIa	1,680	7	155
V, VIb	1,670	7	139
V, VIc	1,420	9	279
V, VId	604	2	151
V, VIg	1,430	10	300
V, VIh	1,330	3	419
V, VIi	944	2	416
VII, VIIIa	1,780	5	126
VII, VIIIb	1,670	8	140
VII, VIIIc	1,360	4	150
VII, VIIIg	1,900	6	120
VII, VIIIh	1,400	4	376
VII, VIIIi	926	4	284
IX, Xa	2,060	5	104
IX, Xb	1,770	5	313
IX, Xc	1,640	10	211
IX, Xd	1,360	1	0
IX, Xg	1,990	5	87
IX, Xh	2,010	5	206
IX, Xi	1,680	5	268

TABLE 4 - Concluded

LOCATION IN SUNSPOT	MEAN FIELD STRENGTH (gauss)	NUMBER OF VALUES AVERAGED	AVERAGE DEVIATION FROM MEAN (gauss)
XIa	1,940	5	126
XIb	1,680	5	139
XIc	1,300	4	169
XIg	2,060	4	58
XIh	2,020	5	202
XIi	1,510	5	120
XIIa	1,750	5	277
XIIb	1,450	5	313
XIIc	1,440	2	225
XIIg	1,840	5	134
XIIh	1,670	5	131
XIIi	1,120	4	170
XIIIa	1,210	5	392
XIIIb	755	2	0
XIIIg	1,580	5	360
XIIIh	1,240	5	187
XIIIi	1,060	2	0
XIVa	966	2	15
XIVb	680	1	0
XIVg	792	2	37
XIVh	754	3	151
XIVi	680	1	0
XVg	755	1	0

NOTE: The mean field strengths have been rounded off to three significant figures.

The uncertainty in field strength corresponding to this wavelength uncertainty is ±75.5 gauss for λ5250.2. That value also represents the minimum field strength that can in principle be detected from these spectroscopic data. In practice, the minimum may be somewhat larger because the resolving power of the spectrograph and the distorting effect of the finite slit width may determine the minimum resolvable separation.

The total probable error for the magnetic field values can be estimated as the root mean square of 180 gauss and 75.5 gauss, or 195 gauss. The probable error in the spectroscopically determined field strengths, therefore, is approximately ±200 gauss.

SUMMARY OF ERROR STUDY

Magnetographs are, in general, subject to large systematic errors. The magnitudes and nature of the errors depend upon the particular type of magnetograph. Numerical error estimates rarely appear in the literature; errors in the range of 10 to 20 percent are generally considered to be moderate (Ref. 40). Most systems are considered to be more reliable for field strengths less than about 1500 gauss than for very large fields.

It may be possible for a large systematic error to go undetected, although fortunately that is less likely now that results from many different instruments can be compared. [In 1962, Stepanov, Shaposhnikova, and Petrova determined that Mt. Wilson measurements underestimated a field of 1000 gauss by no less than 700 gauss, on the average (Ref. 12, p. 205).]

If observations in λ5250.216 are used, all previous experience shows that the calibration must be done by comparing the signal levels to those measured for the same solar features in another line for which a calibration can be made.

Refined error estimates, of course, must wait until the system has been in use long enough for observers to collect a large mass of data and to conduct careful tests for instrumental error. In making a preliminary estimate, no justification exists for assuming the field strengths will have accuracy better than 20 percent of the measured value. Therefore, ±20 percent is recommended as a provisional minimum error estimate.

VARIATION OF CIRCULAR POLARIZATION CONSTANT WITH POSITION ON THE SOLAR DISK

For real-time rapid reduction of magnetograph signals, the relation between degree of circular polarization and magnetic field strength is assumed to be linear, for fields up to about 1000 gauss. The magnetograph calibration includes determining the slope C_1 for this relation. The value of C_1, however, depends explicitly upon position on the solar disk.

If the Unno formulation for polarized residual intensities is used, the variation of C_1 with position on the solar disk can be written as a function of known quantities (the Unno formulation is used because it permits C_1 to be written as a linear function of β_0, the limb darkening constant). The expected variation in C_1 across the disk can then be estimated using a minimum number of line-dependent parameters.

For small magnetic fields, the relation between the mean circular polarization, $\overline{P}_V$, and the magnetic splitting is assumed to be given by

$$\overline{P_v} = (V_H \cos \psi)\, C_1 \tag{3}$$

where

$$C_1 = \frac{-\mu\beta_o \eta_o \displaystyle\int_{v_i - \delta}^{v_i + \delta} \frac{\left[\left. \dfrac{dH(a, v)}{dv} \right|_v \right]}{\left[1 + \eta_o H(a, v)\right]^2} T(v, v_i)\, dv}{\displaystyle\int_{v_i - \delta}^{v_i + \delta} \left[1 + \frac{\mu\beta_o}{1 + \eta_o H(a, v)}\right] T(v, v_i)\, dv} \tag{4}$$

Equations (3) and (4) are taken from Reference 29, p. 1-17; Equation (4) is Equation (1.14) of Reference 29. All symbols have the same meanings as in Reference 29 and will not be redefined here.

Because v is independent of μ and β_0, the three integrals in Equation (4) can be written in a form that is independent of position on the solar disk.

$$\text{Let } A = \int_{v_i - \delta}^{v_i + \delta} \frac{\left[\left. \frac{dH(a, v)}{dv} \right|_v \right]}{\left[1 + \eta_o H(a, v)\right]^2} T(v, v_i)\, dv$$

$$B = \int_{v_i - \delta}^{v_i + \delta} T(v, v_i)\, dv$$

and

$$D = \int_{v_i - \delta}^{v_i + \delta} \frac{T(v, v_i)}{\left|1 + \eta_o H(a, v)\right|} dv .$$

Then

$$C_1 = \frac{-\mu_o \beta_o \eta_o A}{B + \mu \beta_o D} .$$

$$\frac{\partial C_1}{\partial \mu} = \frac{-\beta_o \eta_o A}{(B + \mu \beta_o D)} + \frac{\mu \beta_o^2 \eta_o A D}{(B + \mu \beta_o D)^2}$$

$$\frac{\partial C_1}{\partial \mu} = \frac{C_1}{\mu} - \frac{\beta_o D C_1}{B + \mu \beta_o D} \tag{5}$$

B and D are easily evaluated, and β_0 is known. So Equation (5) can be used to find the change in C_1 for different positions on the solar disk.

Since the value of C_1 at $\mu = 1.00$ has not yet been established, the quantity to be calculated will be

$$\frac{C_1 (\mu)}{C_1 (\mu = 1.00)} .$$

Approximately,

$$\frac{C_1 (\mu)}{C_1 (\mu = 1)} = \frac{C_1 (\mu + \Delta \mu)}{C_1 (\mu = 1)} - \left(\frac{\partial C_1}{\partial \mu}\right)\left(\frac{\Delta\mu}{C_1 (\mu = 1)}\right) \tag{6}$$

So if C_1 ($\mu = 1$) is assumed to be known,

$$C_1 (\mu = 1) = C_1 (\mu = 1)$$

$$\frac{C_1 (\mu = 0.9)}{C_1 (\mu = 1)} = \frac{C_1 (\mu = 1)}{C_1 (\mu = 1)} - \frac{C_1 (\mu = 1)}{C_1 (\mu = 1)} \left[\frac{1}{0.9} - \frac{\beta_o D}{B + 0.9 \beta_o D} \right] (1.0 - 0.9)$$

$$\frac{C_1 (\mu = 0.8)}{C_1 (\mu = 1)} = \frac{C_1 (\mu = 0.9)}{C_1 (\mu = 1)} - \frac{C_1 (\mu = 0.9)}{C_1 (\mu = 1)} \left[\frac{1}{0.8} - \frac{\beta_o D}{\beta + 0.8 \beta_o D} \right] (0.9 - 0.8)$$

etc.

To evaluate D, several spectral line parameters must be known:

$\Delta\lambda_D$ - the Doppler width, which must be known in order to evaluate H(a, v)

a - the damping parameter, which is also required to evaluate H(a, v)

η_o - the ratio of line-to-continuous absorption coefficients.

None of these quantities is well known for λ5250 in sunspots. Fortunately, however, the values found from Equation (5) are far more sensitive to the better-known quantities μ and β_0 than to the three line profile parameters. The use of photospheric values of $\Delta\lambda_D$, a, and η_o should not introduce serious errors.

To investigate this point, a set of maximum and minimum values for C_1 (μ) was calculated by using the smallest and largest values of $\Delta\lambda_D$, a, and η_o which would be expected on the Sun, for any spectral line formed in LTE. The results for λ5250 should lie well within this range. The line profile parameters used for this calculation are given in Table 5. The value of β_o was 1.70 for both cases.

TABLE 5. LINE PROFILE PARAMETER VALUES FOR DETERMINING MAXIMUM AND MINIMUM $C_1(\mu)/C_1(1)$

PARAMETER	VALUE FOR MAXIMUM	VALUE FOR MINIMUM
$\Delta\lambda_D$	5.0 milliangstroms	40.0 milliangstroms
a	0.05	0.295
η_o	5.0	30.0

From Equations (5) and (6), it appears that the smallest possible values that could be obtained for $C_1(\mu)/C_1(1)$ would be found if $\beta_o = 0$. A set of $C_1(\mu)/C_1(1)$ values was calculated for this case; it is tabulated in Table 6 under the heading, "lower envelope". The maximum and minimum values found using the parameters given in Table 5 also are given in Table 6. The difference between these sets of values is an overestimate of the error that would be introduced by using photospheric parameters to calculate $C_1(\mu)$ for sunspots.

When μ is less than 0.5, the maximum error which would be introduced by using photospheric values is certainly only a few percent. It should be emphasized that the range of values covered in Table 5 is truly enormous, and the parameters for any single line can be estimated with reasonable certainty to within much smaller limits.

The results in Table 6 suggest that the $C_1(\mu)$ values for sunspot umbrae can be approximated by using the $\Delta\lambda_D$, a, and η_o values

TABLE 6. RANGE OF VALUES OF $C_1 (\mu)/C_1 (1)$ FOR PHYSICALLY POSSIBLE VALUES OF LINE PROFILE PARAMETERS AND FOR $\beta_0 = 0$

μ	MAXIMUM $C_1 (\mu)/C_1 (1)$	MINIMUM $C_1 (\mu)/C_1 (1)$	LOWER ENVELOPE
1.000	1.000	1.000	1.000
0.917	0.962	0.929	0.909
0.833	0.920	0.855	0.818
0.750	0.873	0.778	0.727
0.667	0.819	0.698	0.636
0.584	0.758	0.614	0.546
0.500	0.686	0.526	0.455
0.417	0.603	0.433	0.364
0.333	0.502	0.335	0.273
0.250	0.382	0.232	0.182
0.167	0.231	0.122	0.092
0.083	0.024	0.003	0.000

which are found for λ5250 in the photosphere. That approximation must be made because of the scarcity of high-quality umbral profiles of λ5250 in unpolarized light. The value of β_0 certainly changes between the photosphere and sunspot umbrae, and this factor is dominant. Fortunately, β_0 for sunspot umbrae can be determined. Two separate calculations of $C_1 (\mu)/C_1 (1)$ were therefore made: one for the photosphere and penumbrae, and one for umbrae.

For the photospheric calculation, the values of $\Delta\lambda_D$, a, and η_0 were found by fitting an absorption profile to M. J. Hagyard's observations of λ 5250 in the photosphere. The values determined were $\Delta\lambda_D$ = 12 milliangstroms, a = 0.2, and η_o = 9. For the photosphere at λ = 5250 angstroms, β_o = 1.70 (Ref. 41, p. 171). According to Moe and Maltby (Ref. 42), "The intensity ratio between the penumbra and the photosphere shows little or no variation with position on the solar disk." The same value of limb darkening constant β_o will therefore be good for both photosphere and penumbra, and the line profile parameters will be the same because good penumbral profiles of λ5250 are as rare as good umbral profiles. The resulting values of $C_1(\mu)/C_1(1)$ are given in Table 7.

TABLE 7. $C_1(\mu)/C_1(1)$ FOR PHOTOSPHERE AND PENUMBRAE

μ	$C_1(\mu)/C_1(1)$
1.000	1.000
0.917	0.957
0.833	0.908
0.750	0.855
0.667	0.796
0.584	0.729
0.500	0.652
0.417	0.566
0.333	0.464
0.250	0.345
0.167	0.202
0.083	0.016

For the umbral calculation, the same values of $\Delta\lambda_D$, a, and η_o will be used, but a new β_o must be found. Wittmann and Schröter (Ref. 43) give center-to-limb intensities of sunspots at $\lambda \approx 4680$ angstroms and 6400 angstroms. On the authority of Figure 3 of

Reference 44, the values for λ = 5250 angstroms can be found by linear interpolation between the two sets of Wittmann-Schröter values. The results are shown in Table 8.

TABLE 8. CENTER-TO-LIMB INTENSITY DISTRIBUTION FOR SUNSPOT UMBRAE AT λ = 5250 ANGSTROMS

μ	I_u (4680 angstroms)	INTERPOLATED I_u (5250 angstroms)	I_u (6400 angstroms)
1.00	3.68	3.77	3.94
0.90	3.66	3.75	3.93
0.80	3.63	3.72	3.90
0.70	3.60	3.69	3.87
0.60	3.56	3.65	3.83
0.50	3.52	3.61	3.78
0.40	3.47	3.55	3.70
0.30	3.35	3.33	3.59
0.20	2.98	3.12	3.40
0.10	2.24	2.50	3.02

The change in intensity between center and limb is quite small.

To obtain β_o, the values of $I_u(\mu)/I_u(\mu = 1)$ are fitted to the form

$$\frac{I_u(\mu)}{I_u(1)} = 1 - u_1 + (u_1)(\mu) \tag{7}$$

where

$$\beta_o = \frac{u_1}{1 - u_1}$$

A simple equation of the form of Equation (7) does not permit a good fit over the entire range of μ values, but an acceptable fit for $1.0 \geqq \mu \geqq 0.4$ can be obtained by setting $\beta_o = 0.093$ ($u_1 = 0.086$). In Table 9, the values of $I_u(\mu)/I_u(1)$ for $\beta_o = 0.093$ are compared to the interpolated measured values.

TABLE 9. VALUES OF UMBRAL LIMB DARKENING FOR $\beta_0 = 0.093$ COMPARED TO MEASURED VALUES

μ	$I_u(\mu)/I_u(1)$, $\beta_0 = 0.093$	$I_u(\mu)/I_u(1)$ FROM TABLE 8
1.00	1.000	1.000
0.90	0.991	0.993
0.80	0.983	0.987
0.70	0.974	0.978
0.60	0.966	0.968
0.50	0.957	0.958
0.40	0.948	0.942
0.30	0.940	0.884
0.20	0.931	0.828
0.10	0.923	0.664
	(β_0 value is less accurate in this range)	

The value $\beta_o = 0.093$ was used to calculate $C_1(\mu)/C_1(1)$ for umbrae. The values of C_1 when μ is less than 0.40 should be given less weight because the approximate limb darkening relation is less accurate in that range.

The line profile parameter whose value in umbrae is most uncertain is probably η_o. Values C_1 were calculated using $\eta_o = 9$, the photospheric value, and $\eta_o = 40$, since η_o may be much larger in umbrae. The results for both η_o values are given in Table 10; they are almost identical.

TABLE 10. $C_1(\mu)/C_1(1)$ FOR SUNSPOT UMBRAE

μ	$C_1(\mu)/C_1(1)$, $\eta_o = 9$	$C_1(\mu)/C_1(1)$, $\eta_o = 40$
1.000	1.000	1.000
0.917	0.915	0.913
0.833	0.827	0.825
0.750	0.740	0.737
0.667	0.652	0.648
0.584	0.562	0.558
0.500	0.471	0.467
0.417	0.380	0.376
0.333	0.286	0.283
0.250	0.192	0.190
0.167	0.098	0.096
0.083	0.000	0.000
	(β_o value is less accurate in this range)	

Should it become necessary to do so, a supplement to Table 10 for $\mu < 0.4$ can be calculated, using a value of β_o which gives a better fit to the umbral intensities near the limb.

The values of Tables 7 and 10 are shown plotted in Figure 5. The relation for the umbra is almost linear.

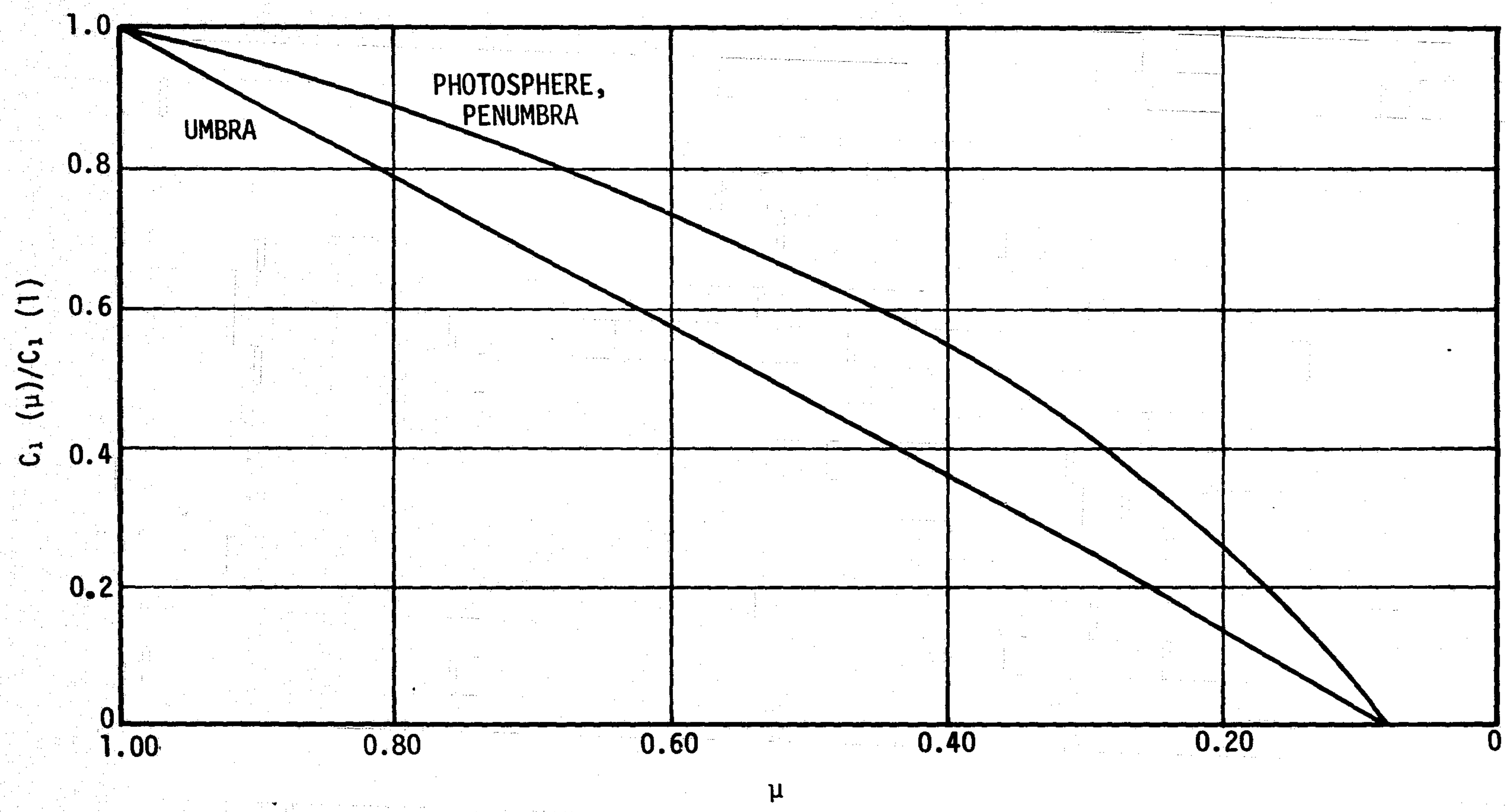

FIGURE 5. C_1 (μ)/C_1 (1) AS A FUNCTION OF POSITION ON SOLAR DISK

PROGRAM TO LOCATE AND PLOT MAGNETIC FIELD NEUTRAL LINES

Two of the properties which are of the greatest interest in solar magnetic field maps are the regions where the magnetic field gradients are steepest and the locations of the boundaries between field regions of opposite polarity. The regions of steep gradient are easily located on magnetic field contour plots because they are the regions where the contours are most closely spaced. However, the boundaries between opposite-polarity field regions (the boundaries will be called "neutral lines" for brevity) are generally less distinctive in appearance on contour plots, and it is convenient to provide a separate program to plot the neutral line locations directly from magnetograph data.

A FORTRAN program to make such plots has been written for the Univac 1108. The position of each neutral line is identified by selecting the coordinates of pairs of adjacent points for which the measured signals are opposite in sign. The program in its present form will analyze a square grid of data 128 points on a side and will store 1998 coordinate values. Places where the signal changes sign because of the sign reversal of the magnetograph calibration curve for large magnetic field values will be identified by the program as portions of neutral lines. When the field strength values at which the calibration curves change sign have been established, the program will be modified to ignore signal sign changes for field strengths in the reversal range.

The program compares points in two adjacent horizontal data rows. Beginning with rows 1 and 2, the signs of pairs of points are compared by taking groups of four data points at a time. The points are labeled as shown in Figure 6; their signs are compared in the order P1, P2; P1, P3; P2, P3; P1, P4. If all four points are of the same sign,

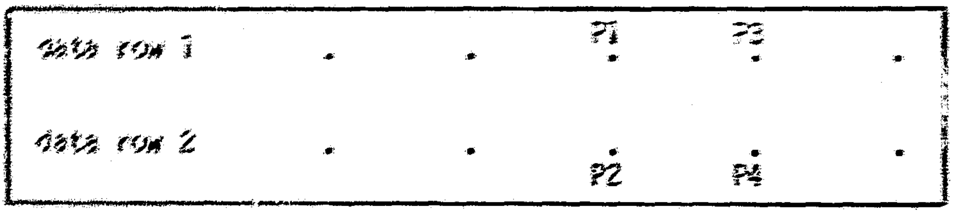

FIGURE 6. POINT LABELING PATTERNS FOR NEUTRAL LINE PROGRAM

points P3 and P4 are relabeled P1 and P2, and the next vertical pair to the right becomes P3 and P4 for a new four-point group. The comparison process is repeated across the data row. When two points of opposite sign are found, their coordinates are stored. In order to save space in memory, the program then stops testing values in a particular four-point group and moves to the next group. This explains why, in the final plots, the lines which connect points of opposite sign may take any of the four directions: they simply record the relative positions of the members of the first pair of points of opposite sign which was found in each group of four points. When the first two data rows have been scanned, the process is repeated with the second and third rows, and the full sequence is repeated until the entire frame has been scanned or until the array reserved for coordinate values has been filled.

After the scanning has been completed, the coordinate values of the pairs of points of opposite sign are plotted by connecting them with short lines. A line drawn joining the midpoints of these short connecting lines will trace the location of a neutral line to the precision allowed by the spatial resolution of the data. To assist in determining the coordinates of the plotted points, grid lines are drawn at every fourth data row and column.

The program was tested on a frame of magnetograph data which was obtained from the Kitt Peak National Observatory and which has been used for testing other magnetograph analysis programs at MSFC. This particular data set forms a grid 120-by-120 data points in size. Three cards were missing from the data deck; one of these contained data which crossed a neutral line and produced a gap in the upper right-hand corner of the final plot. Except for this gap, the plot agrees in every detail with the neutral line pattern obtained from the data by the Kitt Peak Observatory. It also agrees with a hand plot of the data.

The plot of the test data is given in Figure 7. Figure 8 is a flowchart of the test program, which reads data from cards, and Figure 9 is the listing of the test program. For use with real MSFC magnetograph data, the program will be modified to read the appropriate magnetic tape formats.

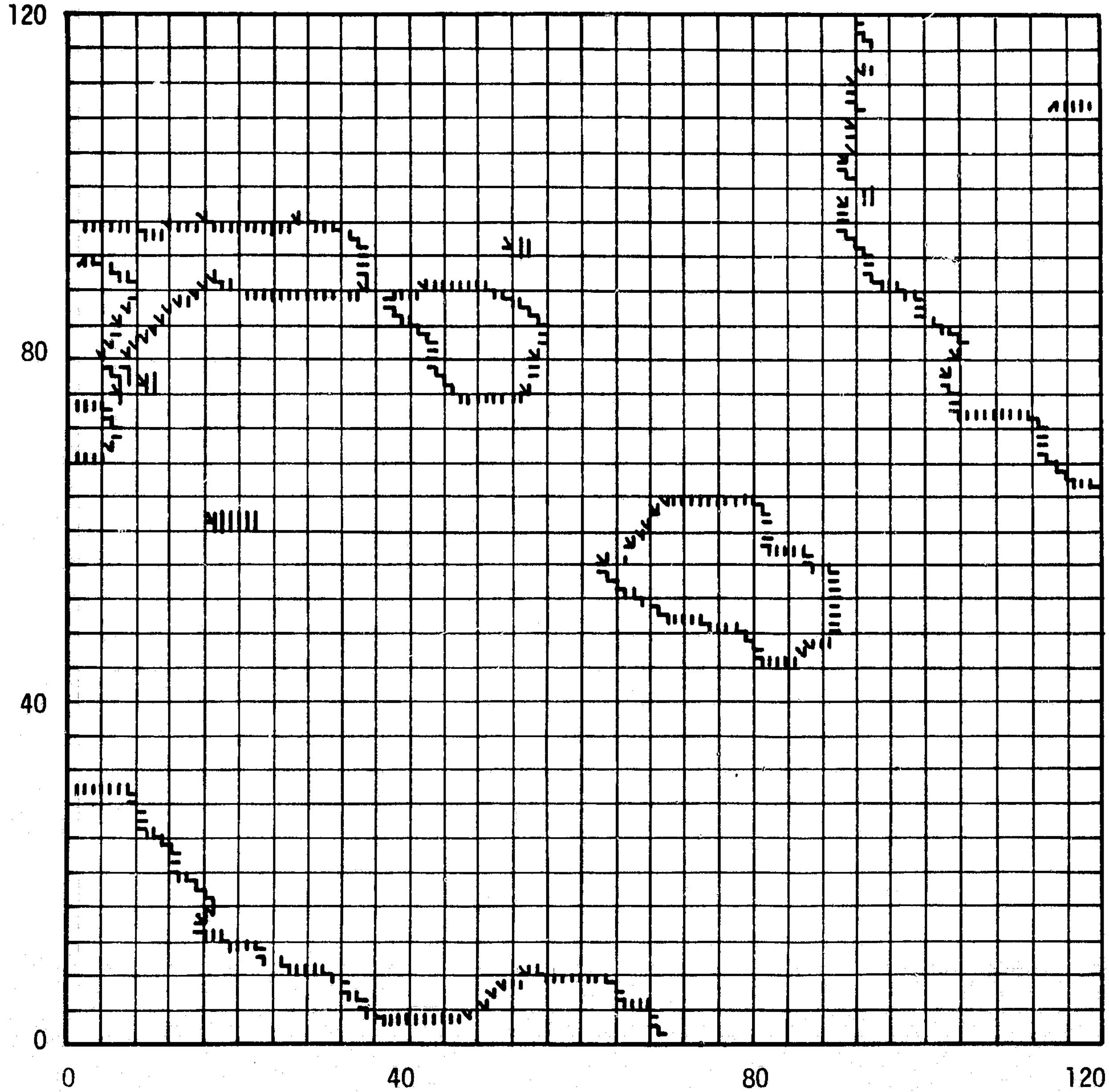

FIGURE 7. PLOT OF NEUTRAL LINES PRODUCED BY TEST PROGRAM

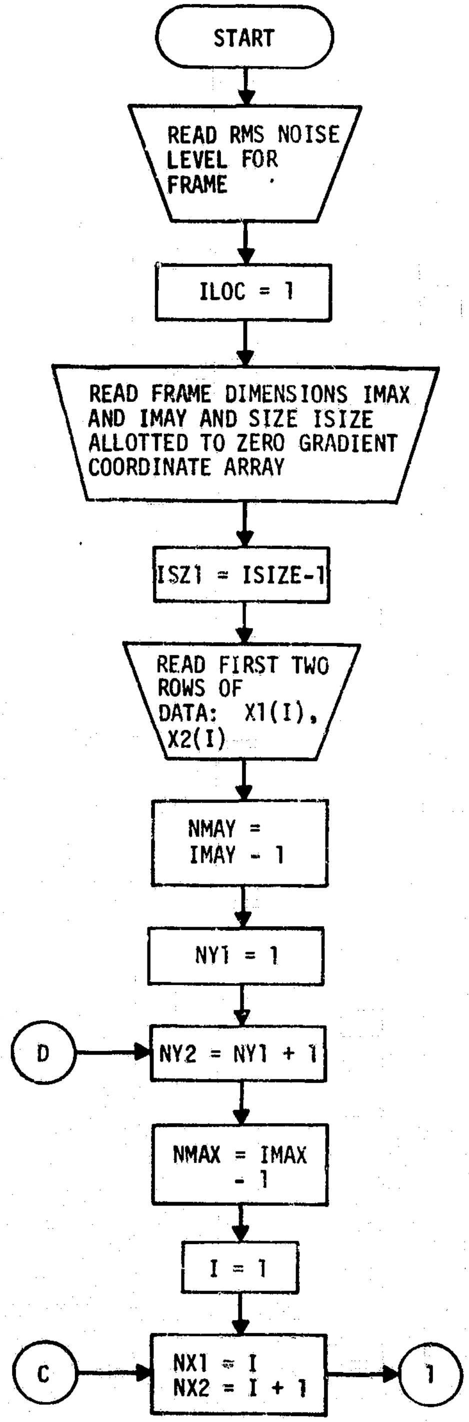

FIGURE 8. FLOWCHART OF TEST PROGRAM

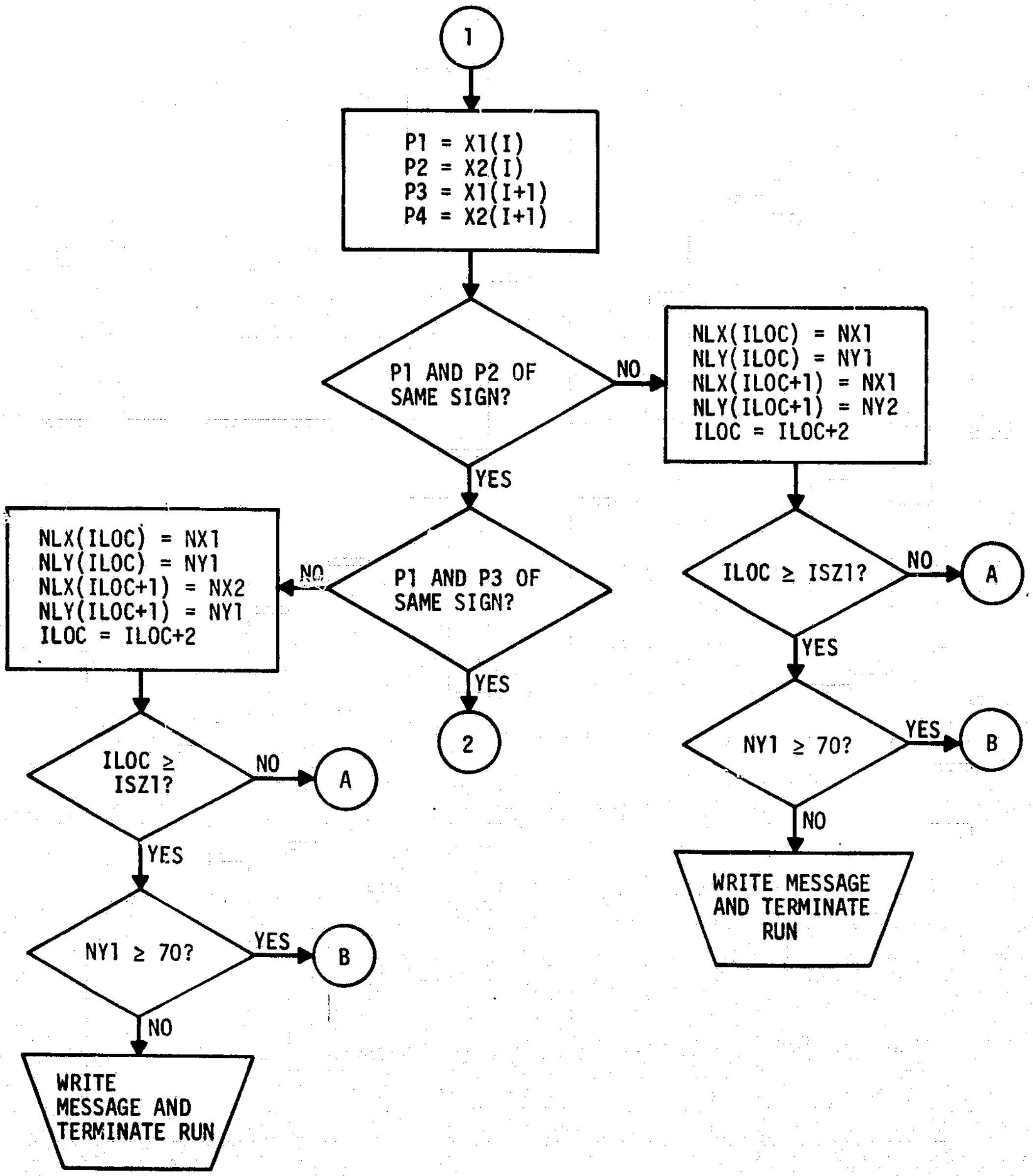

FIGURE 8 - Continued

C-2

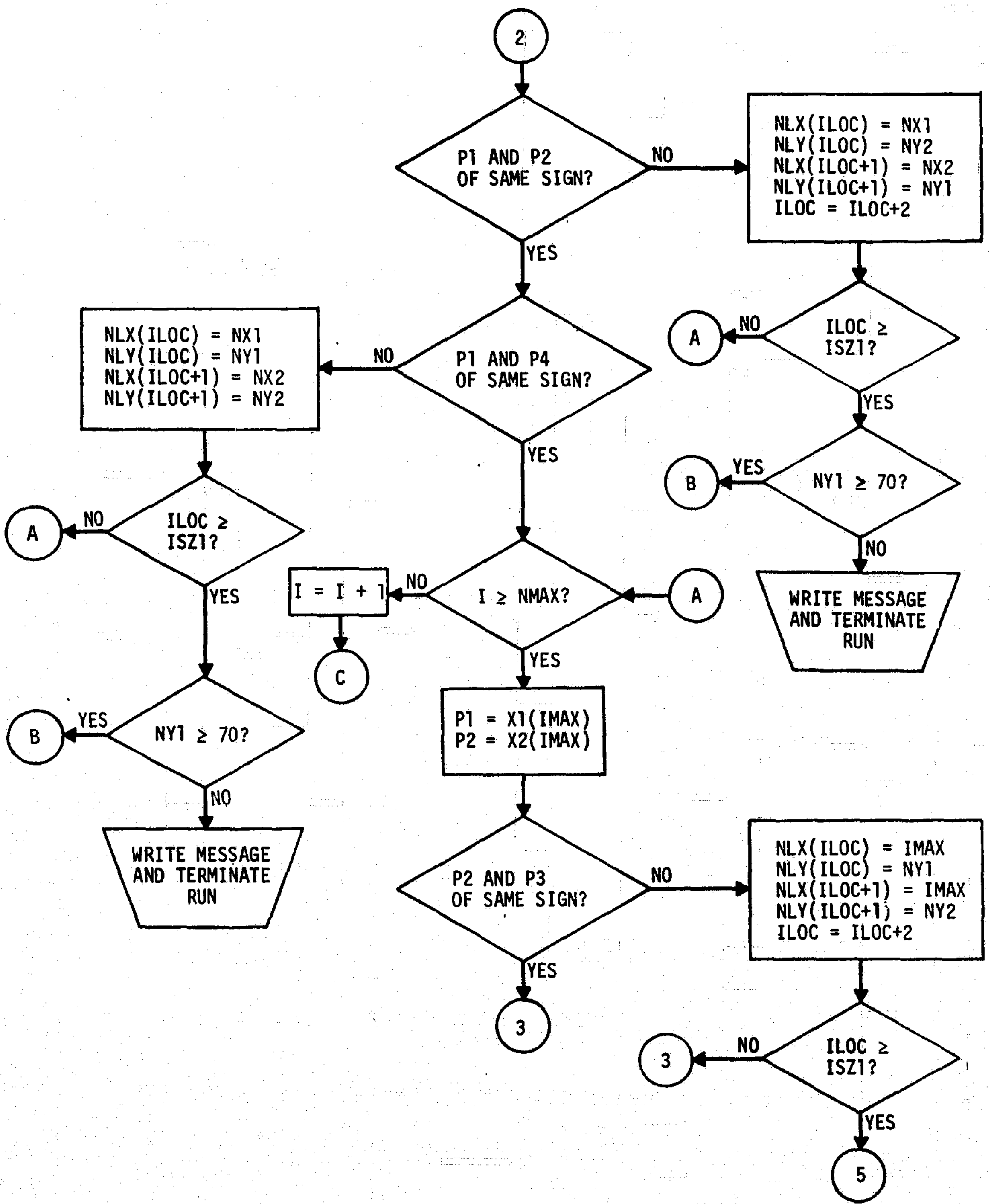

FIGURE 8 - Continued

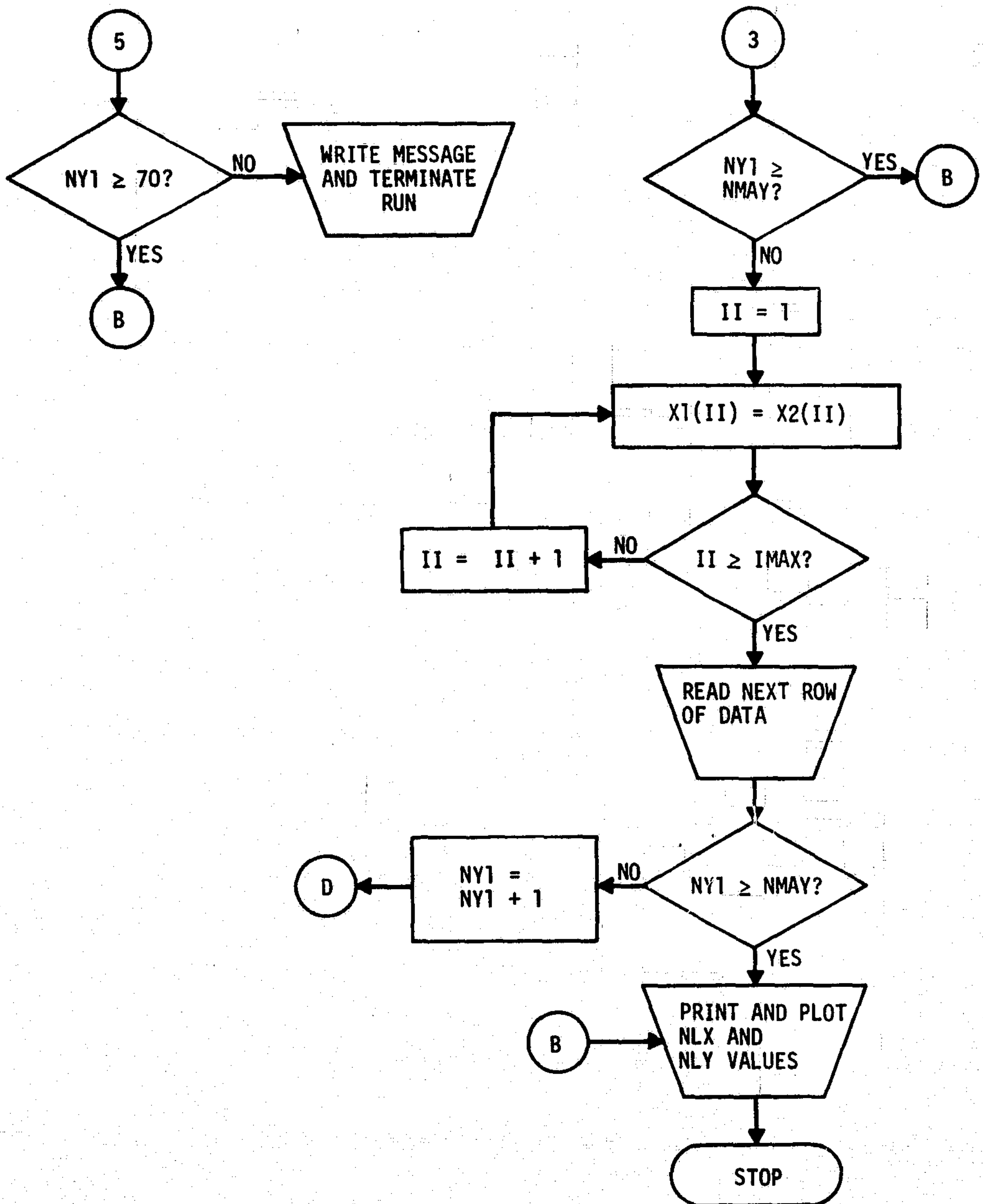

FIGURE 8 - Concluded

```
C     @ZERO GRADIENT@ CONTOURS IN MAGNETOGRAPH DATA
C     VERSION FOR TEST WITH KPNO MAGNETOGRAPH DATA
      DIMENSION X1(128), X2(128), NLX(2000), NLY(2000)
      DIMENSION ARRAY (22)
      DATA (ARRAY(I),I=1,22)/24HHARDCOPY ONLY, ONE COPY ,18,6H
      KRE= 5
      KWR= 6
      READ (KRE, 1) RMSN
C     READ RMS NOISE LEVEL FOR FRAME
    1 FORMAT (F10.0)
      ILOC= 1
C     COUNTER FOR @ZERO@ GRADIENTS
      READ (KRE, 45) IMAX, IMAY, ISIZE
   45 FORMAT (3I10)
C     NO. OF ROWS, NO. OF COLUMNS, NO. OF NEUTRAL LINE POSITIONS TO BE
C     STORED
      IS21= ISIZE - 1
C     READ 1ST 2 ROWS OF DATA
      READ (KRE, 46) (X1(I), I= 1, IMAX)
      READ (KRE, 46) (X2(I), I= 1, IMAX)
   46 FORMAT (12(F5.0, 1X))
C     SET Y COORDINATE COUNTER AND START SEARCH OF FRAME
      NMAY= IMAY - 1
      DO 9 NY1= 1, NMAY
      NY2= NY1 + 1
C     START OF @GRADIENT@ EVALUATION LOOP
      NMAX= IMAX - 1
      DO 10 I= 1, NMAX
C     SET X COORDINATE COUNTER
      NX1= I
      NX2= I + 1
      P1= X1(I)
      P2= X2(I)
      P3= X1(I +1)
      P4= X2(I + 1)
      IF (P1) 104, 3, 103
  103 IF (P2) 4, 3, 3
  104 IF (P2) 3, 3, 4
    4 NLX(ILOC)= NX1
      NLY(ILOC)= NY1
      NLX(ILOC + 1)= NX1
      NLY(ILOC+1)= NY2
      WRITE (KWR, 70) P1, P2, NX1, NY1
   70 FORMAT (1H , 2(E12.5, 5X), 2(I6, 5X))
      ILOC= ILOC + 2
      IF (ILOC-IS21) 10, 5, 5
    5 IF (NY1-70) 6, 7, 7
    6 WRITE (KWR, 8) NY1
    8 FORMAT (1H , 59HARRAY RESERVED FOR ZERO GRADIENT COORDINATES IS FI
     1LLED NY1=, I5)
      WRITE (KWR, 11)
   11 FORMAT (1H , 13HTERMINATE RUN)
      GO TO 999
    3 IF (P1) 112, 12, 113
  112 IF (P3) 12, 12, 13
```

FIGURE 9. LISTING OF TEST PROGRAM

```
  113 IF (P3) 13, 12, 12
   13 NLX(ILOC)= NX1
      NLY(ILOC)= NY1
      NLX(ILOC + 1)= NX2
      NLY(ILOC + 1)= NY1
      WRITE (KWR, 30) P1, P3, NX1, NY1
      ILOC= ILOC + 2
      IF (ILOC-ISZ1) 10, 5, 5
   12 IF (P2) 115, 15, 114
  115 IF (P3) 15, 15, 14
  114 IF (P3) 14, 15, 15
   14 NLX(ILOC)= NX1
      NLY(ILOC)= NY2
      NLX(ILOC + 1)= NX2
      NLY(ILOC + 1)= NY1
      WRITE (KWR, 30) P2, P3, NX1, NY1
      ILOC= ILOC + 2
      IF (ILOC-ISZ1) 10, 5, 5
   15 IF (P1) 110, 10, 116
  116 IF (P4) 16, 10, 10
  110 IF (P4) 10, 10, 16
   16 NLX(ILOC)= NX1
      NLY(ILOC)= NY1
      NLX(ILOC + 1)= NX2
      NLY(ILOC + 1)= NY2
      WRITE (KWR, 30) P1, P4, NX1, NY1
      ILOC = ILOC + 2
      IF (ILOC-ISZ1) 10, 5, 5
   10 CONTINUE
      P1= X1(IMAX)
      P2= X2(IMAX)
      IF (P1) 118, 18, 117
  118 IF (P2) 18, 18, 17
  117 IF (P2) 17, 18, 18
   17 NLX(ILOC)= IMAX
      NLY(ILOC)= NY1
      NLX(ILOC + 1)= IMAX
      NLY(ILOC + 1)= NY2
      ILOC = ILOC + 2
      IF (ILOC-ISZ1) 18, 18, 105
  105 IF (NY1-70) 106, 7, 7
  106 WRITE (KWR, 8) NY1
      WRITE (KWR, 11)
      GO TO 999
   18 IF (NY1-NMAY) 19, 7, 7
   19 DO 20 II= 1, IMAX
      X1(II)= X2(II)
   20 CONTINUE
C     READ NEXT ROW OF DATA
      READ (KRE, 46) (X2(I), I= 1, IMAX)
    9 CONTINUE
C     THIS COMPLETES SEARCH FOR &ZERO GRADIENT& POINTS
    7 IFIN= ILOC - 1
      WRITE (KWR, 132) IFIN
  132 FORMAT (1H , 5HIFIN=, I10)
      WRITE (KWR, 21)
```

FIGURE 9 - Continued

```
   21 FORMAT (1H ,35HX COORD OF ZERO GRADIENT POINTS ARE)
      WRITE (KWR, 22) (NLX(I), I= 1, IFIN)
   22 FORMAT (1H , 5(I5, 5X))
      WRITE (KWR, 23)
   23 FORMAT (1H ,35HY COORD OF ZERO GRADIENT POINTS ARE)
      WRITE (KWR, 22) (NLY(I), I= 1, IFIN)
C     PLOT TAPE
      CALL IDENT (9, ARRAY)
      CALL GRIDIV(0,0.0,120.0,0.0,120.0,4.0,4.0,-5,5,-10,-10,+4,+4)
      IFI= ILOC-2
      DO 800 I= 1, IFI, 2
      X= NLX(I)
      CALL XSCLV1(X, NXP, IERR)
      NX1= NXP
      X= NLX(I+1)
      CALL XSCLV1(X, NXP, IERR)
      NX2= NXP
      Y= (NMAY+1)-NLY(I)
      CALL YSCLV1(Y, NYP, IERR)
      NY1= NYP
      Y= (NMAY+1)-NLY(I+1)
      CALL YSCLV1(Y, NYP, IERR)
      NY2= NYP
      CALL LINEV(NX1,NY1,NX2,NY2)
  800 CONTINUE
      CALL ENDJOB
  999 STOP
      END
```

FIGURE 9 - Concluded

CONCLUSIONS AND RECOMMENDATIONS

Even the best magnetograph results are subject to large uncertainties. It is unwise to assume the uncertainties in results obtained with a new system are less than ±20 percent. They may be larger.

To reduce some of the uncertainties of calibration and interpretation, it is recommended that the magnetograph be modified to operate using a line other than the neutral iron line at 5250.216 angstroms. The new line, of course, should be carefully selected to introduce a minimum number of new uncertainties. If compelling instrumental reasons exist for requiring the new line to be near 5000 angstroms in wavelength, both $\lambda5253$ and $\lambda5324$ would be worthy of closer investigation. Because the amount of Zeeman splitting is proportional to the square of the wavelength, lines of wavelength longer than 5000 angstroms would tend to produce larger splittings and therefore could be advantageous choices. A number of red spectral lines have been suggested by various authors as possible magnetograph lines; two neutral iron lines which should be investigated are $\lambda6173.348$ (lower excitation potential = 2.213 electron volts) and $\lambda6302.508$ (lower excitation potential = 3.671 electron volts) (Ref. 12, p. 179). A number of other candidates may exist.

Evaluation of the characteristics of possible new magnetograph lines should begin with a preliminary study of the type summarized in Table 3. Lines which are not rejected in the preliminary study must then be further examined to prove that their properties are compatible with the assumptions implicit in the magnetograph calibration analysis. As was shown earlier in this report, attempts to calculate line profiles for sunspot models may reveal such incompatibility. The profile calculation thus forms a test which should be applied to each line which is seriously considered for magnetograph operation.

When the magnetograph is operated using $\lambda 5250$, it is recommended that no reliance be placed on calibration systems which require, even indirectly, the calculation of residual intensities of that spectral line in magnetic fields.

REFERENCES - SECTION 2

1. Minnaert, M., G. F. W. Mulders and J. Houtgast, Photometric Atlas of the Solar Spectrum 3332Å to 8771Å, Schnabel, Amsterdam, 1940.

2. Moore, C. E., M. G. J. Minnaert, and J. Houtgast, The Solar Spectrum 2935Å to 8770Å, N.B.S. Monograph No. 61, December 1966.

3. Obridko, V. N., Soviet Physics-Astronomy, 9, 77, 1965.

4. Obridko, V. N., Soviet Astronomy-AJ, 9, 398, 1965.

5. Moe, O. K., and P. Maltby, Astrophysical Journal Letters, 1, 189, 1968.

6. Hénoux, J. C., Astronomy and Astrophysics, 2, 288, 1969.

7. Yun, H. S., Solar Physics, 16, 379, 1971.

8. Beckers, J., Solar Physics, 9, 372, 1969.

9. Göhring, R., Solar Physics, 8, 271, 1969.

10. Moe, O. K., Solar Physics, 4, 267, 1968.

11. Staude, J., Solar Physics, 12, 84, 1970.

12. Bray, R. J., and R. E. Loughhead, Sunspots, Chapman and Hall, 1964.

13. Corliss, C. H., and B. Warner, Astrophysical Journal Supplement, 8, 395, 1964.

14. Withbroe, G. L., Solar Physics, 9, 19, 1969.

15. Hénoux, J. C., Solar Physics, 4, 315, 1968.

16. Beckers, J. M., and E. H. Schröter, Solar Physics, 7, 22, 1968.

17. Lamb, F. K., "The Effect of Collisions on Spectral Line Formation in Solar Magnetic Regions", Solar Magnetic Fields, IAU Symposium No. 43, ed. by R. Howard, D. Reidel, 1971.

18. House, L. L., "Coherence Properties of Polarized Radiation in Weak Magnetic Fields", Solar Magnetic Fields, IAU Symposium No. 43, ed. by R. Howard, D. Reidel, 1971.

19. Harvey, J. W., Solar Physics, 28, 43, 1973.

20. Harvey, J. W., Solar Physics, 28, 9, 1973.

21. Zwaan, C., and J. Buurman, "Magnetic Field Strengths Derived from Various Lines in the Umbral Spectrum", Solar Magnetic Fields, IAU Symposium No. 43, ed. by R. Howard, D. Reidel, 1971.

22. Wittmann, A., Solar Physics, 23, 294, 1972.

23. Wiehr, E., Solar Physics, 9, 225, 1969.

24. Chapman, G. A., and N. R. Sheeley, Jr., Solar Physics, 5, 442, 1968.

25. Harvey, J., W. Livingston, and C. Slaughter, "A Line-Profile Stokesmeter: Preliminary Results on Non-Sunspot Fields", Line Formation in the Presence of Magnetic Fields, NCAR, Boulder, 1972.

26. Stellmacher, G., and E. Wiehr, Solar Physics, 18, 220, 1971.

27. Harvey, J., and W. Livingston, Solar Physics, 10, 283, 1969.

28. Staude, J., Solar Physics, 17, 331, 1971.

29. "Real-Time Solar Magnetograph (First Generation)", ed. by J. R. Watkins, NASA, George C. Marshall Space Flight Center, MISC-SSL-70-5 #3, December 1970.

30. Beckers, J. M., and E. H. Schröter, Solar Physics, 4, 303, 1968.

31. Beckers, J. M., and E. H. Schröter, Solar Physics, 4, 142, 1968.

32. Deubner, F. L., and R. Liedler, Solar Physics, 7, 87, 1969.

33. House, L. L., and L. C. Cohen, Resonance Lines in Astrophysics, NCAR, Boulder, 1968.

34. Moore, C. E., A Multiplet Table of Astrophysical Interest, Contr. from Princeton University Observatory No. 20, 1945.

35. Unno, W., Pub. Astronomical Society of Japan, 8, 108, 1956.

36. Dunn, A. R., Solar Physics, 26, 83, 1972.

37. Grigorjev, V. M., and J. M. Katz, Solar Physics, 22, 119, 1972.

38. Beckers, J. M., "The Measurement of Solar Magnetic Fields", Solar Magnetic Fields, IAU Symposium No. 43, ed. by R. Howard, D. Reidel, 1971.

39. Dunn, A. R., "Analysis of Sunspot Spectral Data", Teledyne Brown Engineering Interim Report SE-SSL-1428, October 1971.

40. Kotov, V. A., "Systematic Errors of the Crimean Vector Magnetograph", Solar Magnetic Fields, IAU Symposium No. 43, ed. by R. Howard, D. Reidel, 1971.

41. Allen, C. W., Astrophysical Quantities, U. of London, 1963.

42. Moe, O. K., and P. Maltby, Solar Physics, 8, 275, 1969.

43. Wittmann, A., and E. H. Schröter, Solar Physics, 10, 357, 1969.

44. Maltby, P., Solar Physics, 13, 312, 1970.

SECTION 3

PROGRAMS FOR PRESENTATION OF VECTOR MAGNETOGRAPH DATA

TABLE OF CONTENTS

LIST OF ILLUSTRATIONS

LIST OF TABLES

INTRODUCTION

This section contains documentation for four programs written for the Univac 1108. Two of them have been described in Teledyne Brown Engineering Interim Report No. EE-MSFC-1815 (May 1974). Some minor changes have been made to these programs, so updated descriptions and current listings are given here. These two programs plot selected portions of Real Time Solar Magnetograph data: one program displays locations of magnetic polarity changes, and the other shows relative steepnesses of magnetic field gradients as a function of location in the data matrix. The third program removes isolated large data values from the data array and replaces each of the removed values by the average of the values surrounding it. The "corrected" array is then written on a new tape in the same format as the original data. The fourth program is a simple routine which combines the "U" and "R" matrices from the original magnetograph data to form the matrix of values corresponding to transverse magnetic field data. This new matrix is written on a new tape in the same format used for the longitudinal data.

MAGNETIC FIELD NEUTRAL LINE PROGRAM

This program locates and plots the locations in the magnetogram at which the magnetic field changes polarity. At these points, the sign of the magnetograph signal changes, so the program really plots the locations where the signs of adjacent signal values are different.

The position of each neutral line is identified by selecting the coordinates of pairs of adjacent points for which the measured signals are opposite in sign. The program in its present form will analyze a square grid of data 128 points on a side and will store 1998 coordinate values. Places where the signal changes sign because of the sign reversal of the magnetograph calibration curve for large magnetic field values will be identified by the program as portions of neutral lines. When the field strength values at which the calibration curves change sign have been established, the program will be modified to ignore signal sign changes for field strengths in the reversal range.

The program compares points in two adjacent horizontal data rows. Beginning with rows 1 and 2, the signs of pairs of points are compared by taking groups of four data points at a time. The points are labeled as shown in Figure 1; their signs are compared in the order P1, P2; P1, P3; P2, P3; P1, P4. If all four points are of the same sign, points P3 and P4 are relabeled P1 and P2, and the next vertical pair to the right becomes P3 and P4 for a new four-point group. The comparison process is repeated across the data row. When two points of opposite sign are found, their coordinates are stored. In order to save space in memory, the program then stops testing values in a particular four-point group and moves to the next group. This explains why, in the final plots, the lines which connect points of opposite sign

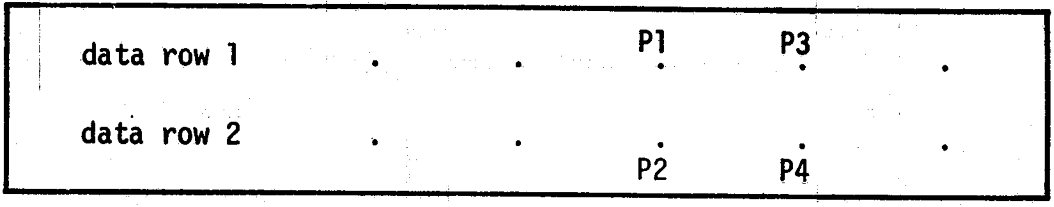

FIGURE 1. POINT LABELING PATTERNS FOR NEUTRAL LINE PROGRAM

may take any of the four directions: they simply record the relative positions of the members of the first pair of points of opposite sign which was found in each group of four points. When the first two data rows have been scanned, the process is repeated with the second and third rows, and the full sequence is repeated until the entire frame has been scanned or until the array reserved for coordinate values has been filled.

After the scanning has been completed, the coordinate values of the pairs of points of opposite sign are plotted by connecting them with short lines. A line drawn joining the midpoints of these short connecting lines will trace the location of a neutral line to the precision allowed by the spatial resolution of the data. To assist in determining the coordinates of the plotted points, grid lines are drawn at every fourth data row and column.

The program uses as data the magnetograph output tapes in their format after undergoing initial processing. In this format, the transverse and longitudinal components are written on separate tapes. Each magnetogram consists of 9 records: a label record of 19 words, and then 8 records of 2049 words each (a counter plus 2048 signal values). In some cases, a few words at the beginning of each magnetogram were lost when the original tapes were processed. The tape read portion of this program contains a short routine to correct for this condition.

Two values must be supplied in order to execute the program. Both of these are entered in DATA statements within the program. The first is the number of longitudinal matrices contained on the tape. This quantity is given the variable name of IPP and is entered as an integer variable. For example, for a tape containing 12 longitudinal matrices, the DATA statement would have the form

```
DATA IPP/12/
```

Only longitudinal matrices are processed by this program. The determination of transverse field strengths from data recorded in the format used here requires that a transverse field value be calculated as the square root of the sum of the squares of its components. The algebraic signs of the transverse field values therefore cannot be determined, and polarity reversals cannot be detected.

The second datum to be supplied is the mean background noise level for the frame of data. This variable is called RMSN; for the matrices that have been processed so far, the value RMSN = 0.05 is usually satisfactory. RMSN is a real variable. The DATA statement which specifies RMSN would be written

```
DATA RMSN/.05/
```

for a typical data frame.

A listing of the program is given in Figure 2. A sample plot is shown in Figure 4.

```
00100   C      'ZERO GRADIENT' CONTOURS IN MAGNETOGRAPH DATA MOD 7/74
00101          DIMENSION NLX(2000),NLY(2000),ARRAY(22),TEMP(5000),Y(32, 128)
00103          DIMENSION LTIME(9)
00104          DIMENSION A(20)
00105          DATA (ARRAY(I),I=1, 22)/24HHARDCOPY ONLY, ONE COPY ,18*6H      /
00107          DATA IPP/12/
00111          DATA HL/8/
00113          DATA RMSN/.05/
00115          KRE= 5
00116          KWR= 6
00117          CALL OPEN(8, 1, 5)
00120          IMAX= 128
00121          IMAY= 128
00122          ISIZE= 2000
00122   C      NO. OF ROWS, NO. OF COLUMNS, NO. OF NEUTRAL LIN E POSITIONS TO BE
00122   C      STORED
00123          ISZ1= ISIZE - 1
00124          CALL IDENT (9, ARRAY)
00124   C      DATA ARE WRITTEN ON TAPE FROM RIGHT TO LEFT, IN ROW ORDER, 8
00124   C      ROWS AT A TIME, PRECEDED BY A RECORD CONTAINING 19 WORDS
00124   C      OF HEADER INFORMATION
00125          DO 999 IP= 1, IPP
00125   C      READ HEADER INFORMATION
00130      300 CALL REDTPR (8, 2, IER, NW, 19, A)
00131          IF (NW-19) 300, 1, 300
00134        1 WRITE (KWR, 990) NW
00137      990 FORMAT (1H , 3HNW=, I5)
00137   C      RMSN IS RMS NOISE LEVEL FOR FRAME
00140          IF (IER - 1) 391, 390, 391
00143      391 WRITE (KWR, 392) IER, NW
00147      392 FORMAT (1H , 2I10)
00147   C      READ 1ST 2 RECORDS OF MAGNETOGRAM
00150      390 DO 65 I= 1, 2
00153          ICT = I
00154          WRITE (KWR, 988) ICT
00157      988 FORMAT (1H , 4HICT=, I5)
00160          J= 2048*(I-1)+1
00161       19 CALL REDTPR (8,2,IER, NW, 1, ICNT,2048,TEMP(J))
00162          WRITE (KWR, 989) NW, ICNT
00166      989 FORMAT (1H ,3HNW=,I7,5X,5HICNT=,I5)
00167          IF (NW-2049) 130, 129, 130
00172      130 WRITE (KWR, 392) NW, ICNT
00176          KK= 2049-NW + 1
00177          JX= 1
00200          DO 121 K= KK, 2049
00203          TEMP(K)= TEMP(JX)
00204          JX = JX + 1
00205      121 CONTINUE
00207          K2= KK - 1
00210          DO 131 K= 1, K2
00213          TEMP(K) = 0.
```

FIGURE 2. LISTING OF NEUTRAL LINE PLOT PROGRAM

ORIGINAL PAGE IS
OF POOR QUALITY

```
00214         131 CONTINUE
00216         129 IF (IER-1) 395, 4650, 395
00221         395 WRITE (KWR, 392) IER, NW
00225        4650 IF (I-1) 65, 465, 65
00230         465 IX = 100
00231             IY= IY  - 50
00232             IDELY= 25
00233             N= FLD(2, 10, TEMP(1))
00234             IDAYS= 200*FLD(26,1,N)+100*FLD(27,1,N)+80*FLD(28,1,N)
00234            1+40*FLD(29,1,N)+20*FLD(30,1,N)+10*FLD(31,1,N)+8*FLD(32,1,N)
00234            2+4*FLD(33,1,N)+2*FLD(34,1,N)+FLD(35,1,N)
00235             N= FLD(18,2, TEMP(1))
00236             FLD(30,4,N)= FLD(12,4,TEMP(1))
00237             IHOURS= 20*FLD(30,1,N)+10*FLD(31,1,N)+8*FLD(32,1,N)
00237            1+4*FLD(33,1,N)+2*FLD(34,1,N)+FLD(35,1,N)
00240             N= FLD(20, 7, TEMP(1))
00241             IMIN= 40*FLD(29,1,N)+20*FLD(30,1,N)+10*FLD(31,1,N)
00241            1+8*FLD(32,1,N)+4*FLD(33,1,N)+2*FLD(34,1,N)+FLD(35,1,N)
00242             N= FLD(27,7,TEMP(1))
00243             ISEC= 40*FLD(29,1,N)+20*FLD(30,1,N)+10*FLD(31,1,N)+8*FLD(32,1,N)
00243            1+4*FLD(33,1,N)+2*FLD(34,1,N)+FLD(35,1,N)
00244             ENCODE (40, LTIME) IDAYS, IHOURS, IMIN, ISEC
00252          40 FORMAT (I4, 5H DAYS,I7,6H HOURS,I8,8H MINUTES, I8,8H SECONDS)
00253             CALL FRAMEV(3)
00254             CALL PRINTV (54, LTIME, IX, IY)
00255             CALL STOPTV
00256          65 CONTINUE
00260             ILOC= 1
00261             IC= 1
00261       C     ICT IS NO. OF RECORDS READ FROM TAPE
00261       C     IC IS NO. OF TIMES READ FROM TAPE IS EXECUTED
00261       C     IC SHOULD BE EQUAL TO ICT - 1
00262             I= 129
00263             DO 68 JJ= 2, 32
00266             DO 70 KK= 1, 128
00271             Y(JJ, KK) = TEMP(I)
00272             I= I + 1
00273          70 CONTINUE
00275          68 CONTINUE
00275       C     REMOVE STRIPE
00277             DO 4056 IM= 1, 32
00302             IX= (IM-1)*128 + 111
00303             TEMP(IX)= TEMP(IX + 1)
00304        4056 CONTINUE
00304       C     SET X COORDINATE COUNTER AND START SEARCH OF FRAME
00306             NMAX= IMAX - 1
00307             II= 2
00307       C     START SEARCHING COLUMNS 2 THROUGH 16
00310             NMAY= IMAY - 1
00310       C     SPIKE NOISE FILTER
00311         211 DO 4050 JJ= 1, 31
00314             DO 4051 KK= 1, 127
00317             XTEM= ABS(RMSN-ABS(Y(JJ,KK)))
00320             IF (XTEM-3.*RMSN) 4051, 4051, 4052
00323        4052 YTEM= ABS(RMSN-ABS(Y(JJ+1,KK)))
00324             IF (YTEM-3.*RMSN) 4053, 4053, 4051
```

ORIGINAL PAGE IS
OF POOR QUALITY

FIGURE 2 - Continued

```
00327        4054 Y(JJ,KK) = RMSN/1.50
00330             GO TO 4051
00331        4053 ZTEM= ABS(RMSN-ABS(Y(JJ,KK+1)))
00332             IF (ZTEM-3.*RMSN) 4055, 4055, 4051
00335        4055 ZZTEM= ABS(RMSN-ABS(Y(JJ+1,KK+1)))
00336             IF (ZZTEM-3.*RMSN) 4054, 4054, 4051
00341        4051 CONTINUE
00343        4050 CONTINUE
00345             DO 9 JJ= I1, 16
00345       C     PREPARE TO GET CORRECT COORDINATES FOR VALUES TO BE STORED
00345       C     MISUNDERSTANDING ABOUT ORDER IN WHICH TAPE WAS WRITTEN
00345       C     SO MUST EXCHANGE X AND Y COORD AFTER THEY ARE DETERMINED
00350             NX1= JJ + (IC - 1) *16
00351             NX2= NX1 + 1
00352             DO 10 I= 1, 127
00352       C     SET Y COORDINATE COUNTER
00355             NY1= I
00356             NY2= I + 1
00357             P1= Y(JJ, I)
00360             P2= Y(JJ, I + 1)
00361             P3= Y(JJ+1, I)
00362             P4= Y(JJ+1, I+1)
00363             PP= ABS(P1)-RMSN
00364             IF (PP) 802, 902, 803
00367         802 PP= 0.
00370         803 IF (P1) 904, 902, 903
00373         904 P1= -PP
00374             GO TO 902
00375         903 P1= PP
00376         902 PP= ABS(P2)-RMSN
00377             IF (PP) 804, 901, 805
00402         804 PP= 0.
00403         805 IF (P2) 905, 901, 916
00406         905 P2= -PP
00407             GO TO 901
00410         916 P2= PP
00411         901 PP= ABS(P3)-RMSN
00412             IF (PP) 806, 912, 807
00415         806 PP= 0.
00416         807 IF (P3) 917, 912, 908
00421         917 P3= -PP
00422             GO TO 912
00423         908 P3= PP
00424         912 PP= ABS(P4)-RMSN
00425             IF (PP) 808, 911, 809
00430         808 PP= 0.
00431         809 IF (P4) 909, 911, 910
00434         909 P4= -PP
00435             GO TO 911
00436         910 P4= PP
00437         911 IF (P1) 104, 3, 103
00442         103 IF (P2) 4, 3, 3
00445         104 IF (P2) 3, 3, 4
00450           4 NLX(ILOC)= NY1
00451             NLY(ILOC)= NX1
00452             NLX(ILOC + 1)= NY2
```

FIGURE 2 - Continued

```
00453              NLY(ILOC + 1)= NX1
00454              WRITE (KWR, 30) P1, P2, NX1, NY1
00462           30 FORMAT (1H , 2(E12.5,5X), 2(I6, 5X))
00463              ILOC= ILOC + 2
00464              IF (ILOC - ISZ1) 10, 5, 5
00467            5 IF (NY1-70) 6, 6, 906
00472            6 WRITE (KWR, 8) NY1
00475            8 FORMAT (6H  NY1=, I7)
00476              WRITE (KWR, 411)
00500              WRITE (KWR, 412)
00502          411 FORMAT (25H ARRAY RESERVED IS FILLED)
00503          412 FORMAT (15H  TERMINATE RUN)
00504          906 IF (ICT-8) 907, 7, 7
00504        C     GO TO END OF MAGNETOGRAM
00507          907 CALL REDTPR (8,2,IER,NW,1,ICNT,2048,TEmp(1))
00510              WRITE (KWR, 989) NW, ICNT
00514              ICT = ICT + 1
00515              WRITE (KWR, 988) ICT
00520              IF (ICT - 8) 907, 7, 7
00520        C     GO TO END OF MAGNETOGRAM, THEN START NExT ONE
00523            3 IF (P1) 112, 12, 113
00526          112 IF (P3) 12, 12, 13
00531          113 IF (P3) 13, 12, 12
00534           13 NLX(ILOC)= NY1
00535              NLY(ILOC)= NX1
00536              NLX(ILOC + 1)= NY1
00537              NLY(ILOC + 1)= NX2
00540              WRITE (KWR, 30) P1, P3, NX1, NY1
00546              ILOC= ILOC + 2
00547              IF (ILOC-ISZ1) 10, 5, 5
00552           12 IF (P2) 115, 15, 114
00555          115 IF (P3) 15, 15, 14
00560          114 IF (P3) 14, 15, 15
00563           14 NLX(ILOC)= NY2
00564              NLY(ILOC)= NX1
00565              NLX(ILOC +1)= NY1
00566              NLY(ILOC + 1)= NX2
00567              WRITE (KWR, 30) P2, P3, NX1, NY1
00575              ILOC= ILOC + 2
00576              IF (ILOC - ISZ1) 10, 5, 5
00601           15 IF (P1) 110, 10, 116
00604          116 IF (P4) 16, 10, 10
00607          110 IF (P4) 10, 10, 16
00612           16 NLX(ILOC)= NY1
00613              NLY(ILOC)= NX1
00614              NLX(ILOC + 1)= NY2
00615              NLY(ILOC + 1)= NX2
00616              WRITE (KWR, 30) P1, P4, NX1, NY1
00624              ILOC = ILOC + 2
00625              IF (ILOC-ISZ1) 10, 5, 5
00630           10 CONTINUE
00632            9 CONTINUE
00634              IF (ICT - 8) 20, 201, 7
00637           20 DO 119 JJ= 1, 16
00642              DO 120 KK= 1, 128
00645              Y(JJ, KK)= Y(JJ+16, KK)
```

FIGURE 2 - Continued

ORIGINAL PAGE IS
OF POOR QUALITY

```
00646        120 CONTINUE
00650        119 CONTINUE
00652            IC = IC + 1
00653            CALL REDTPR(8, 2, IER, NW, 1, ICNT, 2048, TEMP(1))
00654            WRITE (KWR, 989) NW, ICNT
00660            ICT = ICT + 1
00661            WRITE (KWR, 988) ICT
00664            IF (NW-2049) 230, 229, 230
00667        230 WRITE (KWR, 392) NW, ICNT
00673            KK= 2049-NW + 1
00674            J= 1
00675            DO 231 K= KK, 2049
00700            TEMP(K)= TEMP(J)
00701            J= J + 1
00702        231 CONTINUE
00704            K2= KK-1
00705            DO 232 K= 1, K2
00710            TEMP(K)=  0.
00711        232 CONTINUE
00713        229 IF (IER -1) 393, 394, 393
00716        393 WRITE (KWR, 392) IER, NW
00722        394 I= 1
00723            DO 165 JJ= 17, 32
00726            DO 166 KK= 1, 128
00731            Y(JJ, KK)= TEMP(I)
00732            I= I + 1
00733        166 CONTINUE
00735        165 CONTINUE
00735      C     REMOVE STRIPE
00737            DO 4057 IM= 17, 32
00742            IX= (IM-1)*128 + 111
00743            TEMP(IX)= TEMP(IX + 1)
00744       4057 CONTINUE
00746            I1= 1
00746      C     GO SEARCH FIRST 16 COLUMNS AGAIN
00747            GO TO 211
00750        201 DO 219 JJ= 1, 16
00753            DO 220 KK= 1, 128
00756            Y(JJ, KK)= Y(JJ+16, KK)
00757        220 CONTINUE
00761        219 CONTINUE
00763            IC = IC +1
00764            ICT= 10
00765            I1= 1
00766            GO TO 211
00766      C     THIS COMPLETES SEARCH FOR 'ZERO GRADIENT' POINTS
00767          7 IFIN= ILOC -1
00770            WRITE (KWR, 132) IFIN
00773        132 FORMAT (1H , 5HIFIN=, I10)
00773      C     INVERT X ARRAY FOR PLOTTING
00774            DO 1801 I= 1, IFIN
00777            NX= MLX(I)
01000            MLX(I)= IMAX+1-NX
01001       1801 CONTINUE
01001      C     PLOT TAPE
01003             CALL GRIDIV(0.0,0.0,128.0,0.0,128.0,4.0,4.0,-5,5,-10,-10,+4,+4)
```

FIGURE 2 - Continued

ORIGINAL PAGE IS
OF POOR QUALITY

```
01004         IFI= ILOC-2
01005         DO 800 I= 1, IFI, 2
01010         X= NLX(I)
01011         CALL XSCLVI(X, NXP, IERR)
01012         NX1= NXP
01013         X= NLX(I+1)
01014         CALL XSCLVI(X, NXP, IERR)
01015         NX2= NXP
01016         YY= (NMAY+1)-NLY(I)
01017         CALL YSCLVI(YY, NYP, IERR)
01020         NY1= NYP
01021         YY= (NMAY+1)-NLY(I+1)
01022         CALL YSCLVI(YY, NYP, IERR)
01023         NY2= NYP
01024         CALL LINEV(NX1, NY1, NX2, NY2)
01025     800 CONTINUE
01027     999 CONTINUE
01031         CALL ENDJOB
01032         STOP
01033         END

      END OF COMPILATION:       NO  DIAGNOSTICS.
```


FIGURE 2 - Concluded

MAGNETIC FIELD GRADIENT PROGRAM

One way to represent magnetic field energy distributions in sunspots is to plot values of magnetic field gradient as a function of position in the spot. A second special-purpose program has been written to generate such displays.

The value actually plotted is not the value of magnetic field gradient; instead, it is the difference between signal values of adjacent grid positions. This procedure was chosen for several reasons. First, it gives the most direct representation of the actual data. Second, the plotted values are independent of uncertainties in the field strength calibration of the signal. Third, evaluation of distances on the solar surface and foreshortening corrections are not required, so the plot is independent of the assumptions which must be introduced to make those calculations. Fourth, if differences only are used, the evaluation of a numerical derivative is avoided; that procedure is notoriously unstable. The final plot is presented in the original magnetogram grid format, so it can be easily compared with contour plots and with photographs of the scope display at the time of observation. A label page giving the date and time of the observation is written for each plot.

Difference values in three size ranges are plotted. The scale factor used for demonstration was the approximate mean noise level of the observations, XNSE, but any interesting scale factor could be substituted. The plotting symbols were chosen to give an appearance of increased density as the signal difference value increased. The difference ranges and corresponding symbols are listed in Table 1.

The magnetograph signal data are read from magnetic tapes in the same format as are used for the neutral line program. In addition

TABLE 1. GRADIENT PLOT PROGRAM SYMBOLS

GRADIENT DIFFERENCE	SYMBOL
$2 \cdot \mathrm{XNSE} \leq \mathrm{difference} < 5 \cdot \mathrm{XNSE}$	o
$5 \cdot \mathrm{XNSE} \leq \mathrm{difference} < 10 \cdot \mathrm{XNSE}$	+
$\mathrm{difference} \geq 10 \cdot \mathrm{XNSE}$	*

to the data tape, a mean noise level or other plotting scale factor must be specified. This value is supplied in a DATA statement by assigning a value to a variable called XNS; the appropriate noise value, XNSE, is later calculated from XNS. In the sample given here, XNS = 0.05. As in the neutral line program, the number of matrices to be processed is supplied in a DATA statement. Again, the variable name assigned to this quantity is IPP, and again it is an integer variable. This program processes either longitudinal or transverse data but cannot do both types in a single run. If longitudinal data are to be plotted, the magnetograph data tape, after initial processing, is used as the data source. IPP is the number of longitudinal matrices on the tape. A third DATA statement must be included:

```
DATA LT/1/
```

and will cause the program to select the correct procedure for reading and plotting the longitudinal data. If transverse data are to be plotted, the data tape must be generated by the fourth program described in this section. IPP is the number of transverse matrices to be plotted, and LT must be supplied by the DATA statement

```
DATA LT/2/
```

No separate data deck is required.

The logic of the program is like that of the neutral line plot program, except that value differences instead of sign differences are recorded. Sequences of small grids, numbered P1, P2, P3, P4 as shown in Figure 1, are used to evaluate the differences across the magnetogram. The plot symbol is assigned to the coordinates of either P1 or P2. The coordinates of P1 are used if one of the differences (P1-P2), (P1-P3), or (P1-P4) is plotted; the coordinates of P2 are used if (P2-P3) or (P2-P4) is plotted. The value plotted is the largest difference found in the small four-point grid. No difference values smaller than 2·XNSE and no isolated difference values larger than 6·XNSE are plotted.

A listing of the program is given in Figure 3, and a sample plot is shown in Figure 5.

```
C     GRADIENT CONTOURS IN MAGNETOGRAM
C     BLANK IS PLOTTED IF GRADIENT VALUE IS LESS THAN 2X NOISE;
C     0 IF GRADIENT IS 2 TO 5X NOISE; * IF GRADIENT IS MORE THAN
C     10X NOISE.  ALL GRADIENTS MORE THAN 2X NOISE ARE PRINTED.
      DIMENSION XTWO(1000),YTWO(1000),XFIVE(1000),YFIVE(1000)
      DIMENSION XTEN(500),YTEN(500),TEMP(5000),Y(32, 128)
      DIMENSION ARRAY(22), GTEM(5)
      DIMENSION FLDX(12), FLDY(12,
      DIMENSION A(19)
      DIMENSION LTIME(9)
      DIMENSION TEME (2049)
      DATA IPP/38/
      DATA (FLDY(I), I= 1, 12)/12*6H          /
      DATA FLDX(2)/6H      /
      DATA (FLDX(I), I= 4, 12)/9*6H      /
      DATA (ARRAY(I), I= 1, 22)/24H HARDCOPY ONLY, ONE COPY, 18*6H
      DATA HL/8/
      DATA LT/1/
C     LT=1 IF LONGITUDINAL, 2 IF TRANSVERSE
      DATA XNS/.05/
      KRE= 5
      KWR= 6
      CALL OPEN(8, 1, 5)
      IMAX= 128
      IMAY= 128
      ISIZE = 1000
C     NO. OF ROWS, NO. OF COLUMNS, NO. OF GRADIENT VALUES STORED
      IS1= 1000
      IS2= 1000
      IS3= 500
      ISZ1= ISIZE - 1
      CALL IDENT (9, ARRAY)
      DO 997 IP= 1, IPP
C     READ HEADER INFORMATION
  300 CALL REDTPR (8, 2, IER, NW, 19, A)
      IF (NW-19) 300, 1, 300
    1 WRITE (KWR, 990) NW
  990 FORMAT (1H , 3HNW=, I5)
      IF (IP-30) 997, 700, 700
  700 CONTINUE
      IF (LT-1) 170, 170, 171
  170 XNSE= A(7)*(XNS-A(13))
      GO TO 172
  171 XNSE= SQRT(A(8)*SQRT(XNS))
C     XNSE IS MEAN NOISE LEVEL
  172 TXNS= XNSE*2.00
      FXNS= XNSE*5.00
      DXNS= XNSE*10.00
      FLDX(1)= A(3)
```

FIGURE 3. LISTING OF MAGNETIC FIELD GRADIENT PLOT PROGRAM

```
00175            FLDX(3)= A(4)
00176            IF (IER = 1) 391, 390, 391
00201       391 WRITE (KWR, 392) IER, NW
00205       392 FORMAT (1H , 2I10)
00206       390 WRITE (KWR, 67) (A(I), I= 1, 19)
00214        67 FORMAT (1H , 6(1X, O12))
00215            WRITE (KWR, 167) (A(I), I= 1, 4)
00223       167 FORMAT (1H ,2(I10,1X), 2(A12,2X))
00224            WRITE (KWR, 169) (A(I), I= 5, 11)
00232       169 FORMAT (1H ,5(E12.5,2X),2(I10,2X))
00233            WRITE (KWR, 168) (A(I), I= 12, 19)
00241       168 FORMAT (1H , 8(E12.5, 2X))
00241    C       READ 1ST 2 RECORDS OF MAGNETOGRAM
00242            DO 65 I= 1, 2
00245            ICT = I
00246            WRITE (KWR, 988) ICT
00251       988 FORMAT (1H ,4HICT=, I5)
00252            J= 2048*(I-1)+1
00253        19 CALL REDTPR (8, 2, IER, NW, 1, ICNT, 2048, TEMP(J))
00254            WRITE (KWR, 989) NW, ICNT
00260       989 FORMAT (1H , 3HNW=, I7, 5X, 5HICNT=, I5)
00261            IF (NW-2049) 130, 129, 130
00264       130 WRITE (KWR, 392) NW, ICNT
00270            DO 122 IB= 1, 3
00273       122 TEME(IB)= TEMP(IB)
00275            IMB= 4
00276            DO 123 IB= 11, 2049
00301            TEME (IB)= TEMP(IMB)
00302            IMB= IMB + 1
00303       123 CONTINUE
00305            DO 124 IB= 4, 10
00310       124 TEME(IB)= XNSE
00312            DO 125 IB= 1, 2049
00315       125 TEMP(IB)= TEME(IB)
00315    C       REMOVE STRIPE
00317       129 DO 4056 IM= 1, 16
00322            IX= (IM-1)*128+J-1+111
00323            TEMP(IX)= XNSE
00324      4056 CONTINUE
00326            IF (IER-1) 395, 4650, 395
00331       395 WRITE (KWR, 392) IER, NW
00335      4650 IF (I-1) 65, 465, 65
00340       465 IX = 100
00341            IY= IY - 50
00342            IDELY= 25
00343            N= FLD(2, 10, TEMP(1))
00344            IDAYS= 200*FLD(26,1,N)+100*FLD(27,1,N)+80*FLD(28,1,N)
00344           1+40*FLD(29,1,N)+20*FLD(30,1,N)+10*FLD(31,1,N)+8*FLD(32,1,N)
00344           2+4*FLD(33,1,N)+2*FLD(34,1,N)+FLD(35,1,N)
00345            N= FLD(18,2, TEMP(1))
00346            FLD(30,4,N)= FLD(12,4,TEMP(1))
00347            IHOURS= 20*FLD(30,1,N)+10*FLD(31,1,N)+8*FLD(32,1,N)
00347           1+4*FLD(33,1,N)+2*FLD(34,1,N)+FLD(35,1,N)
00350            N= FLD(20, 7, TEMP(1))
00351            IMIN= 40*FLD(29,1,N)+20*FLD(30,1,N)+10*FLD(31,1,N)
00351           1+8*FLD(32,1,N)+4*FLD(33,1,N)+2*FLD(34,1,N)+FLD(35,1,N)
```

FIGURE 3 - Continued

ORIGINAL PAGE IS
OF POOR QUALITY

```
00352          N= FLD(27,7,TEMP(1))
00353          ISEC= 40*FLD(29,1,N)+20*FLD(30,1,N)+10*FLD(31,1,N)+8*FLD(32,1,N)
00353         1+4*FLD(33,1,N)+2*FLD(34,1,N)+FLD(35,1,N)
00354          ENCODE (40, LTIME) IDAYS, IHOURS, IMIN, ISEC
00362       40 FORMAT (I4, 5H DAYS,I7,6H HOURS,I8,8H MINUTES, I8,8H SECONDS)
00363          CALL FRAMEV(3)
00364          CALL PRINTV (54, LTIME, IX, IY)
00365          CALL STOPTV
00366       65 CONTINUE
00370          IC= 1
00370     C    ICT IS NO. OF RECORDS READ FROM TAPE
00370     C    IC IS NO. OF TIMES READ FROM TAPE IS EXECUTED
00370     C    IC SHOULD BE EQUAL TO ICT - 1
00370     C    WRITE 1ST 2 RECORDS INTO Y ARRAY
00371          I= 129
00372          DO 68 JJ= 2, 32
00375          DO 70 KK= 1, 128
00400          Y(JJ, KK)= TEMP(I)
00401          I= I + 1
00402       70 CONTINUE
00404       68 CONTINUE
00404     C    SET X COORDINATE COUNTER AND START SEARCH OF FRAME
00406          NMAX= IMAX -1
00407          J1= 1
00410          J2= 1
00411          J3=1
00412          I1= 2
00412     C    START SEARCHING COLUMNS 2 THROUGH 16
00413          NMAY= IMAY - 1
00413     C    SPIKE NOISE FILTER
00414      211 DO 4050 JJ= 1, 31
00417          DO 4051 KK= 1, 127
00422          XTEM= ABS(XNSE-ABS(Y(JJ,KK)))
00423          IF (XTEM-3.*XNSE) 4051, 4051, 4052
00426     4052 YTEM= ABS(XNSE-ABS(Y(JJ+1,KK)))
00427          IF (YTEM-3.*XNSE) 4053, 4053, 4051
00432     4054 Y(JJ,KK)= XNSE
00433          GO TO 4051
00434     4053 ZTEM= ABS(XNSE-ABS(Y(JJ,KK+1)))
00435          IF (ZTEM-3.*XNSE) 4055, 4055, 4051
00440     4055 ZZTEM= ABS(XNSE-ABS(Y(JJ+1,KK+1)))
00441          IF (ZZTEM-3.*XNSE) 4054, 4054, 4051
00444     4051 CONTINUE
00446     4050 CONTINUE
00450          DO 9 JJ= I1, 16
00450     C    PREPARE TO GET CORRECT COORDINATES FOR GRADIENT VALUES TO
00450     C    BE STORED
00450     C    MISUNDERSTANDING ABOUT ORDER IN WHICH TAPE WAS WRITTEN
00450     C    SO MUST EXCHANGE X AND Y COORD AFTER THEY ARE DETERMINED
00453          NX1= JJ + (IC-1)*16
00454          NX2= NX1 + 1
00455          DO 10 I= 1, 127
00455     C    SET Y COORDINATE COUNTER
00460          NY1= I
00461          NY2= I + 1
00462          P1= Y(JJ, I)
```

FIGURE 3 - Continued

ORIGINAL PAGE IS
OF POOR QUALITY

```
00463              P2= Y(JJ, I + 1)
00464              P3= Y(JJ + 1, I)
00465              P4= Y(JJ+1, I+1)
00466              GTEM(1)= P1 - P2
00467              GTEM(2)= P1-P3
00470              GTEM(3)=P1-P4
00471              GTEM(4)= P2-P3
00472              GTEM(5)= P2-P4
00473              GMAX= ABS(GTEM(1))
00474              IG = 1
00475              DO 299 I2= 2, 5
00500              IF (ABS(GTEM(I2))-GMAX) 299, 301, 301
00503          301 GMAX= GTEM(I2)
00504              IG= I2
00505          299 CONTINUE
00507              IF (IG-4) 297, 298, 298
00512          297 IF (GMAX-TXNS) 10, 295, 295
00512        C     COORD OF P1 WILL BE STORED
00515          295 IF (GMAX-FXNS) 294, 302, 302
00520          294 WRITE (KWR, 26) NX1, NY1, GMAX
00525           25 FORMAT (1H ,4HNX1=,I7,9H     NY1=,I7,9H    GMAX=,E12.5)
00526              XTWO(J1)= NY1
00527              YTWO(J1)= NX1
00530              J1= J1 + 1
00531              IF (J1-IS1) 10, 5, 5
00534          302 IF (GMAX-DXNS) 303, 304, 304
00537          303 WRITE (KWR, 25) NX1, NY1, GMAX
00544              XFIVE(J2)= NY1
00545              YFIVE(J2)= NX1
00546              J2= J2 + 1
00547              IF (J2-IS2) 10, 5, 5
00552          304 WRITE (KWR, 25) NX1, NY1, GMAX
00557              XTEN(J3)= NY1
00560              YTEN(J3)= NX1
00561              J3 = J3 + 1
00562              IF (J3-IS3) 10, 5, 5
00565          298 IF (GMAX-TXNS) 10, 307, 307
00565        C     COORD OF P2 WILL BE STORED
00570          307 IF (GMAX-FXNS) 308, 309, 309
00573          308 WRITE (KWR, 26) NX2, NY1, GMAX
00600           26 FORMAT (1H ,4HNX2=,I7,9H     NY1=,I7,9H    GMAX=,E12.5)
00601              XTWO(J1)= NY1
00602              YTWO(J1)= NX2
00603              J1= J1 + 1
00604              IF (J1-IS1) 10, 5, 5
00607          309 IF (GMAX - DXNS) 310, 311, 311
00612          310 WRITE (KWR, 26) NX2, NY1, GMAX
00617              XFIVE(J2)= NY1
00620              YFIVE(J2)= NX2
00621              J2= J2 + 1
00622              IF (J2-IS2) 10, 5, 5
00625          311 WRITE (KWR, 26) NX2, NY1, GMAX
00632              XTEN(J3)= NY1
00633              YTEN(J3)= NX2
00634              J3= J3 + 1
00635              IF (J3-IS3) 10, 5, 5
```

FIGURE 3 - Continued

```
00640        5 IF (NX1 - 70) 6, 6, 906
00643        6 WRITE (KWR, 8) NY1
00646        8 FORMAT (6H  NY1=, I7)
00647          WRITE (KWR, 27) J1, J2, J3
00654          WRITE (KWR, 11)
00656          WRITE (KWR, 12)
00660       11 FORMAT (40H ARRAY RESERVED FOR GRADIENTS IS FILLED.)
00661       12 FORMAT (15H TERMINATE RUN.)
00662      906 IF (ICT - 8) 907, 7, 7
00662    C     GO TO END OF MAGNETOGRAM
00665      907 CALL REDTPR (8, 2, IER, NW, 1, ICNT, 2048, TEMP(1))
00666          WRITE (KWR, 989) NW, ICNT
00672          ICT = ICT + 1
00673          WRITE (KWR, 988) ICT
00676          IF (ICT-8) 907, 7, 7
00676    C     GO TO END OF MAGNETOGRAM, THEN START NEXT ONE
00701       10 CONTINUE
00703        9 CONTINUE
00705          IF (ICT - 8) 20, 201, 7
00710       20 DO 119 JJ= 1, 16
00713          DO 120 KK= 1, 128
00716          Y(JJ, KK)= Y(JJ + 16, KK)
00717      120 CONTINUE
00721      119 CONTINUE
00723          IC = IC + 1
00724          CALL REDTPR (8, 2, IER, NW, 1, ICNT, 2048, TEMP(1))
00724    C     REMOVE STRIPE
00725          DO 4057 IM= 1, 16
00730          IX= (IM-1)*128+111
00731          TEMP(IX)= XNSE
00732     4057 CONTINUE
00734          WRITE (KWR, 989) NW, ICNT
00740          ICT = ICT + 1
00741          WRITE (KWR, 988) ICT
00744          IF (NW-2049) 230, 229, 230
00747      230 WRITE (KWR, 392) NW, ICNT
00753          KK= 2049 - NW + 1
00754          J= 1
00755          DO 231 K= KK, 2049
00760          TEMP(K)= TEMP(J)
00761          J= J + 1
00762      231 CONTINUE
00764          K2= KK - 1
00765          DO 232 K= 1, K2
00770          TEMP(K)= 0.
00771      232 CONTINUE
00773      229 IF (IER-1) 393, 394, 393
00776      393 WRITE (KWR, 392) IER, NW
01002      394 I= 1
01003          DO 165 JJ= 17, 32
01006          DO 166 KK= 1, 128
01011          Y(JJ, KK)= TEMP(I)
01012          I= I + 1
01013      166 CONTINUE
01015      165 CONTINUE
01017          I1= 1
```

FIGURE 3 - Continued

```
01017      C      GO SEARCH FIRST 16 COLUMNS AGAIN
01020             GO TO 211
01021         201 DO 219 JJ= 1, 16
01024             DO 220 KK= 1, 128
01027             Y(JJ, KK)= Y(JJ + 16, KK)
01030         220 CONTINUE
01032         219 CONTINUE
01034             IC= IC + 1
01035             ICT = 10
01036             I1= 1
01037             GO TO 211
01037      C      THIS COMPLETES CALC OF GRADIENT VALUES
01040           7 WRITE (KWR, 27) J1, J2, J3
01045          27 FORMAT (1H , 3HJ1=,I5,5X,3HJ2=,I5,5X,3HJ3=,I5)
01045      C      INVERT X AND Y ARRAYS FOR PLOTTING
01046             J1= J1 - 1
01047             DO 800 I= 1, J1
01052             NX= XTWO(I)
01053             NY= YTWO(I)
01054             XTWO(I)= NMAX+1-NX
01055             YTWO(I)= NMAY +1-NY
01056         800 CONTINUE
01060             J2= J2 -1
01061             DO 799 I= 1, J2
01064             NX= XFIVE(I)
01065             NY= YFIVE(I)
01066             XFIVE(I)= NMAX + 1 -NX
01067             YFIVE(I)= NMAY +1 -NY
01070         799 CONTINUE
01072             J3= J3-1
01073             DO 798 I= 1, J3
01076             NX= XTEN(I)
01077             NY= YTEN(I)
01100             XTEN(I)= NMAX + 1-NX
01101             YTEN(I)= NMAY + 1 -NY
01102         798 CONTINUE
01104             CALL QUIK3L (-1,0.0,128.0,0.0,128.0,1H0,FLDX,FLDY,J1,XTWO,YTWO)
01105             CALL QUIK3L (0,0.0,128.0,0.0,128.0,1H*,FLDX,FLDY,J2,XFIVE,YFIVE)
01106             CALL QUIK3L (0,0.0,128.0,0.0,128.0,1H*,FLDX,FLDY,J3,XTEN,YTEN)
01107         997 CONTINUE
01111             CALL ENDJOB
01112         998 STOP
01113             END

     END OF COMPILATION:        NO  DIAGNOSTICS.
```

FIGURE 3 - Concluded

ORIGINAL PAGE IS
OF POOR QUALITY

RESULTS OF PLOT PROGRAMS

Figures 4 and 5 show results of the two plot programs for the same frame of data (23 October 1973, $23^h\ 41^m\ 9^s$ U. T.). Figure 4 is the neutral line plot and Figure 5 the field gradient plot. Figure 6 is a contour plot of the same data frame, made by the Computer Sciences Corporation. (The orientation of Figure 6 is reversed both vertically and horizontally from Figures 4 and 5.) The contour intervals of Figure 6 are labeled according to the code given in Table 2.

TABLE 2. CONTOUR LABELS FOR FIGURE 6

LABEL	FIELD STRENGTH (gauss)
A	-2.581×10^3
B	-1.290×10^3
C	-6.452×10^2
D	-2.581×10^2
E	-2.581×10^1
F	0.000
G	$+2.581 \times 10^1$
H	$+2.581 \times 10^2$
I	$+6.452 \times 10^2$
J	$+1.290 \times 10^3$
K	$+2.581 \times 10^3$

The position of the solar limb shows clearly in each of these three figures. (The vertical streak in Figures 5 and 6 is a flaw on the magnetograph vidicon tube. The gradient plotting program now contains a routine which removes this streak.) In addition, the active region shown contains two neutral lines which run across the regions of steepest magnetic field gradient. There is also some evidence, in Figures 4 and 6, of a weak but complex field structure near the limb.

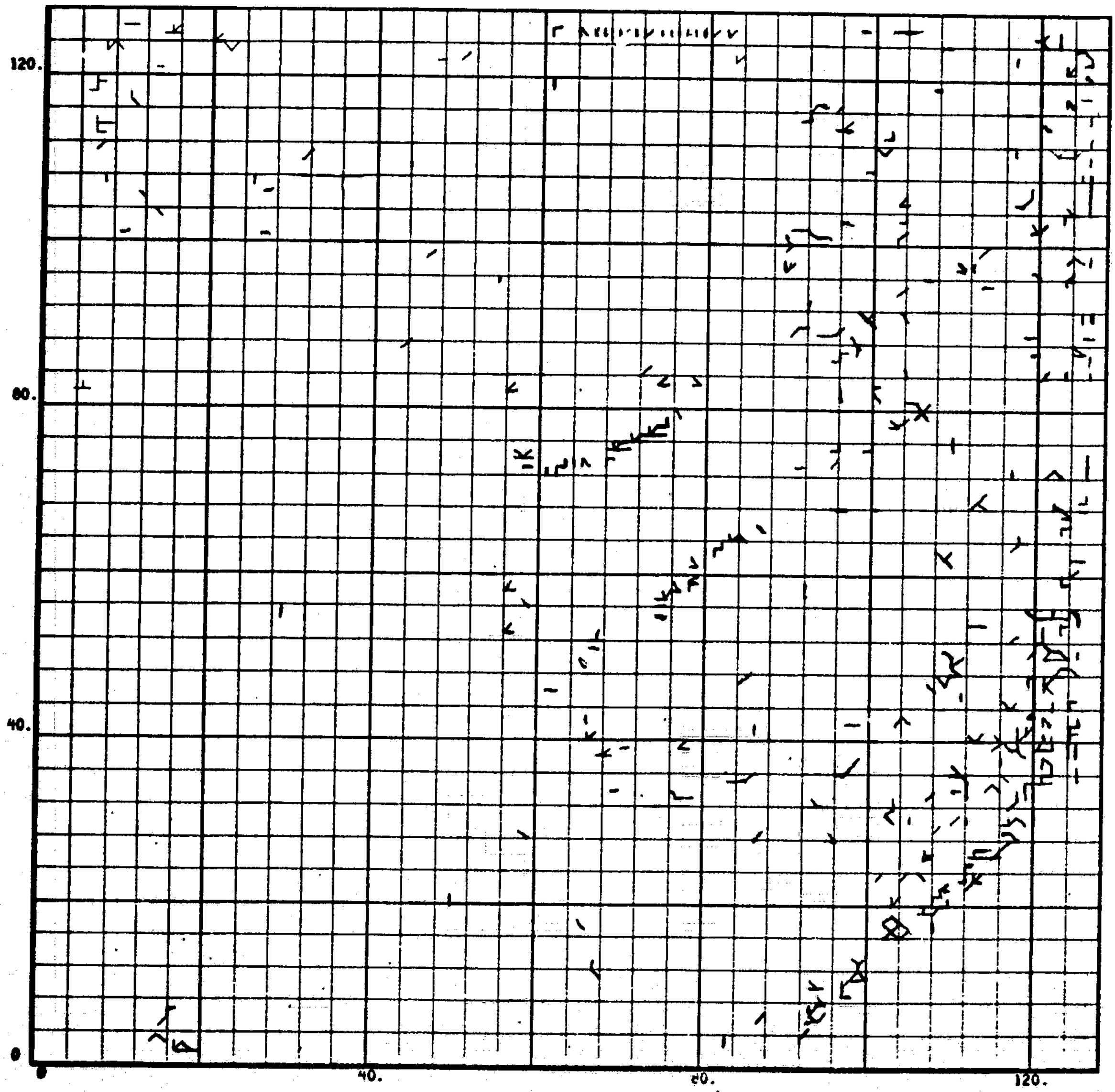

FIGURE 4. SAMPLE NEUTRAL LINE PLOT

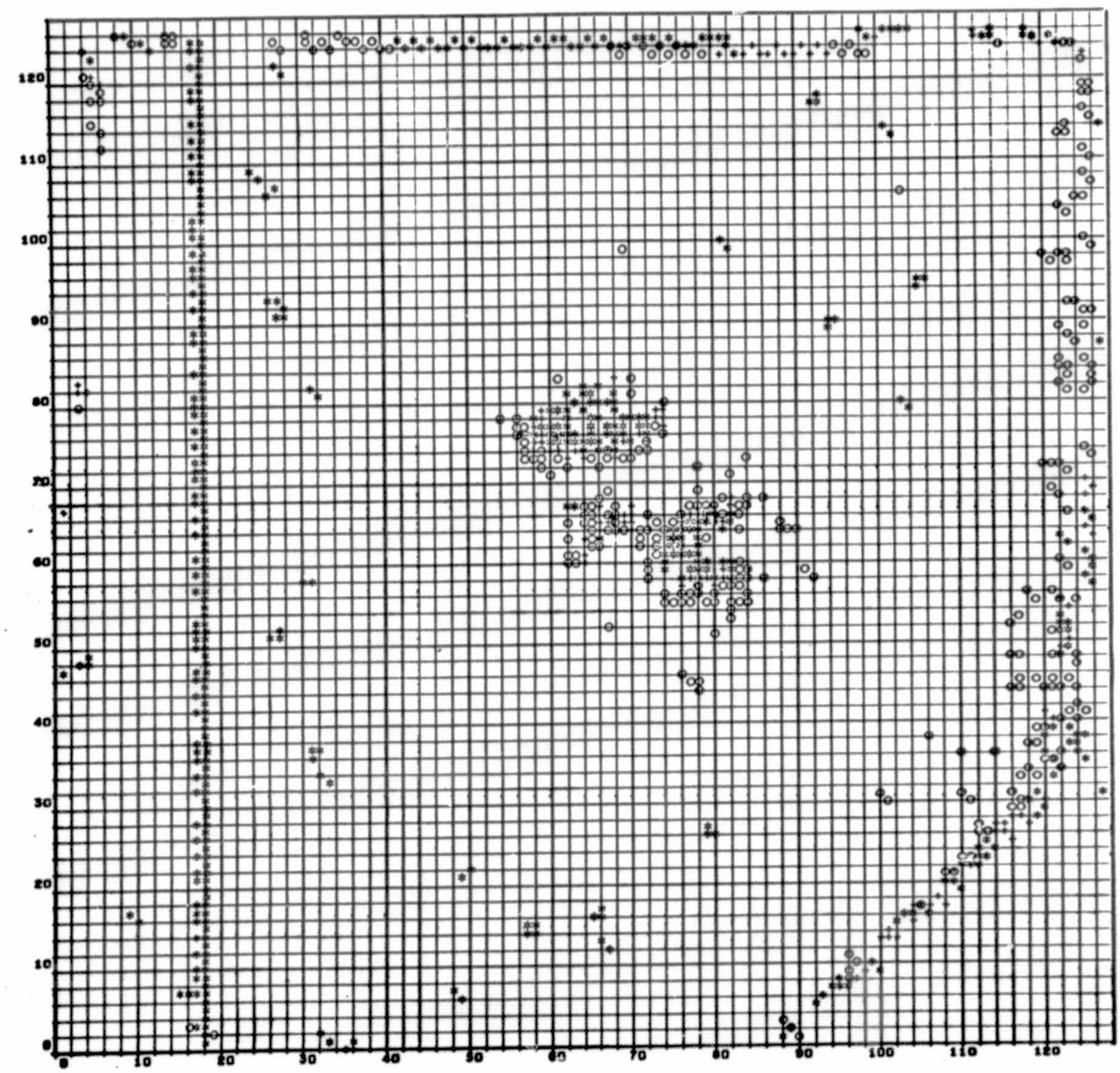

FIGURE 5. SAMPLE GRADIENT PLOT

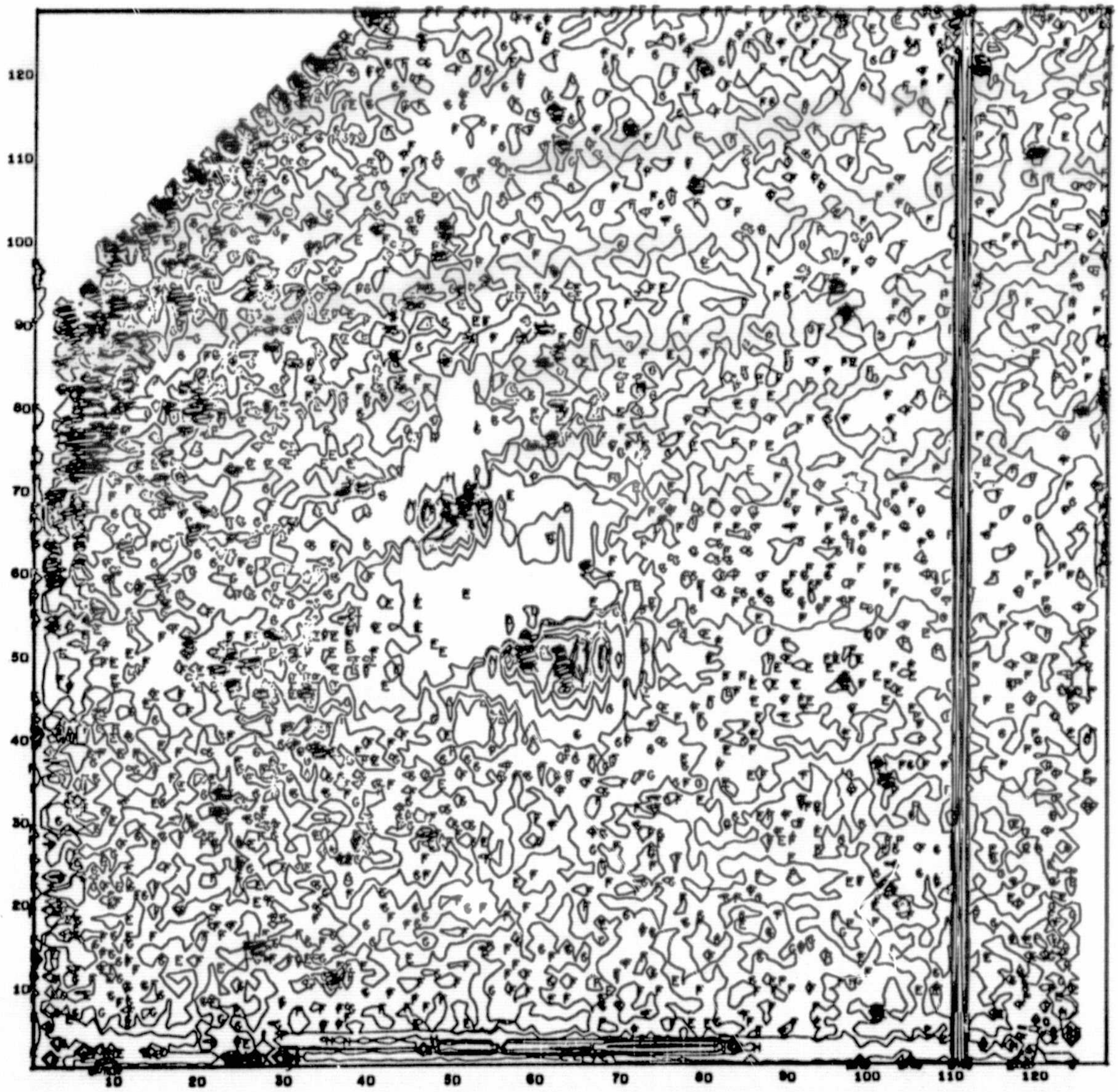

FIGURE 6. MAGNETIC FIELD CONTOURS FOR DATA PLOTTED IN FIGURES 4 AND 5

NOISE REMOVAL PROGRAM

Some of the data matrices contain noise values which appear as single values much larger than any other values near them. This program removes each of these values, replaces it by the average of the points surrounding the removed value, and writes a new tape containing the corrected matrices in the same format as on the original tape. Both longitudinal and transverse matrices can be corrected in one pass.

The program also removes the vertical streak which appears in Figures 5 and 6. This stripe always occurs in column 111 of the data matrix as it is read in (the matrix is stored reading from right to left across the frame). Because the location is always the same, the stripe can be removed as soon as the matrix has been read. The value in the location X = 111 in each line is replaced by the value X = 112 in the same line.

The isolated values to be removed are identified by comparing them to criterion values which are supplied as data. Two criterion values are needed, one for longitudinal data and one for transverse. The data tapes used are the magnetograph data tapes after the initial processing, so the data values are signal values, not field strengths. Also, the transverse criterion value is the criterion for the U or the R component, not for the resultant transverse field vector. It is assumed that the same criterion value can be used for the U and R matrices.

After a matrix is read, the proper criterion value is chosen, and the absolute value of each matrix data point is compared to the criterion value. If the matrix value is more than six times the criterion value, the adjacent matrix points are examined. If one or more of the adjacent values is greater in absolute value than six times the criterion, the tested value is assumed to be valid. If none of the adjacent values is greater in absolute value than six times the criterion, the tested value is assumed to be invalid and is replaced by the average of the adjacent values.

The magnetograph data for the program are taken from the data tapes after initial processing. These tapes have the general format shown in Figure 7.

```
               { HEADER
               { LONGITUDINAL DATA MATRIX
MAGNETOGRAM    { INTENSITY DATA MATRIX
    #1         { U MATRIX (ONE COMPONENT OF TRANSVERSE DATA)
               { R MATRIX (OTHER COMPONENT OF TRANSVERSE DATA)

               { HEADER
               { LONGITUDINAL DATA MATRIX
MAGNETOGRAM    { INTENSITY DATA MATRIX
    #2         { U MATRIX
               { R MATRIX

     .               .
     .               .
     .               .

               { HEADER
               { LONGITUDINAL DATA MATRIX
MAGNETOGRAM    { INTENSITY DATA MATRIX
   #NMAT       { U MATRIX
               { R MATRIX

                 END OF FILE
```

FIGURE 7. MAGNETOGRAPH DATA TAPE FORMAT

On any tape, the longitudinal matrix may or may not be present, the intensity matrix may or may not be present, and the U-R matrix pair may or may not be present. This program will process any combination of matrices if the correct data are supplied. (It is assumed, however, that the intensity matrices are either always present or always absent. All tapes processed so far have complied with this assumption.)

In addition to the tape, values must be furnished to the program through four DATA statements. The contents and formats of these statements are described in Table 3.

TABLE 3. DATA STATEMENTS FOR SPIKE NOISE REMOVAL PROGRAM

VARIABLE NAME	VARIABLE DEFINITION	MODE (REAL OR INTEGER)	EXAMPLE OF DATA STATEMENT
NMAT	Number of magnetograms on tape (i.e., number of groups of matrices as shown in Figure 7)	Integer	DATA NMAT/7/
XNA	Criterion value for longitudinal data = six times largest valid isolated signal value	Real	DATA XNA/.005/
XNB	Criterion value for each component of transverse data = six times largest valid isolated signal value expected in U and R matrices	Real	DATA XNB/.002/
DINT	DINT = 1.0 if intensity matrices are present on tape and = 0.0 if no intensity matrices were recorded	Real	DATA DINT/0.0/

After the matrix has been corrected, the program writes it on tape in the same format in which it was read and reads the next matrix. The tape which is produced contains NMAT groups of matrices; each group contains the same number of matrices as were in that group on the original tape.

A listing of the program is given in Figure 8.

```
C     REMOVE SPIKE NOISE VALUES
      DIMENSION TEMP(16384),A(15),IA(4),Y(128,128)
      DIMENSION TEME(2049)
      DIMENSION XNSE(4)
C     NMAT= NO. OF MAGNETOGRAMS ON DATA TAPE
      DATA NMAT/7/
      DATA XNA/.00583/
      DATA XNB/.00156/
C     XNA IS LIMIT FOR L MATRIX
C     XNB IS LIMIT FOR T MATRIX
      DATA DINT/1.0/
```

FIGURE 8. LISTING OF NOISE REMOVAL PROGRAM

```
00113   C      DINT=0 IF NO INTENSITY MATRICES, =1 IF INTENSITY MATRICES
00113   C      PRESENT
00115          KRE= 5
00116          KWR= 6
00117          CALL OPEN (8,1,5)
00120          CALL REWIND (8)
00121          CALL OPEN (9, 1, 5)
00122          CALL REWIND(9)
00123          DO 100 IMAT= 1, NMAT
00123   C      READ HEADER
00126        1 CALL REDTPR (8,2,IER,NW,2,IA(1),7,A(1),2,IA(3),8,A(8))
00127          CALL WRITER (9,2,IER,2,IA(1),7,A(1),2,IA(3),8,A(8))
00130          IF (NW-19) 1, 17, 1
00133       17 WRITE (KWR, 21) NW
00136       21 FORMAT (4H NW=, I5)
00137       26 WRITE (KWR, 167) IA(1), IA(2), A(1), A(2)
00145      167 FORMAT (1H ,2(I10,1X),2(A12,2X))
00146          WRITE (KWR, 169) ((A(I),I= 3, 7),IA(3),IA(4))
00156      169 FORMAT (1H ,5(E12.5,2X),2(I10,2X))
00157          WRITE (KWR, 168) (A(I),I= 8, 15)
00165      168 FORMAT (1H , 8(E12.5,2X))
00166          WRITE (KWR, 299) IA(2), IMAT
00172      299 FORMAT (1H , 2(I10, 5X))
00173          IF (DINT) 2, 2, 3
00176        2 IF (IA(2)-5) 4, 5, 5
00201        4 IRUN= 1
00202          XNSE(1)= XNA
00203          GO TO 50
00204        5 IF (IA(2)-61) 6, 6, 7
00207        6 IRUN= 2
00210          XNSE(1)= XNB
00211          XNSE(2)= XNB
00212          GO TO 50
00213        7 IRUN= 3
00214          XNSE(1)= XNA
00215          XNSE(2)= XNB
00216          XNSE(3)= XNB
00217          GO TO 50
00220        3 IF (IA(2) - 5) 8, 8, 9
00223        8 IRUN= 2
00224          XNSE(1)= XNA
00225          XNSE(2)= XNA
00226          GO TO 50
00227        9 IF (IA(2)-61) 10, 10, 11
00232       10 IRUN= 3
00233          XNSE(1)= XNA
00234          XNSE(2)= XNB
00235          XNSE(3)= XNB
00236          GO TO 50
00237       11 IRUN = 4
00240          XNSE(1)= XNA
00241          XNSE(2)= XNA
00242          XNSE(3)= XNB
00243          XNSE(4)= XNB
00244          GO TO 50
00245       50 DO 51 I= 1, IRUN
```

ORIGINAL PAGE IS
OF POOR QUALITY

FIGURE 8 - Continued

```
00245      C     READ MATRIX
00250              J= 1
00251           52 CALL REDTPR(8,2,IER,NW,1,ICNT,2048,TEMP(J))
00252              WRITE (KWR, 989) NW, ICNT
00256          989 FORMAT (1H , 3HNW=,I7,5X,5HICNT=,I5)
00256      C       CHECK FOR WRONG RECORD LENGTH IN 1ST RECORD
00257              IF (NW-2049) 130, 59, 130
00262          130 WRITE (KWR, 989) NW, ICNT
00266              WRITE (KWR, 1130) (TEMP(IL),  IL= 1, 20)
00274         1130 FORMAT (5(1H , E12.5))
00275              DO 122 IB= 1, 3
00300          122 TEME(IB)= TEMP(IB)
00302              IMB= 4
00303              DO 123 IB= 11, 2048
00306              TEME(IB)= TEMP(IMB)
00307              IMB= IMB + 1
00310          123 CONTINUE
00312              DO 124 IB= 4, 10
00315          124 TEME(IB)= XNSE(1)
00317              DO 125 IB= 1, 2048
00322          125 TEMP(IB)= TEME(IB)
00324              WRITE (KWR, 1130) (TEMP(IL),  IL= 1, 20)
00332           59 J= J + 2048
00333           53 CALL REDTPR(8,2,IER,NW,1,ICNT,2048,TEMP(J))
00334              WRITE (KWR, 989) NW, ICNT
00340              IF (ICNT-8) 12, 129, 129
00343           12 J= J + 2048
00344              GO TO 53
00344      C       REMOVE STRIPE
00345          129 DO 4056 IM= 1, 128
00350              IX= (IM-1)*128+11
00351              TEMP(IX)= TEMP (IX + 1)
00352         4056 CONTINUE
00352      C       WRITE MATRIX INTO Y ARRAY
00354              IY= 1
00355              DO 68 JJ= 1, 128
00360              DO 70 KK= 1, 128
00363              Y(JJ,KK)= TEMP(IY)
00364              IY= IY + 1
00365           70 CONTINUE
00367           68 CONTINUE
00367      C       SPIKE NOISE FILTER
00371          211 DO 4050 JJ= 1, 127
00374              DO 4051 KK= 1, 127
00377              XTEM= ABS(XNSE(1)-ABS(Y(JJ,KK)))
00400              XMG= Y(JJ,KK)
00401              IF (XTEM-5.*XNSE(1)) 4051, 4051, 4052
00404         4052 YTEM= ABS(XNSE(1)-ABS(Y(JJ+1,KK)))
00405              IF (YTEM-5.*XNSE(1)) 4053, 4053, 4051
00410         4054 TTM1= (Y(JJ,KK+1)+Y(JJ+1,KK)+Y(JJ+1,KK+1))/3.
00411              IF (JJ-1) 3000, 3000, 3001
00414         3001 TTM2= (TTM1+Y(JJ-1, KK)+Y(JJ-1,KK+1))/3.
00415              GO TO 3002
00416         3000 TTM2= TTM1
00417         3002 IF (KK-1) 3003, 3003, 3004
00422         3004 TTM3= (TTM2+Y(JJ, KK-1)+Y(JJ+1, KK-1))/3.
```

FIGURE 8 - Continued

```
00423                IF (JJ-1) 3005, 3005, 3006
00426           3006 TTM4= (TTM3+Y(JJ-1, KK-1))/2.
00427                GO TO 3010
00430           3005 TTM4= TTM3
00431                GO TO 3010
00432           3003 TTM4= TTM2
00433           3010 Y(JJ, KK)= TTM4
00434                WRITE (KWR, 4049) JJ, KK, XMG, Y(JJ, KK)
00442           4049 FORMAT (1H , I5, 5X, I5, 2(5X, E12.5))
00443                GO TO 4051
00444           4053 ZTEM= ABS(XNSE(I)-ABS(Y(JJ, KK+1)))
00445                IF (ZTEM-5.*XNSE(I)) 4055, 4055, 4051
00450           4055 ZZTEM= ABS(XNSE(I)-ABS(Y(JJ+1, KK+1)))
00451                IF (ZZTEM-5.*XNSE(I)) 4054, 4054, 4051
00454           4051 CONTINUE
00456           4050 CONTINUE
00456           C    REWRITE CORRECTED Y ARRAY IN TEMP
00460                IY= 1
00461                DO 171 JJ= 1, 128
00464                DO 170 KK= 1, 128
00467                TEMP(IY)= Y(JJ,KK)
00470                IY= IY + 1
00471            170 CONTINUE
00473            171 CONTINUE
00473           C    WRITE TAPE RECORD
00475                J= 1
00476                ICNT = 1
00477             55 CALL WRITER (9, 2,IER,1,ICNT,2048,TEMP(J))
00500                IF (ICNT-8) 54, 56, 56
00503             54 J= J + 2048
00504                ICNT= ICNT + 1
00505                GO TO 55
00506             56 WRITE (KWR, 57) IMAT
00511             57 FORMAT (18H WROTE MATRIX NO. , I4)
00512             51 CONTINUE
00514            100 CONTINUE
00516                CALL CLOSE (9,3)
00517                STOP
00520                END

        END OF COMPILATION:        NO  DIAGNOSTICS.
```

FIGURE 8 - Concluded

ORIGINAL PAGE IS
OF POOR QUALITY

TRANSVERSE MATRIX GENERATION PROGRAM

This is a very simple program which reads a magnetograph data tape, selects the U and R matrices, and calculates the transverse component T of the signal according to $T = (U^2 + R^2)^{\frac{1}{2}}$, for each matrix point. The matrix of T values is then written on a new tape. The tape written by this program is not in the same format as the original tapes; it consists only of header records and T matrices.

The data tapes for this program are the same as for the other programs described in this section. Two data values must be supplied through DATA statements; these are NMAT and DINT. The definitions of these variables and formats of the DATA statements are exactly the same as for the Noise Removal Program. Note, in particular, that NMAT is the total number of magnetograms on the tape, whether or not all those magnetograms contain transverse data matrices. On the output tape, however, headers and matrices are written only for those magnetograms which contained transverse data.

A listing of the program is given in Figure 9.

```
C     WRITE TAPE FOR PLOTTING TRANSVERSE FIELD PATTERNS
      DIMENSION U(16384), R(2048), HT(2048)
      DIMENSION A(15), IA(4)
C     NMAT= NO. OF MAGNETOGRAMS ON DATA TAPE
      DATA NMAT/14/
      DATA DINT/0.0/
C     DINT=0 IF NO INTENSITY MATRIX PRESENT, =1 IF INTENSITY MATRIX
C     PRESENT
      KRE= 5
      KWR = 6
      CALL OPEN (8, 1, 5)
      CALL REWIND (8)
      CALL OPEN (9, 1, 5)
      CALL REWIND (9)
      IMAT = 1
C     SKIP DOWN TO FIRST U MATRIX
    1 CALL REDTPR (8,2,IER,NW,2,IA(1),7,A(1),2,IA(3),8,A(8))
   21 FORMAT (4H NW=, I5)
```

FIGURE 9. LISTING OF TRANSVERSE MATRIX GENERATION PROGRAM

```
00121                IF (NW-19) 1, 17, 1
00124             17 WRITE (KWR, 21) NW
00127             26 WRITE (KWR, 167) IA(1), IA(2), A(1), A(2)
00135            167 FORMAT (1H , 2(I10, 1X), 2(A12, 2X))
00136                WRITE (KWR, 169) ((A(I), I= 3, 7), IA(3), IA(4))
00146            169 FORMAT (1H , 5(E12.5,2X), 2(I10, 2X))
00147                WRITE (KWR, 168) (A(I), I= 8, 15)
00155            168 FORMAT (1H , 8(E12.5, 2X))
00156             22 FORMAT (4H NW=, I5, 6X,5HICNT=, I5)
00157                AMG= 5.0
00160                WRITE (KWR, 299) IA(2), IMAT, AMG
00165            299 FORMAT (1H , 2(I10,5X), F10.0)
00166                IF (IA(2)-5) 201, 209, 208
00166        C       CASE 1.  SKIP TO NEXT HEADER
00171            201 CALL REDTPR (8,2,IER,NW,2,IA(1),7,A(1),2,IA(3),8,A(8))
00172                IF (NW-19) 201, 202, 201
00175            202 IMAT = IMAT + 1
00176                AMG= 1.0
00177                WRITE (KWR, 299) IA(2), IMAT, AMG
00204                GO TO 17
00205            208 IF (IA(2)-61) 209, 210, 210
00210            209 IF (DINT) 3, 3, 203
00210        C       CASE 2.  SELECT 1ST AND 2ND MATRICES
00210        C       CASE 3.  SELECT 2ND AND 3RD MATRICES
00213            203 CALL REDTPR(8, 2, IER, NW, 1, ICNT, 2048, U(1))
00214                AMG= 2.0
00215                WRITE (KWR, 299) IA(2), IMAT, AMG
00222                IF (ICNT-8) 203, 3, 3
00225            210 IF (DINT) 203, 203, 204
00225        C       CASE 4.  SELECT 3RD AND 4TH MATRICES
00230            204 IDEX= 0
00231                AMG= 3.0
00232                WRITE (KWR, 299) IA(2), IMAT, AMG
00237                CALL REDTPR (8, 2, IER, NW, 1, ICNT, 2048, U(1))
00240                IF (ICNT-8) 204, 205, 205
00243            205 IF (IDEX) 206, 206, 3
00246            206 IDEX = 1
00247                AMG=  4.0
00250                WRITE (KWR, 299) IA(2), IMAT, AMG
00255                GO TO 204
00255        C       3RD MATRIX ON TAPE IS 1ST U MATRIX IF I MATRIX IS PRESENT
00256              3 IU = 1
00257              6 CALL REDTPR (8, 2, IER, NW, 1, ICNT, 2048, U(IU))
00260                WRITE (KWR, 22) NW, ICNT
00264              4 IU= IU + 2048
00265                IF (ICNT-8) 6, 7, 7
00265        C       HAVE STORED 1ST U MATRIX.  NOW READ 1ST RECORD OF R MATRIX
00270              7 CALL REDTPR( 8, 2, IER, NW, 1, ICNT, 2048, R(1))
00271                WRITE (KWR, 22) NW, ICNT
00275              9 DO 8 J= 1, 2048
00300                HT(J)= SQRT(SQRT(U(J)*U(J)+R(J)*R(J)))
00301              8 CONTINUE
00303                I1= 2048
00303        C       FIRST 4 WORDS OF HT MATRIX ARE GARBAGE
00304                CALL WRITER (9, 2, IER, 2, IA(1),7,A(1),2,IA(3),8,A(8))
00305                CALL WRITER (9, 2, IER, 1, ICNT, 4, U(1), 2044, HT(5))
```

FIGURE 9 - Continued

ORIGINAL PAGE IS
OF POOR QUALITY

```
00306          13 CALL REDTPR (8, 2, IER, NW, 1, ICNT, 2048, R(1))
00307             WRITE (KWR, 22) NW, ICNT
00313             DO 10 J= 1, 2048
00316             I= J + I1
00317             HT(J)= SQRT(SQRT(U(I)*U(I)+R(J)*R(J)))
00320          10 CONTINUE
00322             I1= I1 + 2048
00323             CALL WRITER (9, 2, IER, 1, ICNT, 2048, HT(1))
00324             IF (ICNT-8) 13, 12, 12
00324      C      HAVE REACHED END OF R MATRIX
00327          12 WRITE (KWR, 14) IMAT
00332          14 FORMAT (21H WROTE HT MATRIX NO. , I3)
00333             IF (IMAT - NMAT) 15, 16, 16
00336          15 IMAT = IMAT + 1
00337             GO TO 1
00340          16 CALL CLOSE (9, 3)
00341             STOP
00342             END

      END OF COMPILATION:        NO  DIAGNOSTICS.
```

FIGURE 9 - Concluded

ORIGINAL PAGE IS
OF POOR QUALITY